

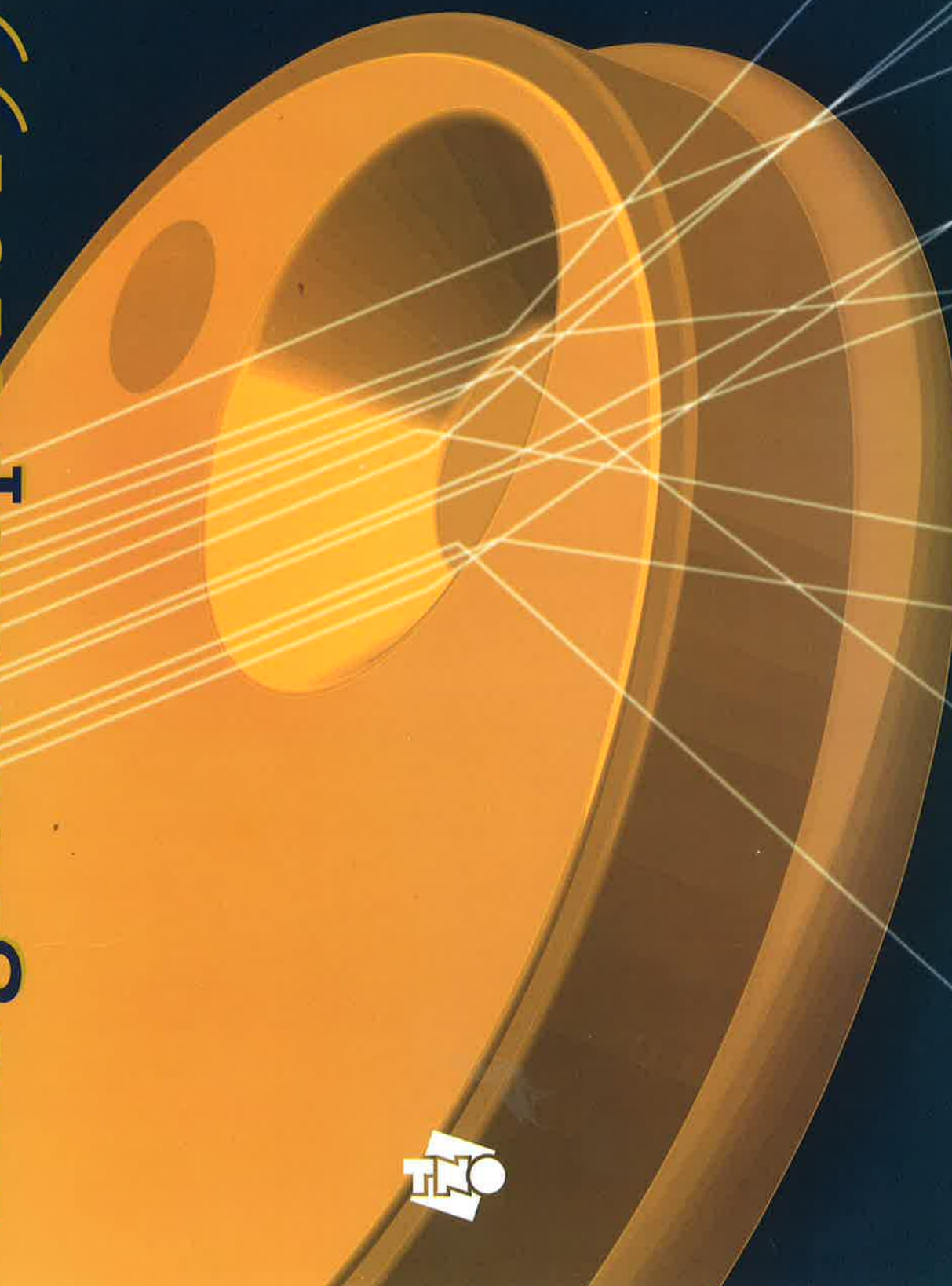
TNO VOEDING ZEIST
BIBLIOTHEEK

10 d(96-99)

Centre for Radiological Protection
Dosimetry

© TNO – All rights reserved

Progress Report 1996-1999



Quotations from articles in this report
should be referred to as "personal communication".

TNO Centre for Radiological Protection and Dosimetry

Progress Report 1996 - 1998

Editors: H.B. Kal and P.A.J. Bentvelzen

Typing: Hetty Jense

Graphical design and lay out: J.L.A. van der Brugge

Printed by: ArtByte Reclame en Pre-Press



Utrechtseweg 310
P.O. Box 9034
6800 ES Arnhem
The Netherlands
Telephone:
+31.26.356.30.55
Telefax:
+31.26.445.07.87
E-mail:
secretariat@csd.tno.nl





TNO Centre for Radiological Protection and Dosimetry

H.W. Julius, director Arnhem (till 1 August 1997)
J.J. Broerse, advisor Rijswijk
G. Gerritse, interim-manager (from 1 August 1997)

Staff members:

A. van Aersen-Groot Hulze	Arnhem	P. de Jong	Arnhem/Rijswijk
R.W. Bartstra	Rijswijk	H.B. Kal	Rijswijk
P.A.J. Bentvelzen	Rijswijk	V.C. Lossau	Arnhem
L. van den Berg	Arnhem/Rijswijk	J.C. Moor	Arnhem
H. Bruger	Arnhem	J.W. Noomen	Rijswijk
F.A.I. Busscher	Arnhem	J.H. Reumer	Arnhem
J.W.E. van Dijk	Arnhem	A. van Rotterdam	Rijswijk
W. van Dijk	Arnhem	F.W. Schultz	Rijswijk
H.H. Goedoen	Rijswijk	A. Teunissen	Arnhem
Th.G.L. Heijmans	Arnhem	C.W. Verhoef	Arnhem
W.P. Hiestand	Arnhem	D. de Vries-Kolder	Arnhem
J.Th.M. Jansen	Rijswijk	J. Zoetelief	Rijswijk

PREFACE

I am proud to present the Progress Report 1996-1998 of the TNO Centre for Radiological Protection and Dosimetry (TNO-CSD). At first glance, a comparison of the present report with the Progress Report 1995 shows continuity. Continuity in that knowledge has been further developed and intensified in the research areas mentioned in the former report. There is also continuity in the provision of services by TNO-CSD to the radiological workers in The Netherlands, in particular by the issuing, reception, readout and registration of 30.000 personal dosimeters per month. Research and the provision of services, two clusters of activities for which TNO-CSD has earned international recognition and which are a continuous source of pride to the TNO Centre for Radiological Protection and Dosimetry.

However, the image of continuity is only partially true. Two important developments during the past two years will affect TNO-CSD. Firstly, the retirement at August 1, 1997 of Han Julius as director of TNO-CSD. Han Julius initiated the development of the renowned individual dosimeter of TNO. He directed the process of its innovation, research, development and finally implementation in an enrapturing and creative way. For more than twenty years he managed the TNO Radiological Service, which in 1994 became a major part of TNO-CSD. He was nation-wide and internationally the image of TNO in the field of personal dosimetry. Moreover, Han was the image of The Netherlands in these fields in various international circles. In many different ways Han has contributed much to the profession of radiological protection. He therefore merits our appreciation and gratitude. TNO-CSD is pleased to have attracted Han Julius as its advisor. It is clear, however, that this retirement as a director in view of his status and imprint on TNO-CSD, will have a great impact.

The second development with a major impact on the future of TNO-CSD is that the field of radiological protection in The Netherlands is in motion. For instance, the public discussion on nuclear energy in The Netherlands resulted in the termination of energy production by the nuclear power plant at Dodewaard. In the year 2002 the nuclear power plant at Borssele will most likely end its activities. In this area will therefore be a diminishing need for research and services in radiological protection and dosimetry. In The Netherlands 90 per cent of exposure to ionising radiation resulting from man-made sources is due to medical applications. The need for both research and services will be, therefore, directed more towards medical applications.

It is up to TNO-CSD to realise these new ambitions. This will not be a simple task, but is quite a challenge. There will be many changes at TNO-CSD, but we will ensure and even improve the quality of both the research and the provisions of services. The present Progress Report provides a survey of the quality of the research and services. I hope that this report will meet your interest and appreciation.

G. Gerritse



Contents

I. RESEARCH AND DEVELOPMENT

1. Individual monitoring

- 1.1. Quo Vadis in radiological protection? *H.W. Julius* 2
- 1.2. Ten years of performance monitoring of the TNO-individual monitoring service. *J.W.E. van Dijk* 5
- 1.3. Effective dose per unit fluence calculated for adults and a 7-year old girl in broad antero-posterior beams of monoenergetic electrons of 0.1 to 10 MeV. *F.W. Schultz and J. Zoetelief* 7

2. Medical applications

- 2.1. Patient dose due to colon examinations: dose assessment and results from a survey in The Netherlands. *J. Geleijns, J.G. van Unnik, J.J. Broerse, M.P. Chandie Shaw, F.W. Schultz, W. Teeuwisse and J. Zoetelief* 11
- 2.2. Assessment of lifetime gained as a result of mammographic breast cancer screening using a computer model. *J.Th.M. Jansen and J. Zoetelief* 12
- 2.3. Determination of average glandular dose with modern mammography units for two large groups of patients. *R. Klein, H. Aichinger, J. Dierker, J.Th.M. Jansen, S. Joite-Barfuss, M. Säbel, R. Schulz-Wendtland and J. Zoetelief* 16
- 2.4. Survey of CT techniques and absorbed dose in various Dutch hospitals. *J.G. van Unnik, J.J. Broerse, J. Geleijns, J.Th.M. Jansen, J. Zoetelief and D. Zweers* 19
- 2.5. Guidelines for quality control of equipment used in diagnostic radiology in The Netherlands. *L. van den Berg* 20
- 2.6. Calculation of effective dose for irradiation of Graves' ophthalmopathy. *J.J. Broerse, J.T.M. Jansen, C. Klein, M.H. Seegenschmiedt, A. Snijders-Keilholz and J. Zoetelief* 22

3. Environmental protection

- 3.1. Efficacy of air treatment devices in controlling indoor radon decay products. *P. de Jong and W. van Dijk* 27
- 3.2. The efficacy of the composition and production process of concrete on the ^{222}Rn exhalation rate. *P. de Jong and W. van Dijk* 27
- 3.3. The effective dose of radon in The Netherlands. *H.B. Kal* 30
- 3.4. The epidemiology of the association between domestic radon concentrations and lung cancer mortality: an ever ending story? *P.A.J. Bentvelzen, A. van Rotterdam and R.W. Bartstra* 31
- 3.5. Health effects on rats exposed to radon in utero. *H.B. Kal, H.H. Goedoen, J.W. Noomen and R.W. Bartstra* 32

4. Radiation dosimetry research

- 4.1. Calculated energy response correction factors for thermoluminescent dosimeters (TLD) employed in the seventh EULEP dosimetry intercomparison. *J. Zoetelief and J.Th.M. Jansen* 35
- 4.2. Recent EULEP dosimetry intercomparisons for whole body irradiation of mice. *J. Zoetelief, J.J. Broerse, F.A.I. Busscher, W.P. Hiestand, H.W. Julius and J.Th.M. Jansen* 39
- 4.3. Relative neutron sensitivity of tissue-equivalent ionisation chambers in an epithermal neutron beam for boron neutron capture therapy. *J.Th.M. Jansen, C.P.J. Raaijmakers, B.J. Mijnheer and J. Zoetelief* 41
- 4.4. Compartmental models for internal dosimetry. *F.W. Schultz and A. van Rotterdam* 44

5. Biological consequences of exposure to radiation

- 5.1. Induction of mammary tumours in rats by single dose gamma irradiation at different ages. *R.W. Bartstra, P.A.J. Bentvelzen, J. Zoetelief, A.H. Mulder, J.J. Broerse and D.W. van Bekkum* 49
- 5.2. Introduction of a molecular tumour marker in rat lung tumour cells for detection of minimal tumour load. *P.J.M. Meijnders and H.B. Kal* 52
- 5.3. Sensitivity of low tumour load in rats for high dose chemotherapy with bone marrow rescue. *P.J.N. Meijnders and H.B. Kal* 52
- 5.4. Thermosensitivity of experimental rat lung tumours. *P.J.N. Meijnders and H.B. Kal* 54
- 5.5. Long-term deterministic effects of high-dose total-body irradiation on the heart of rhesus monkeys; are changes in circulating atrial natriuretic peptide relevant? *J. Wondergem, C.C.M. Persons, M. Fröhlich, C. Zurcher and J.J. Broerse* 56

II. SERVICES

1.	Thermoluminescence dosimetry. <i>J.W.E. van Dijk</i>	62
2.	Radioactivity analyses. <i>P. de Jong and W. van Dijk</i>	62
3.	Quality assurance in diagnostic radiology. <i>L. van den Berg and J. Moor</i>	63
4.	Radiation safety at the workplace. <i>L. van den Berg and J. Moor</i>	63
5.	Calibration of instruments. <i>L. van den Berg and J. Moor</i>	64
6.	Monte Carlo computer codes. <i>F.W. Schultz</i>	64
7.	Patient dosimetry and assessment of image quality in medical diagnostic radiology. <i>J. Zoetelief, J.T.M. Jansen and F.W. Schultz</i>	65

III. LIST OF PUBLICATIONS AND REPORTS

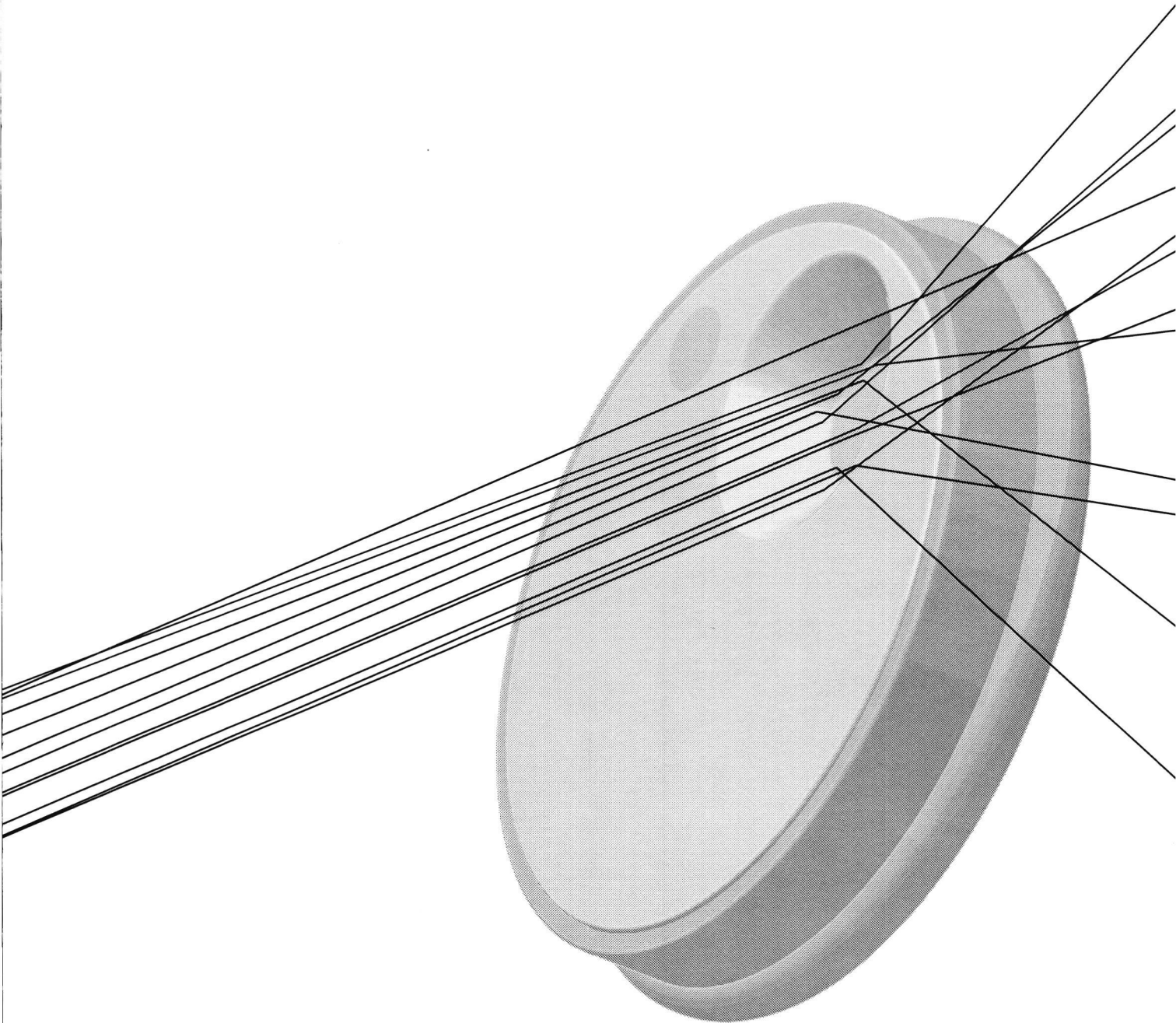
69



I. Research and Development

II. Services

III. Publications and Reports





1. Individual monitoring

Core business of the TNO Centre for Radiological Protection and Dosimetry (TNO-CSD) is the individual monitoring of radiation workers. Approximately 85 per cent of the radiation workers in The Netherlands is covered by the TNO Individual Monitoring Service. In addition, TNO-CSD runs the National Dose Registration and Information System (NDRIS), containing the occupational dose data of all radiation workers in The Netherlands. In the following contributions Quo Vadis in radiological protection is described (1.1), ten years of performance monitoring of the individual monitoring service (1.2) and interesting results obtained with Monte Carlo calculations of the effective dose for adults and a child, are presented.



1.1. Quo vadis in radiological protection?

H.W. Julius

Introduction

Since about a century the scientific community is familiar with the phenomenon of ionising radiation. To mention only a few names: Wilhelm Conrad Röntgen (Nobel prize 1901), Henri Becquerel (Nobel prize 1903), Marie Curie-Slodowska (Nobel prize 1903 and 1911). Already in the early days, practical applications of radiation developed, the first and most important being diagnostic radiology, using Röntgen's X rays. But also the biological effects of ionising radiation, both beneficial and harmful, became apparent soon. Indeed, ionising radiation was in more than one sense a very exciting new tool.

Although scientists were well alert of the adverse effects of ionising radiation the public at large, however, was completely unaware of the problems. And this remained the case until, in 1945, the alarm bell set off as atomic bombs exploded over Hiroshima and Nagasaki. These events still today have a significant impact on the public opinion regarding radiation in general and nuclear processes in particular. The negative attitude of 'the man in the street', although based on insufficient knowledge, greatly stimulated scientific research and sharpening of the regulations - all over the world. As far as science is concerned two main streams developed:

- radiobiology, focusing on the effects of ionising radiation by analysing phenomenological data to quantify the dose-effect relationship and
- applied radiological protection (often referred to as 'health physics'), focusing on the quantitative measurement of radioactivity, radiation fields and radiation doses received by individuals.

Mainly having been involved in the second stream I would like to say a little more about where we are today and where we will be tomorrow. Applied Radiological Protection roughly covers three main fields of interest in which scientific research and services are combined.

Occupational radiation hygiene

TNO's activities in this field have been for a great deal in Individual Monitoring. When I joined TNO, more than 30 years ago, photographic film dosimetry - then 40 years old already - was still the standard technique used for personal dosimetry. But a new technique, Thermo-luminescence Dosimetry (TLD) had already attracted the attention of dosimetrists. TNO jumped into it by doing scientific research and technical development and - much later than was anticipated originally - introduced TLD in routine operation in the early eighties. The very last film dosimeter was issued in 1987, 11 years ago.

In our rapidly changing world the question may arise: Is TLD getting old and obsolete? To answer the question, let us see what is going on elsewhere in the world. In the United States more than 50 per cent of the dosimetry for workers is still based on photographic film. Similar situations exist in countries such as the UK, France and Germany. Some European countries are even still in the process of considering switching from film to TLD. It is beyond doubt that promising new techniques - such as Electronic Personal Dosimetry (EPD), Direct Ion Storage (DIS) and Optically Stimulated Luminescence (OSL) - will, on the long run, replace TLD. But I anticipate that many more tons of cadmium will still be dumped into the River Rhine before this will be the case.

Since 1989 TNO operates the Dutch National Dose Registration and Information System (NDRIS), which contains all occupational radiation doses in The Netherlands. Other countries now have similar facilities. I expect the time will come soon that these systems will be connected and become part of a European network. This will greatly improve the protection of workers travelling between countries.

Medical application of ionising radiation

Diagnostic radiology and nuclear medicine are responsible for, roughly speaking, 90 per cent of the radiation dose to the population caused by non-natural sources. This is a field, which requires the interest and assistance of the radiological protectionist and dosimetrist. The challenges for the future are twofold: Firstly, more sophisticated technological means need to be developed to find better ways to assess the radiation dose to the patient under practical conditions in such a way that experimental results from various investigators are comparable. Secondly, better ways are to be found to quantify the quality of diagnostic images on the basis of which medical diagnoses are made. Both are necessary to provide a better balance between the quality of the diagnostic information and radiation risks for the patient.

Radiation fields and radioactivity in the environment.

In The Netherlands, like in all Western countries, the pollution of the environment is a hot political issue. The main pollutants attracting attention these days are CO₂ and NO_x (the main greenhouse gasses), noise and toxic substances that pollute our soil. As far as radiation and radioactivity in the environment are concerned, the media are relatively silent these days. But the problems are there:

Radon and radon daughters in the in-house environment and the related radioactivity of building materials, radioactive waste from non-nuclear industries, dose limits at the boundary of sites where radiation sources are installed, etc. The Dutch Ministry of Housing, Physical Planning and Environment is in a continuous process of developing, discussing and revising regulations. Sure enough, not an easy task! Not only difficult because of lack of scientific evidence for the risks of low levels of radiation, but also because the proposed dose limits tend to be of the same order of magnitude as the variations in the natural background.

It is in this context that I -although not a radiobiologist- cannot resist briefly touching stochastic effects of ionising radiation, because these provide the basis of risk assessments and hence of the radiological protection regulations. At high and medium dose levels the effects are relatively well known. However, as soon as it comes to low and very low dose levels, hard scientific data are scarce or missing entirely. We are left with no other option than extrapolation. How to extrapolate is still subject of discussion. The linear-non-threshold extrapolation hypothesis is generally used to estimate the radiation risk at low and very low doses because it is the most conservative way to go.

Hardly anybody will argue that this approach is not suitable for setting dose limits for the professional worker. Modern safe guards make it easy to comply. The situation is different, however, when it comes to setting dose limits for the population at large. The combination of conventional risk concepts and the linear-non-threshold concept has significant implications, both for the need to construct heavy and expensive shielding of radiation sources (including those in hospitals) and for setting acceptable concentration levels of radioactivity in the outdoor environment and in building materials and the related concentration of radon and radon daughters in the indoor environment.

In view of the above, it seems justified to, instead of cutting down budgets, stimulate radiobiological research and strengthen the basis for radiation risk assessments and hence for future regulations. Our environment as well as our society deserve to be treated in a fair way.

Quo vadis in radiological protection?

The profession may look forward to many interesting challenges. But it should certainly also anticipate some significant problems. During the seventies and eighties Radiation Protection was in excellent shape, for two reasons:

First of all: There were lots of problems. Think of the increasing interest in the protection of the patient in diagnostic radiology and nuclear medicine, the growing emphasis on environmental aspects and the problems related with the expansion of nuclear energy and the associated

waste problems.

Secondly: Plenty of money was available to be spent for solving -or at least aiming at solving- these problems.

The present situation, however, is quite different. Most of the problems seem to have been solved and some people argue that The Netherlands is a non-problem country! I am not sure this is true, but indeed: Radiation protection in hospitals has been improved significantly and implementing further improvements is considered a matter of routine, radioactivity in the environment is not the hot issue anymore as it used to be and nuclear energy production is not very popular and therefore is almost banned in this country (a rather misleading and hypocrite political decision, taking into account that we freely import electricity generated by nuclear power at a stone's throw distance).

The budgets available for scientific research and development are shrinking every year. This is not typical for our profession, it happens in many other fields as well. It is neither typical for The Netherlands, similar trends develop in many other countries, even on both sides of the Atlantic. The generally adopted philosophy is: Scientific research should pay off, literally. Meaning: Science and its products should be paid for by the customer and hence needs to be marketed and sold. This is exactly what the Universities are doing these days. Unfortunately, research in radiation protection and dosimetry clearly does not generate products that can easily be sold, simply because the need for them is based on legal requirements and nobody is eager to spend the extra money. Society will, however, suffer for it when it comes to another Chernobyl-like disaster, which may happen every day, taking into account the technical state of nuclear power plants in countries not too far from here.

The changing society and the subsequent weakening position of Radiological Protection requires changing the structure of the profession. It is my strong believe that, in our country, we badly need a 'Centre of Excellence' where scientific research and public services are combined and which, at the same time, serves as an advisory body for the government and society as a whole.

Actually, many, if not most, countries operate a 'National Institute for Radiological Protection'. Well known is the National Radiological Protection Board, in the UK. But also Germany, France, Sweden, Ireland and other countries, including the young Czech Republic, have such National Institutes. These Institutes play a vital role in the communication with the public, in the communication between nations and in the relation with the European Union. The latter is of particular importance as far as acquiring research contracts is concerned. Our country deserves the creation of a National Institute for Radiological Protection.

1.2. Ten years of performance monitoring of the TNO-Individual Monitoring Service

J.W.E. van Dijk

Introduction

The Quality Assurance (QA) programme of an approved dosimetry service, aims at attaining and sustaining a level of performance that meets the expectations of both the customer and the authorities. This includes the level of dosimetric performance, the level of service to the customers (i.e., giving adequate advice and effective handling of complains) and the level of operational efficiency, administrative accuracy and commercial performance (1,2). The Quality Assurance subscription is one of the possible ways of monitoring continuously most aspects of a dosimetry service. This QA-subscription is the subscription on the service of a dummy customer as mentioned in the EC Recommendations (2). In this paper the results of 10 years QA-subscription at the TNO Individual Monitoring Service (IMS) are presented and discussed.

TNO Individual Monitoring Service

The TNO Individual Monitoring Service (IMS) is a, by the Ministry of Social Affairs and Employment, approved dosimetry service (ADS), monitoring about 27,000 radiological workers. An in-house developed TLD system that consists of a pool of about 58,000 two- or three-element dosimeters and three automatic reader systems is used. The dosimeters contain $\text{LiF}_{\text{Ti,Mg}}$ (TLD100) detectors behind a 340 mg/cm^2 plastic filter for the measurement of $H_p(0.07)$ and TLD100 detectors behind 2 mm aluminium for the measurement of $H_p(10)$. For the measurement of beta doses, the dosimeters contain additionally either a 20 mg.cm^2 $^7\text{LiF}_{\text{Ti,Mg}}$ (TLD720) detector or a carbon loaded $\text{LiF}_{\text{Ti,Mg}}$ detector (3).

The detectors in the dosimeters are calibrated individually; re-calibration is done after being issued 15 times (on average once every one or two years). The TLD reader systems are calibrated daily. ^{60}Co sources, of which the dose rates are traceable to the primary standard, are used for the irradiations.

QA-subscription

In order to continuously monitor the quality of the TNO Individual Monitoring Service, a Quality Assessment Subscription was started 10 years ago, in October 1987 (5). The QA-subscription is the subscription to our services of a dummy customer. There is a biweekly subscription of 10 dosimeters and a four-weekly and a quarterly subscription of 6 dosimeters.

Together with and indistinguishable from the dosimeters for the normal customers, every issuing period a number of randomly chosen dosimeters is sent by regular mail to the private address of a member of the staff. Two dosimeters are

placed in a lead pig and two are placed in the MS processing area. In our calibration irradiation facility, two dosimeters are irradiated to 2.00 mSv using ^{60}Co sources. The remaining four biweekly issued dosimeters are, in duplicate, irradiated to 0.20 and 12.00 mSv. At the end of the issuing period the dosimeters are taken back home again and returned to the laboratory by regularly mail.

Evaluation of the dosimeters and reporting of the results is done together with and indistinguishable from the bulk of the returned dosimeters. Copies of the reports are sent to the responsible staff members as are all other documents that are sent to the normal customers, including annual reports and invoices.

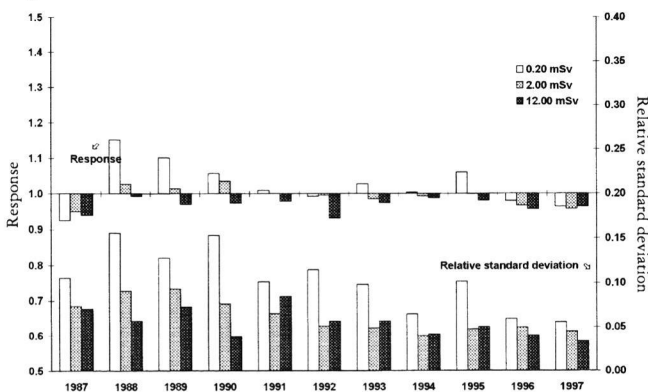
Checking the dosimeters and documents received and analysing the dosimetric data, results in the overall monitoring of the service as suggested in the EC Technical Recommendations that were referred to in the introduction.

Results

Statistical analysis of the results of the QA-subscriptions gives both the accuracy (how far does the result deviate from the true value) and the precision (what are the confidence limits of the dose reported) of the dosimetry system under routine conditions.

Figure 1 shows for each of the 10 years the relative response

Figure 1.



($H_p(10)_{\text{measured}}/H_p(10)_{\text{true}}$) and the variation coefficient (relative standard deviation) for the irradiated dosimeters of the biweekly QA-subscription.

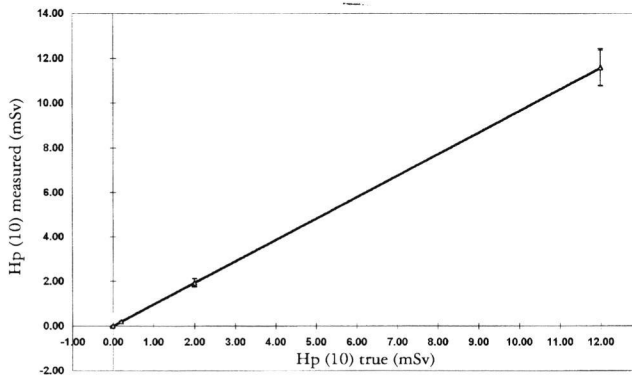
At the bottom of the graph, the bars represent the variation coefficient (right value-axis) calculated using all measurements of one year (in general 52). Starting in the earlier years with a coefficient of variation of about 10 per

cent the performance in terms of precision has improved to about 5 per cent in recent years.

At half height of the figure the bars represent the deviation from unity for the relative response. Although the deviations in the earlier years are larger there seems to be a tendency for slightly (about 3 per cent) underestimating the dose.

Figure 2 shows for 1997 the results for both the stored and

Figure 2.

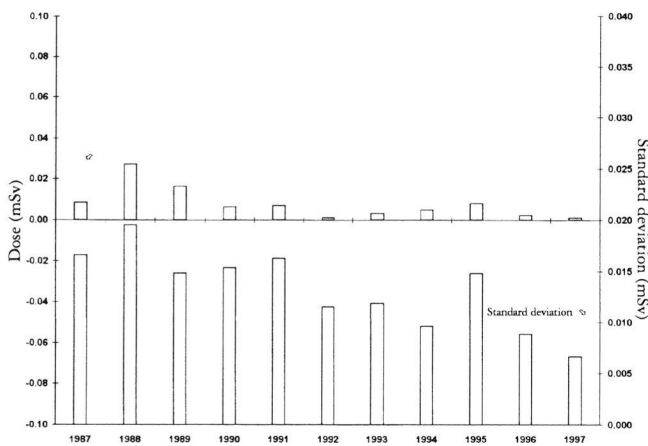


the irradiated dosimeters. At the bottom axis the conventionally true value for the dose is given and on the left value-axis the measured dose.

The solid line is the calculated regression function and the vertical bars represent the standard deviation. The correlation is virtually perfect but the slope indicates an under response of 3.4 per cent.

Figure 3 shows the results of the QA-subscription of the

Figure 3.



dosimeters that are kept in the mail processing area of our service.

At the bottom of the graph, the bars represent the standard deviation (right value-axis) calculated using all

measurements of one year (in general 52). Starting in the earlier years with a standard deviation of about 0.017 mSv it has improved to less than 0.01 mSv in recent years.

At half height of the figure the bars represent the deviation of the measured dose from zero. Although the deviations in the earlier years are occasionally larger, the average is in most years much less than 0.01 mSv.

For assessing the performance of the dosimetry system at low dose levels, in addition to the data obtained with the QA-subscription, frequency analysis on the results of all issued dosimeters gives very useful information. This analysis, for which all 400,000 measurements, which are done in a year, are used, shows that the standard deviation in an occupational dose of 0.00 mSv is 0.011 mSv for a monitoring period of two weeks. Part of this standard deviation is due to variations in the contribution of the natural background. If these variations are eliminated the standard deviation in a single dose measurement under routine conditions is about 0.006 mSv.

Discussion

The logistics of dosimeter distribution is such that from the entire pool of available dosimeters a dosimeter is randomly chosen and assigned to a worker. This strategy not only has great advantages from the logistics point of views over the system in which each worker has been assigned a fixed set of two or three dosimeters, but also from the dosimetric point of view. This strategy ensures that random and systematic errors in the dosimeter calibration are averaged out over the entire population of monitored workers resulting in a lower error in the total annual dose for each individual worker.

Because the QA-subscription dosimeters are issued in the same routine as those for the normal customers, the same statistical argument applies for these dosimeters. Thus the precision and accuracy found with the QA-subscription is representative for the precision and accuracy of the doses reported to the normal customers.

In many situations, the provisions made for the safe operation of radiation emitting equipment and the handling of radioactive materials is such that it is virtually impossible to commit doses that approach the legal limits. Thus, in many practical situations the dose measured by an approved dosimetry service are not primarily of importance to verify compliance with regulations but to verify the compliance with, often very strict, ALARA goals. This means that many customers expect a good performance of the dosimetric system at dose levels approaching those of the natural background.

It should be stressed however, that, doses higher than the natural background level, the results of the QA-subscription are only valid for one radiation quality (^{60}Co) and normal

incidence. As discussed elsewhere (4), the random errors determined with the QA-subscription must be added to the (randomised) systematic errors due to energy and angular dependence which can be determined from type-tests results (3). Taking this into account, we find the following performance parameters for 1997:

- 0.006 mSv: Standard deviation in very low doses excluding variations in the natural background;
- 0.01 mSv: Standard deviation in very low doses.
- 0.03 mSv: Detection limit (4).
- 4 per cent: Variation coefficient, excluding systematic errors.
- 16 per cent: Variation coefficient, including systematic errors (4).

The art of using the QA-subscription for improving the level of performance of the service is to look at least as critical at the dose reports and the other documents send as a critical customer might do. The study of the statistical results, together with the possibility to do simulation experiments on the raw data that are stored on tape, helped to improve the dosimetric performance. On several occasions staff

discussions on the QA-subscription, combined with comments from customers have resulted in improvements in user friendliness of our services. O

1. JC Dutt and L Lindborg.

Quality control and quality assurance in individual monitoring of ionizing radiations. *Radiat Prot Dosim* 54, 337-342, 1994.

2. Commission of the European Communities, 1994.

Technical recommendations for monitoring individuals occupationally exposed to external radiation. CEC EUR 5287, Chapter 9.

3. HW Julius, TO Marshall, P Christensen and JWE van Dijk.

Type testing of personal dosimeters for photon energy and angular response. *Radiat Prot Dosim* 54, 373-377, 1994.

4. JWE van Dijk and HW Julius.

Dose thresholds and quality assessment by statistical analysis of routine individual monitoring TLD data. *Radiat Prot Dosim* 66, 17-22, 1996.

5. JWE van Dijk.

Quality assurance in individual monitoring: 10 years of performance monitoring of the TLD based TNO Individual Monitoring Service. *Radiat Prot Dosim* 77, 235-244, 1998.

1.3. Effective dose per unit fluence calculated for adults and a 7-year old girl in broad antero-posterior beams of monoenergetic electrons of 0.1 to 10 MeV

F.W. Schultz and J. Zoetelief

The International Commission on Radiological Protection (ICRP) has recommended the use of effective dose (E) as the radiological protection quantity to assess radiation risk (1). The derivation of E requires knowledge of organ doses that in general cannot be directly measured. It therefore is common practice to measure operational quantities instead of effective dose that the International Commission on Radiation Measurements and Units (ICRU) has defined for external radiation. They are ambient, directional and personal dose equivalents ($H^*(d)$, $H'(d)$, $H_p(d)$), and are based on dose absorbed at some depth (d) in a spherical or slab phantom (2, 3). These quantities are assumed to yield a good estimate of E, but this assumption has not yet been properly verified in the case of external radiation with electrons of low energy (<10 MeV). Information on organ

doses due to external low-energy electron radiation is sparse, but in principle can be generated by means of Monte Carlo (MC) simulation of radiation transport. A condition is the availability of (complex) mathematical anthropomorphic phantoms. Rather than absolute values, MC simulation will yield organ doses normalised to a radiation field quantity, like particle fluence.

Each of three anthropomorphic phantoms were placed in broad unidirectional (antero-posterior, AP) beams of monoenergetic electrons (electron energies from 0.1 to 10 MeV) travelling through empty space. This is a worst case for radiological protection because in AP direction the more radiosensitive organs are exposed most. Furthermore, there is no attenuation due to air and no dose reduction by wearing protective clothing. The phantoms are based on descriptions

by the German GSF-Forschungszentrum für Umwelt und Gesundheit and contain all organs that are important with respect to radiological protection. They represent the reference adult male (70 kg, length 1.70 m) and female (60 kg, 1.60 m), and a seven years old girl (24 kg, 1.15 m). Using the general purpose MC simulation code MCNP, version 4.2, developed at the Los Alamos National Laboratory, USA, organ doses per unit fluency were calculated. It was taken into account that cells in the top layer of the skin (70 μm) are insensitive to radiation. The fact that dose absorbed here does not contribute to E appeared to be significant when electron energy falls below 0.4 MeV. E was calculated according to ICRP Report 60 (1). Tissue weighting factors were not re-normalised, i.e., their sum equals 1, 0.95 and 1.05 for the average adult, the male and the female phantoms, respectively.

Plotting doses per unit fluency as a function of electron energy on logarithmic scales, three types of qualitative behaviour can roughly be distinguished, i.e., for surface, peripheral and deep organs, respectively. For skin, the dose per unit fluency initially is relatively high ($1\text{-}2 \times 10^{-11} \text{ Gy.cm}^2$) and increases slowly with increasing electron energy to arrive at a more or less steady level ($2\text{-}4 \times 10^{-10} \text{ Gy.cm}^2$) when electron energy exceeds about 1 MeV. Similar

magnitude lower.

Differences in corresponding organ doses in different phantoms cannot be generalised, although most often they are greater for child compared to adult than for adults compared mutually. This is attributable to phantom size. Possible influence of tissue compositions being different in child or adult has not been investigated. Dose ratios with respect to the average adult (Table 1) are often negligible (close to one), sometimes considerable but insignificant, rarely considerable and significant. Dose ratios above 10 occur but are rare.

For the various phantoms E as a function of electron energy is shown in Fig. 1. Organs with low doses, which, especially for deeper organs and lower electron energies, often have larger (statistical) uncertainties, usually do not contribute much to E. Therefore, the uncertainty in E remains very acceptable (at most 6% for adults, 18% for the child). Below electron energy of 0.6 MeV, skin is the main contributor to E. Phantom dependence of E for adult cases is pronounced at electron energies above 3 MeV due to different organ contributions in males and females, and at 1 MeV because of the large contribution of breasts in the female only. In general, E calculated for the average adult does not deviate too seriously from the separate curves for male and female

Table 1. Dose ratios, phantom/average adult: median value and (range) over all energies for a surface organ, two peripheral organs and a deep organ, and for effective dose.

Organ	ADAM		Phantom EVA		CHILD	
	Median	(Range)	Median	(Range)	Median	(Range)
Skin	0.98	(0.92-1.02)	1.02	(0.98-1.03)	1.00	(0.97-1.04)
Breasts	1.00				1.60	(0.10-306)
Liver	1.13	(0.34-1.90)	0.87	(0.10-1.66)	1.29	(0.51-92.6)
Pancreas	1.06	(0.37-2.00)	0.92	(0.36-1.63)	0.75	(0.49-5.39)
E	1.02	(0.81-1.25)	0.98	(0.75-1.19)	1.29	(0.98-22.6)

behaviour is seen for the other surface organs (eye lenses). Peripheral organs like testes and breasts, but also thymus, liver and bone marrow, start from much lower values (about $5 \times 10^{-16} \text{ Gy.cm}^2$) and end at levels between 5×10^{-11} to $3 \times 10^{-10} \text{ Gy.cm}^2$ for 10 MeV. The sigmoid curves show a transition point near 0.8 MeV, $3 \times 10^{-13} \text{ Gy.cm}^2$. Dose per unit fluency in deep organs, like lungs, stomach or kidneys, stays much longer (up to 2-3 MeV electron energy) at the low initial level (about $5 \times 10^{-16} \text{ Gy.cm}^2$). Then it increases rather steeply to values similar to the ones for peripheral organs at 10 MeV. Only for deep organs near the centre of the body, e.g., oesophagus or ovaries, does the dose for 10 MeV electron energy remain about two orders of

adults (less than 25% over- or underestimation). However, above 0.4 MeV electron energy the average adult curve underestimates E for the child significantly. The underestimation is largest in the energy range of 1.5-3 MeV, up to a factor of 23 (due to the large contribution of the girl's breast tissue), which is unacceptable for radiological protection purposes. For energies over 3 MeV the underestimation is smaller again (a factor of 1.8 or less). Comparing E with literature data on operational quantities determined for weakly penetrating radiation (4, 5, 6), it appears that in the considered energy range the directional ($H'(0.07)$) and personal ($H_p(0.07)$) dose equivalents overestimate the radiation risk from ten- to a thousand-fold.

The dose equivalents themselves are in agreement, whether obtained for the ICRU sphere or a slab of water. As estimators of radiation risk they are, however, unnecessarily safe for external electron beams of low energy.

1. ICRP (1991)

1990 Recommendations of the International Commission on Radiological Protection. ICRP Report 60. Pergamon Press.

2. ICRU (1985)

Determination of dose equivalents from external radiation sources. ICRU Report 39. Bethesda MD, International Commission on Radiation Units and Measurements.

3. ICRU (1988)

Determination of dose equivalents from external radiation sources, Part 2. ICRU Report 43. Bethesda MD, International Commission on Radiation Units and Measurements.

4. WG Cross, PY Wong and NO Freedman.

Dose distributions for electrons and beta rays incident normally on water. Radiat Prot Dosim 35,77-91, 1991.

5. A Ferrari and M Pelliccioni.

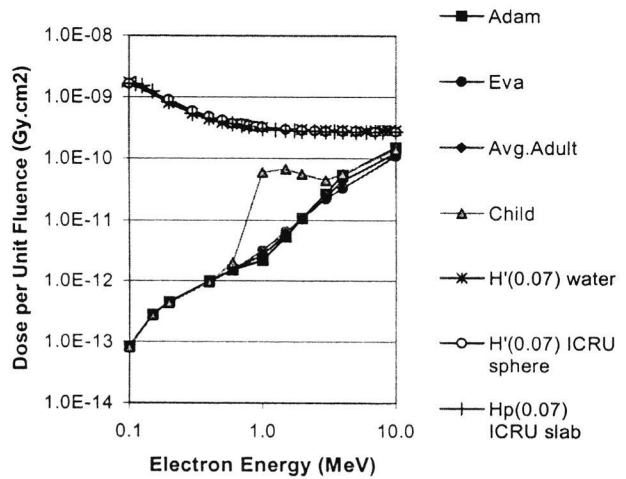
Dose equivalents for mono-energetic electrons incident on the ICRU sphere. Radiat Prot Dosim 55, 207-210, 1994.

6. JL Chartier, B Grosswendt, GF Gualdrini, H Hirayama, CM Ma, F Padoani, N Petoussi, SM Seltzer and M Terrissol.

Reference fluence-to-dose-equivalent conversion coefficients and angular dependence factors for 4-element ICRU tissue, water and PMMA slab phantoms irradiated by broad electron beams. Radiat Prot Dosim 63, 7-14, 1996.

Figure 1.

Effective Dose & Operational Quantities



2. Medical applications

Medical applications of ionising radiation are causing by far the largest radiation burden to the population due to man-made sources. Among the medical applications, diagnostic radiology is contributing by about 16.5 per cent and nuclear medicine by about 1.4 per cent to the average annual radiation exposure per caput of the Dutch population, which amounts about 2.7 mSv.

The general radiation protection principle of the International Commission on Radiological Protection (ICRP) postulates that all exposures 'should be kept as low as reasonably achievable'. In the case of medical applications, this implies that each procedure (treatment or diagnosis) is justified and optimised. For diagnostic radiology and nuclear medicine imaging optimisation means that the radiation dose to the patients should be kept as low as possible, but still providing images compatible with the clinical requirements.

The majority of the studies carried out within TNO-CSD on medical applications of ionising radiation concerns diagnostic radiology. The contributions to this chapter concern methods for assessment of (effective) doses in the patient due to diagnostic radiology (2.1 to 2.4); assessment of lifetime gained as a result of mammographic breast cancer screening (2.5) and a description of guidelines for quality control of equipment used in diagnostic radiology (2.6).

2.1. Patient dose due to colon examinations: dose assessment and results from a survey in The Netherlands

J. Geleijns¹, J.G. van Unnik², J.J. Broerse, M.P. Chandie Shaw¹,
F.W. Schultz, W. Teeuwisse¹ and J. Zoetelief

This study aimed at deriving effective dose (E) to the patient due to colon examinations. Special attention was paid to the relation between patient dose and the application of screen-film radiography and digital imaging. Patient dose incurred due to a biphasic colon examination was compared to patient dose from double contrast studies.

The integral dose-area product (DAP) was measured at 10 X-ray units in 9 hospitals during colon examinations of 1733 patients, aged 18 years or older. Effective dose was estimated from DAP through computer simulations of radiation transport in anthropomorphic phantoms. DAP to effective dose conversion factors of 0.29 mSv/Gy.cm² and 0.27 mSv/Gy.cm² were derived for the biphasic and the double contrast study, respectively. Average DAP for the biphasic colon examination was 21 Gy.cm² from which 13 Gy.cm² should be attributed to the double contrast views. The survey yielded an average DAP value of 29 Gy.cm² (range 18 to 53 Gy.cm²) and an average effective dose of 4.7 mSv (range 2.7 to 8.4 mSv, table 1).

The average DAPs that are derived from this study are within the range of values that are reported by other authors (table 2). The reference level that is recommended for the United Kingdom in a protocol of the Institute of Physical Sciences in Medicine (1) should be considered as a national investigation level. Evaluation of the Dutch data showed that it is not realistic to apply the IPSM reference level also to the Dutch situation since this level seems to be rather high. For the Dutch situation a more restrictive value of for example 40 Gy.cm² could probably be applied. Patient dose incurred during the biphasic colon examination was surprisingly low due to careful selection of the radiological technique. It is recommended to apply additional filtration of at least 0.1 mm copper and to use a screen-film combination with a speed class of at least 400. Dose reduction when using digital techniques is often not realised in clinical practice.

¹Department of Radiology of the Leiden University Medical Center and the

²Department of Radiology of the Onze Lieve Vrouwe Gasthuis, Amsterdam.

Table 1. Average effective dose (mSv) incurred during colon studies at nine Dutch hospitals.

	All Hospitals	A-conv	A-dig	B	C	D	E	F	G	H	I
Average dose	4.7	5.5	4.9	2.7	6.5	3.8	8.4	5.0	3.3	4.2	4.9
Standard dev.	2.4	2.9	3.1	1.2	3.9	2.1	3.5	2.7	1.2	1.7	2.7
Median	4.1	5.0	4.0	2.6	5.2	3.2	7.7	4.4	3.4	3.8	4.3
Min. dose	0.3	0.5	0.7	0.3	2.5	1.2	3.1	0.4	1.1	1.7	0.8
Max. dose	25.3	25.3	22.3	6.7	20.6	12.7	22.9	13.7	7.0	9.3	17.4
No of patients	1733	497	456	128	31	131	80	137	81	69	123

Table 2. Comparison of average DAP, range of DAP values and reference DAP.

Author	DAP, (Gy.cm ²)	No of colon examinations
Dose surveys		
Martin and Hunter (2)	25	8-39
This study	31	18-53
Drouillard, digital (3)	32	
IPSM (1)	41	6-272
Drouillard, analogue (3)	56	
Reference value		
IPSM, reference dose	60	

1. Institute of Physical Sciences in Medicine; National Radiological Protection Board and College of Radiographers.

National protocol for patient dose measurements in diagnostic radiology. Chilton, England, 1992.

2. CJ Martin and S Hunter.

Reduction of patient doses from barium meal and barium enema examinations through changes in equipment factors. *Br J Radiol* 67, 1196-1205, 1994.

3. J Drouillard.

Evaluation of the DSI digital fluorography system. *Medica Mundi* 36, 3-13, 1991.

2.2 Assessment of lifetime gained as a result of mammographic breast cancer screening using a computer model

J.Th.M. Jansen and J. Zoetelief

A computer model for the simulation of breast cancer screening (MBS) is used to calculate the results of screening in terms of lifetime (1). To optimise breast cancer screening protocols, risk (lifetime lost due to radiation induced tumours) versus benefit (lifetime gained due to early detection and treatment of breast cancer) analyses are performed for a simulated stable Swedish female population. The present study focuses on the results of different screening strategies employing single view mammography, including starting and finishing ages of screening and time interval between successive screening sessions, based on lifetime lost or gained. To establish the stability of the recommendations with respect to possible changes in the variables used in MBS, calculations are performed for high risk factors for breast tumour induction using both the additive and multiplicative risk models.

The results of the simulation of annual screening of women of ages above 20 years for a stable Swedish population of one million women followed throughout their lives are given in Table 1. Starting at the youngest ages, the lifetime lost due to spontaneously discovered tumours per year increases rapidly with age, reaching a maximum at ages 50-54 years followed by a decrease. Lifetime gained due to early detection alone is increasing at young ages, reaches a maximum at ages 50-54 years and decreases afterwards to approach zero at high ages. The risk of screening, i.e., the lifetime lost due to induced fatal breast tumours, decreases with age to approximately zero for women older than 85 years. This zero risk is due to the latency period and the limited lifetime expectancy at high ages.

Total lifetime gained by screening is negative at young ages,

becomes positive as age increases and reaches a maximum in the age group of 50-54 years, followed by a decrease to approximately zero (Table 1). The maximum effect of annual screening occurs earlier when the results are expressed in terms of lifetime gained (50-54 years) compared with expression in terms of the number of fatal tumours (60-64 years) (2). This shift is due to the lifetime lost per fatal tumour, which is larger at younger ages. At young ages, i.e., 25-29 years, for the present screening conditions, the number of fatal breast tumours can be increased compared with the situation without screening. In terms of lifetime gained, screening can still be beneficial. This is owing to the relatively short survival time after the detection of a fatal tumour, compared with the long survival time after the induction of a fatal tumour as a result of the latency and risk periods. This especially holds true for the multiplicative risk model that predicts that induction of fatal tumours is becoming manifest at older ages, where the natural background breast tumour mortality is high. If annual screening is applied from ages 35 to 75 years, the lifetime lost due to breast cancer is calculated to be reduced by 46 per cent compared with the non-screening situation.

The results for increased risk factors for induction of fatal tumours, i.e., average values plus one standard deviation, according to Miller et al. (3), for both the additive and the presently preferred multiplicative risk model are given in Table 2. For both risk models and for ages equal to or above 35 years, the high (excess) risk factor is about six times the average (excess) risk factor. For ages below 35 years, the ratio is between a factor of three and six. For the multiplicative risk model the given ratio refers to excess risk.

The risk factors presented by Miller et al. are considered most appropriate as these data refer to women in a western country, fractionated irradiation and to a radiation quality not too far from the X-rays used in mammography. For ages above 25 years, the multiplicative risk model predicts less lifetime lost for younger women and more lifetime lost for older women, i.e., in excess of 60 years compared with the additive risk model. The largest difference between the additive and multiplicative risk models for ages above 35 years is 86 per cent, found for the age group 35-39 years. For the age group 35-39 years and employing high risk factors the lifetime gained by early detection with screening is more than 3 times the lifetime lost due to an induced fatal tumour (additive model). When applying annual screening to women aged 35-75 years, the lifetime gained is only marginally influenced by the use of high risk factors (44%) or average risk factors (46%). Assuming an average glandular dose of 4 mGy per screening session (two-view mammography), high risk factors and no improved benefit, the lifetime gained is 42 per cent. It is concluded that the influence of a doubling of the dose marginally affects the results for the age group 35-75 years. However, for the age group 35-40 years, the situation is different, as according to the additive risk model (Table 2), the benefit to risk ratio would reduce to 1.5 which leaves little margin for error.

The present calculations are performed for a standard Swedish population. It is possible to identify subgroups within this population which will have a lower benefit risk ratio. An example of such a subgroup is women with larger compressed breast thicknesses or denser breasts who will receive a higher average glandular dose and consequently will have a higher radiation risk at about the same benefit. Individual average glandular doses of three times the average glandular dose are not uncommon, due to variation among individuals (4). For this subgroup, using high risk factors and the additive risk model approximately no lifetime will be gained for ages 35-39 years.

To estimate the influence of various times between successive screening sessions on the lifetime gained by screening, calculations with semi-annual, annual, biennial and triennial screening are performed for ages from 35 to 77 years. The results of these calculations are shown in Table 3. For the youngest screened age group an increase of screening with a factor of 3 from triennial to annual more than doubles (2.4) the lifetime gained. However, for the oldest screened age group the same increase in screening only increases the lifetime gained by 17 per cent. For the same screening frequency increase, the highest relative increase in lifetime gained is for the age group 35-40 years and the highest number of years of lifetime gained is for the age group 47-52 years. This indicates that, especially for relative

young ages, a relatively high screening frequency should be chosen. For relatively high ages a lower screening frequency would only result in a marginally lower lifetime gained by screening compared with a high frequency. Lifetime lost due to breast cancer is reduced by 52, 47, 38 and 31 per cent for semi-annual, annual, biennial and triennial screening, respectively, for the age group 35-77 years compared with the situation without screening. As an example, it is assumed that a difference of less than 25 per cent in lifetime gained due to an increased screening frequency is not worthwhile the following schedule results: ages 35-40 years semi-annual, ages 40-55 years annual, ages 55-65 years biennial, ages 65-75 triennial. This schedule yields a 44 per cent reduction in lifetime lost due to breast cancer.

Although, in terms of lifetime, a theoretical benefit is shown for women in the age group 35-40 years, screening of this age group remains questionable. (1) Uncertainties in the risk factors do not exclude the possibility that the benefit to risk ratio is close to 1. (2) Subgroups might have higher risks either due to higher average glandular doses or to differences in radiation susceptibility of individuals. (3) The cost effectiveness is smaller by a factor of more than two for semi-annual screening for ages 35-40 years compared with annual screening for ages 41-46 years (4). In terms of reduction in the number of fatal tumours a starting age of 40 years seems more realistic. (5) It will be more difficult to detect in a trial lifetime gained compared with a reduction in the number of fatal tumours. Consequently, screening of the age group 35-40 years cannot (yet) be recommended. It should be demonstrated first that screening in the age group 40-50 years is effective. When this is the case, a trial for ages 35-40 years might be considered. The present calculations indicate that trials on the effectiveness of breast cancer screening at younger ages should preferably be performed in terms of lifetime gained.

1. JThM Jansen and J Zoetelief.

MBS: A model for risk benefit analysis of Breast cancer Screening. Br J Radiol 68, 141-149, 1995.

2. JThM Jansen and J Zoetelief.

Optimisation of mammographic breast cancer screening using a computer simulation model. Eur J Radiol 24, 137-144, 1997.

3. AB Miller, GR Howe, GJ Sherman et al.

Mortality from breast cancer after irradiation during fluoros-copic examinations in patients being treated for tuberculosis. N Engl J Med 321, 1285-1289, 1989.

4. H Aichinger, J Dierker, M Säbel and S Joite-Barfuss.

Image quality and dose in mammography. Electromedica 58, 61-66, 1994.

Table 1. Annual screening of a simulated stable Swedish population. Lifetime (years) lost or gained per year, if one million women are followed throughout their lives is given.

Age (year)	Lifetime lost due to spontaneous tumours (year)	Lifetime gained due to early detection (year)	Lifetime lost due to induced fatal tumours ¹ (year)	Total lifetime gained by screening ² (year)
20-24	244	87	960	-873
25-29	1322	436	301	135
30-34	4217	1652	284	1369
35-39	8271	3652	103	3549
40-44	12193	5764	90	5674
45-49	14979	8828	75	8753
50-54	16248	10457	58	10398
55-59	15806	9383	42	9342
60-64	14158	7505	27	7478
65-69	11350	5211	15	5196
70-74	8161	3096	7	3088
75-79	5140	1491	3	1489
80-84	2628	546	1	546
85-89	1012	134	0	134
90-94	242	15	0	15
95-99	18	0	0	0

¹ Lifetime lost due to radiation-induced fatal tumours according to the multiplicative risk model.

² Total lifetime gained (negative values indicate a lifetime lost) due to screening.

Table 2. Annual screening of a simulated stable Swedish population. Lifetime (years) lost or gained per year, if one million women are followed throughout their lives. For tumour induction the high risk factors (average plus one standard deviation) are used.

Age (year)	Lifetime gained due to early detection (year)	Lifetime lost due to radiation induced tumours		Lifetime gained by screening ³ (year)
		Mult. ¹ (year)	Add. ² (year)	
20-24	87	3799	2900	-3711
25-29	436	1106	1523	-670
30-34	1652	1042	1214	610
35-39	3652	629	1167	3023
40-44	5764	549	878	5215
45-49	8828	455	634	8373
50-54	10457	353	435	10103
55-59	9383	253	279	9130
60-64	7505	164	163	7340
65-69	5211	93	84	5118
70-74	3096	44	36	3052
75-79	1491	16	12	1476
80-84	546	4	3	543
85-89	134	0	0	134
90-94	15	0	0	15
95-99	0	0	0	0

¹ Lifetime lost due to radiation induced fatal tumours, multiplicative risk model.

² Lifetime lost due to radiation induced fatal tumours, additive risk model.

³ Total lifetime gained by screening, induced fatal tumours according to the multiplicative risk model.

Table 3. Semi-annual, annual, biennial and triennial screening commencing 35 years of age for a simulated stable Swedish population, employing average risk factors and an absorbed dose of 2 mGy per session. Lifetime (years) lost or gained per year, if one million women are followed throughout their lives.

Screening interval: Age (year)	Lifetime lost due to spontaneous tumours (year)	^{1/2} a (year)	Total lifetime gained due to screening, using the multiplicative risk model		
			1 a (year)	2 a (year)	3 a (year)
0-34	861	0	0	0	0
35-40	8660	5069	3966	2483	1644
41-46	13198	7300	6197	4409	3209
47-52	15742	11694	10281	8053	6069
53-58	16118	10447	9722	8259	7033
59-64	14326	8162	7691	6794	5977
65-70	11043	5199	4980	4514	4101
71-76	7215	2648	2554	2372	2191
77-99	1444	0	0	0	0

2.3 Determination of average glandular dose with modern mammography units for two large groups of patients

R. Klein¹, H. Aichinger², J. Dierker², J.Th.M. Jansen,
S. Joite-Barfuss², M. Säbel³, R. Schulz-Wendtland⁴ and J. Zoetelief

Until recently, for mammography Mo-anode Mo-filter X-ray tube assemblies were almost exclusively used. Modern mammography units provide the possibility to employ a variety of anode-filter combinations with the aim of adapting the X-ray spectrum to compressed breast thickness and composition. The present contribution provides information on the radiation exposure of two large groups of patients (one of 1678 and one of 945 women) who were mammographed with modern X-ray equipment, and on the dosimetry necessary for the evaluation.

For dosimetric purposes spectral information is essential. X-ray spectra have been determined for various anode-filter combinations from measurements with a Ge detector. Based on these spectra, conversion factors from air kerma free-in-air to average glandular dose (*g* factors) have been calculated for different anode-filter combinations, compressed breast thicknesses ranging from 2 to 9 cm and breast compositions varying from 0 to 100 per cent glandular tissue. Table 1 shows the factor *g* for a breast composition of 50 per cent adipose and 50 per cent glandular tissue for various breast thicknesses, anode-filter combinations and tube voltages. Data on *g* factors for 100 per cent adipose and 100 per cent glandular tissue as well as an interpolation formula to derive *g* factors for intermediate tissue compositions are presented elsewhere (1). Determinations of various quantities, including entrance surface air kerma (ESAK), tube output, tube loading (TL), fraction of glandular tissue (FGL) and compressed breast thickness, were made during actual mammography. The fraction of glandular tissue for actual breasts was derived from a comparison of TL (tube-current exposure-time product) at a given breast thickness to values of TL derived from phantoms of varying compositions at the same thickness (1). Average glandular dose (AGD) was determined using *g* factors corrected for tissue composition as well as *g* values for standard breast composition, i.e., 50 per cent adipose tissue and 50 per cent glandular tissue by mass. It is shown that, on average, the influence of the actual breast composition causes variations of the order of about 15 per cent.

For group 1 and group 2, the mean values of average glandular dose (using *g* factors corrected for tissue composition) were 1.59 and 2.07 mGy respectively. The number of exposures per woman was on average 3.4 and 3.6, respectively. The mean value of compressed breast thickness was 55.9 and 50.8 mm, respectively. The mean age of group 1 was 53.6 years (for group 2 the age was not recorded).

The fraction by mass of glandular tissue (FGL) decreases with increasing compressed breast thickness (Fig. 1) and age

of patient (Fig. 2) (from 75 per cent at 25 mm to 20 per cent at 80 mm, and from 65 per cent at 20 years to 30 per cent at 75 years). For a medium-sized breast, i.e. a compressed breast thickness of 55 mm, FGL is about 35 per cent, indicating that the standard mix (FGL = 50 per cent) might need some modification, particularly because of additional evidence from another investigation (2) with similar results on FGL.

¹Institut für Medizinische Physik, Universität Erlangen-Nürnberg;

²Siemens AG, Bereich Medizinische Technik, Erlangen;

³Klinik für Frauenheilkunde, Universität Erlangen-Nürnberg;

⁴Institut für Diagnostische Radiologie, Universität Erlangen-Nürnberg, Germany

1. H Klein, J Aichinger, J Dierker, JThM Jansen, S Joite-Barfuss, M Säbel, R Schulz-Wendtland and J Zoetelief.

Determination of average glandular dose with modern mammography units for two large groups of patients. *Phys Med Biol* 42, 651-671, 1997.

2. RA Geise and A Palchevsky.

Composition of mammographic phantom materials. *Radiology* 198, 347-350, 1996.

Table 1. Factor g (mGy mGy^{-1}), for conversion of air kerma free-in-air at the entrance position of the breast into average glandular dose, for a breast composition of 50 per cent adipose and 50 per cent glandular tissue by mass and various breast thicknesses, anode-filter combinations and tube voltages. The first HVL is calculated for the spectra behind a 3-mm thick PMMA compression plate. The relative standard deviation is less than 1 per cent for each conversion factor.

anode material	filter thickness (μm)	filter material	tube voltage (kVp)	first HVL (mm Al)	g for breast thickness (mm)								
					20	30	40	50	60	70	80	90	
Mo	30	Mo	25	0.35	0.407	0.284	0.213	0.168					
Mo	30	Mo	28	0.39		0.313	0.237	0.187	0.154	0.130			
Mo	30	Mo	30	0.40				0.198	0.163	0.137	0.118		
Mo	30	Mo	32	0.42					0.170	0.143	0.124	0.109	
W	60	Mo	25	0.39	0.444	0.314	0.236	0.186					
W	60	Mo	28	0.41		0.325	0.246	0.195	0.160	0.135			
W	60	Mo	30	0.42				0.206	0.170	0.144	0.124		
Mo	25	Rh	28	0.44				0.216	0.178	0.151	0.130		
Mo	25	Rh	30	0.46					0.186	0.158	0.136	0.120	
Mo	25	Rh	32	0.47					0.192	0.163	0.141	0.124	
Rh	25	Rh	28	0.45				0.229	0.190	0.161	0.140		
Rh	25	Rh	30	0.48					0.205	0.175	0.152	0.134	
Rh	25	Rh	32	0.51					0.218	0.186	0.162	0.142	
W	50	Rh	28	0.54				0.267	0.222	0.189	0.164		
W	50	Rh	30	0.56				0.278	0.232	0.198	0.172		
W	50	Rh	32	0.58					0.237	0.202	0.176	0.155	
W	50	Rh	34	0.60					0.246	0.210	0.183	0.162	

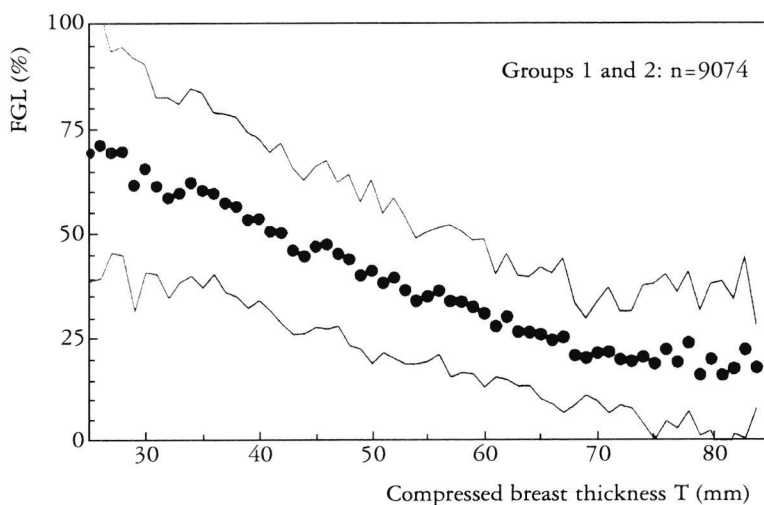


Figure 1. Mean value and standard deviation (all exposures at compressed breast thickness T) of the fraction of glandular tissue, FGL, as a function of compressed breast thickness T .

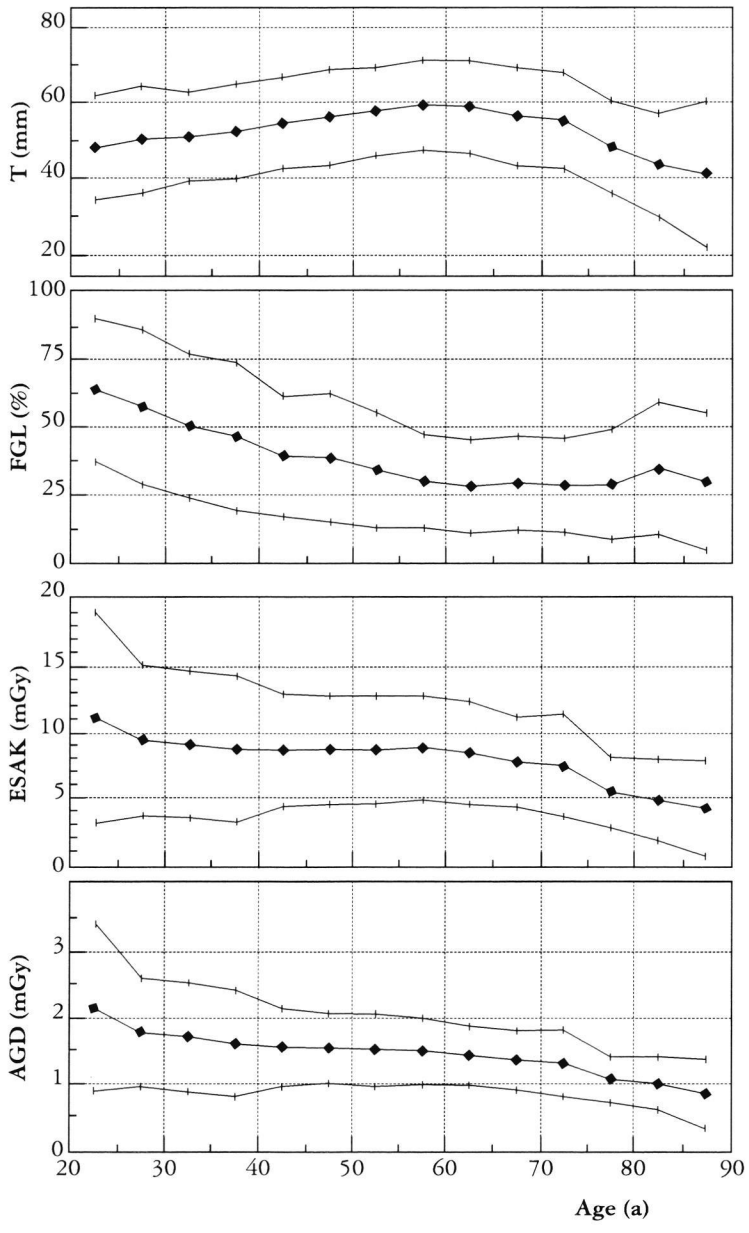


Figure 2. Compressed thickness, T, fraction by mass of glandular tissue FGL, entrance surface air kerma ESAK and average glandular dose AGD as a function of patient age (mean value and standard deviation of 5 classes) for group 1.

2.4 Survey of CT techniques and absorbed dose in various Dutch hospitals

J.G. van Unnik¹, J.J. Broerse, J. Geleijns², J.Th.M. Jansen, J. Zoetelief and D. Zweers²

Studies carried out in different countries have shown a relatively high radiation burden to the patient due to computed tomography (CT) examinations. They revealed important variations in absorbed dose (1).

The purpose of this study was to make an inventory of the radiation dose of computed tomography in The Netherlands and to relate the dose to the way the examination was performed. Details were obtained from approximately 3000 CT examinations carried out in 20 hospitals (22 CT scanners). The effective dose was calculated for each examination using CTDI-to-effective dose conversion factors. For most scanners, the conversion factors were available from the literature, for some they had to be derived with a computer model using a Monte Carlo algorithm. In the hospitals the mean effective doses from a brain CT range from 0.8 - 5 mSv, from a lumbar spine CT 2-12 mSv, from a chest CT 6-18 mSv and from an abdominal CT 6-24 mSv. Figure 1 gives the distribution of mean effective doses from abdominal CT scans. In this and other studies no clear correlation was found between effective dose and image quality. Therefore, a significant dose reduction can be obtained when e.g., the eleven hospitals with mean effective doses of 16 mSv and larger would take measures to lower the dose to 15 mSv or even lower.

The most important indications for the various CT examinations were as follows: for the brain ischemia and malignancy, for the lumbar spine disc herniation and for the chest and abdomen a known malignancy. This explain the relatively advanced age of the patients as shown for patients with abdominal CT's (Fig. 2). In many hospitals I.V. contrast is less used than recommended in current literature.

A full paper on this subject appeared under the same title in *The British Journal of Radiology* 70, 367-371, 1997. *J*

¹ Department of Radiology, Onze Lieve Vrouwe Gasthuis, Amsterdam;

² Department of Clinical Oncology, Leiden University Medical Center, Leiden.

1. PC Shrimpton, DG Jones, MC Hillier et al.

Survey of CT practice in the UK (NRPB R249) (NRPB, Chilton), 1991.

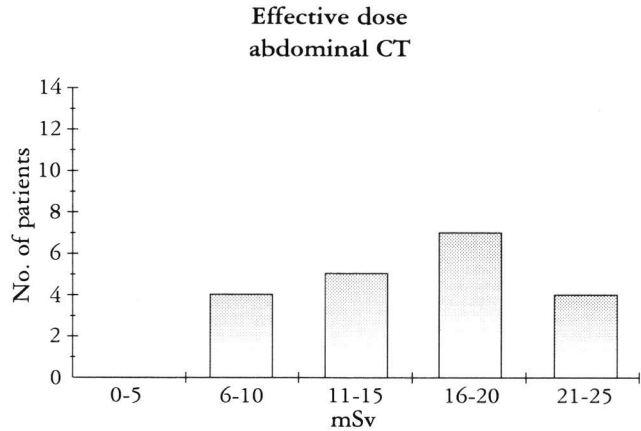


Figure 1. The frequency distribution of mean effective dose to patients from abdominal CT scans in 20 hospitals.

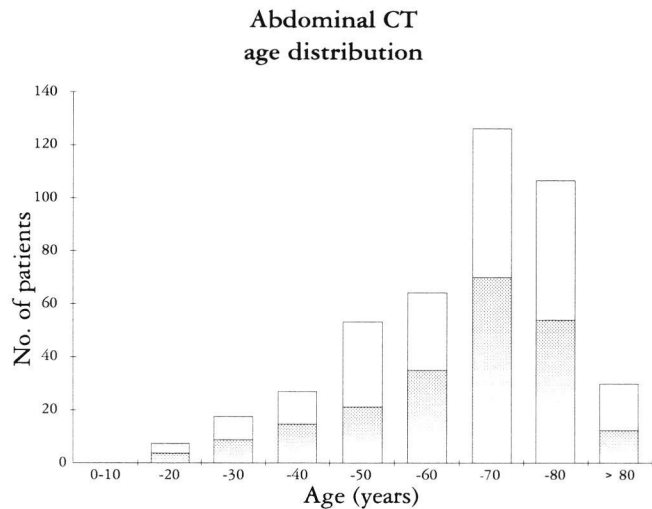


Figure 2. The age distribution of 415 patients who had abdominal CT in this survey. Open bars: females; shaded bars: males.

2.5. Guidelines for quality control of equipment used in diagnostic radiology in The Netherlands

L. van den Berg

The Council Directive 84/466/Euratom (1) regarding the radiation protection of persons undergoing medical examination or treatment (Patient Directive) has been implemented into Dutch law by an amendment (2), to the Dutch Decree on Radiation Protection (3). In an annex to this amendment, criteria for five technical parameters for equipment are included and no measurement methods are indicated or referred to.

In addition to the formal implementation of the "Patient Directive", the Dutch Ministry of Health, Welfare and Sports (VWS) invited professional societies to participate in a working group on "Quality criteria for equipment used in diagnostic radiology" with the aim to add technical criteria and to formulate guidelines for quality control (QC). Each guideline should include criteria for technical parameters and accompanying measurement methods.

Four societies participated in the working group. These are The Netherlands Society for Radiology, The Netherlands Society of Radiographers and Radiological Technologists, The Netherlands Society for Radiological Protection and The Netherlands Society for Clinical Physics. TNO Centre for Radiological Protection and Dosimetry gave scientific and secretarial support to the working group. The working group aimed at the establishment of guidelines including limiting values and measurement methods for conventional installations. Eleven technical parameters having a major impact on image quality and patient dose were selected (Table 1). Radiographers, instrumental engineers and medical physicists from 20 departments of radiology of academic and peripheral hospitals tested drafts of the guidelines. These tests resulted in suggestions for improvements that were implemented into the guidelines where appropriate.

In September 1997 the guidelines were finalised (4) and distributed among all diagnostic departments in The Netherlands.

Each guideline consists of the following chapters: 1) Scope and field of application, 2) Background information on physical and technical aspects and impact on image quality and patient dose 3) Test procedures, 4) Test frequencies, 5) Registration of measurements results and calculations, 6) Evaluation and interpretation, comparison of results with limiting values, corrective actions, trend analysis, 7) Test report with a completed registration form.

Chapter 3 includes both the principles of the test method and a step by step description of the procedures. The principles of the test procedure provide a basis for adaptation to local circumstances. The step by step test procedure allows performing quality control measurements with limited

physical knowledge of the equipment.

The final document (4) has been accepted by the professional societies in The Netherlands and the Dutch Minister of Health as a reference set of tools to perform Quality Control of equipment used for conventional diagnostic radiology.

The Minister of Health recommends that holders of radiological installations gain experience with these guidelines to be able to meet the future requirements (5). As mentioned before, the guidelines are restricted to conventional X-ray installations. For other types of radiological equipment, such as computed tomography systems, fluoroscopy and digital imaging systems, additional guidelines should be formulated.

1. European Commission.

Council Directive of 3 September 1984 (84/466/Euratom) laying down the basic measures for the radiation protection of persons undergoing medical examination or treatment, Official Journal of the European Communities No. L 265, 1984.

2. Decree of May 25 1993.

Amendment of Decree on Radiation Protection, Gazette of The Netherlands 317, 1993.

3. Decree of 10 September 1986.

Enforcement of the articles 28 up to and including 32 and the application of article 34 of the Atomic Energy Act (Decree on Radiation protection Atomic Energy Act), Gazette of The Netherlands 465, 1986.

4. Richtlijnen voor kwaliteitsbewaking van radiodiagnostiek-apparatuur,

samengesteld door de werkgroep "Kwaliteitscriteria voor radiodiagnostiekapparatuur", 1997

5. European Commission.

Council Directive 97/43/Euratom of 30 June 1997 on health protection of individuals against the dangers of ionising radiation in relation to medical exposure, and repealing Directive 84/466/Euratom, Official Journal of the European Communities No. L 180/22, 1997.

Table 1. Technical parameters influencing the performance of X-ray equipment with the accompanying limiting values and measurement methods.

Parameter	Limiting values	Measurement method or equipment
Tube voltage	5% accuracy; 2.5% precision	Electronic kVp-meter
Automatic exposure control	Optical density of the film between 1.10 OD and 1.50 OD	Exposing film at selected tube voltages and thickness' of the PMMA-phantom
Film processing	Maximal deviation fog ± 0.05 OD; speed and contrast ± 0.15 OD	Constancy test using film exposed with a sensitometer
Film screen combination	Maximal deviation of the same speed class ± 0.10 OD; no artefacts	Exposure of 4 films simultaneously to a given radiation quality, e.g. 80 kV and 25 mm Al-filter
Light tightness and illumination of the darkroom	Maximal increment 0.10 OD after 4 minutes exposure of a pre-exposed film	Film, pre-exposed with a sensitometer, kept to various dark-room conditions
Half value layer and filtration	Inherent filtration > 2.5 mm Al _{eq} . It is recommended to add Cu-filter for > 100 kV	Measurement of the HVL at 80 kV and use of look-up diagrams for filtration
Light beam alignment	Edges light and X-ray beam within 1% focus-film distance	Use of a specific alignment phantom
Grid	Transmission factor $> 64\%$; ratio 6:1, grid factor < 3 ; no artefacts	Dose measurements of primary and scattered radiation in the presence and the absence of the grid
Focal spot size	In compliance with the specification of the manufacturer	Star pattern phantom according to the IEC-336
Viewing boxes	> 3000 cd.m ⁻² and 25 % homogeneity; ambient light sources < 25 lux	cd.m ⁻² -meter for brightness of the viewing box; lux-meter for ambient light
Geometrical indicators of the x-ray unit	Readouts < 1 cm; $< 1^\circ$; orthogonality X-ray beam to table $< 1^\circ$	Measuring tape, goniometer and orthogonality phantom

2.6. Calculation of effective dose for irradiation of Graves' ophthalmopathy

*J.J. Broerse, J.Th.M. Jansen, C. Klein¹, M.H. Seegenschmiedt¹,
A. Snijders-Keilholz² and J. Zoetelief*

Medical applications of ionising radiation carry the risk of late deterministic and stochastic effects. In general, the dose distribution in the body will be inhomogeneous and the exposed organs have different susceptibilities for tumour induction. The risk of radiation carcinogenesis can be assessed by deriving an effective dose for a standard patient on the basis of the tissue-weighting factors as defined by the ICRP (1) and Monte Carlo radiation transport codes (2). The calculations of the effective dose for retro-orbital irradiations were initiated by the referral of a 22-year old woman with an early stage of Graves' disease to the Department of Clinical Oncology at the Leiden University Medical Center (LUMC). As can be concluded from Figure 1, the attributable life-time risk from small doses is considerably larger at young age than later in life. It is therefore relevant to investigate the consequences for the effective dose of a reduction of the treatment field and the target dose as applied at the Alfried Krupp Hospital in Essen.

The location of relevant organs in the body can be simulated by mathematical models such as the GSF-EVA and GSF-ADAM phantoms. According to the ICRP (1) the effective dose is defined as $E = \sum wTHT$, where wT is the tissue weighting factor and HT the equivalent dose in the respective tissues. The probability coefficients for stochastic effects and associated tissue weighting factors are summarised in Table 1.

For the situation at Leiden the effective dose was calculated for a bilateral retrobulbar irradiation with 5 MV photons, a field size of $5 \times 5 \text{ cm}^2$ and a target dose of 20 Gy in 10 fractions of 2 Gy over 2 weeks (3). The doses in various surrounding tissues were derived from Monte Carlo simulations of the interaction processes of the primary photons and the associated secondary particles. The results for this geometry for a male person are included in Table 2. Other groups involved in retro-orbital irradiation (4,5) showed their appreciation for our theoretical approach but also expressed their concern on specific aspects of our calculation. Blank et al. (4) argued against our choice of a tissue weighting factor of 0.025 for the brain and suggested to replace it by 0.01. Our dose calculations were based on the geometry of a male ADAM phantom assuming a homogeneous distribution of 8.3 per cent of the total bone marrow in the skull and an amount of approximately 2 per cent bone marrow in the field. As indicated in ICRP publication 23 (6), other sources mention a value of 13.1 per cent for red marrow in the head. Blank et al. (4) are correct to indicate that the distribution of the bone marrow in the head is not uniform. They estimated the amount in the orbital region to be 0.5 per cent. The rest being located in

the scalp, base of skull and mandible. The images provided by Alavi et al. (7), however, do not allow a refined calculation for unequal distribution of bone marrow in the skull. Anyway, the use of blocks to shape the field according to the conical outline of the orbit will reduce the dose in the bone marrow and in the brain. This is accomplished in Essen for irradiations with 12 MV photons, a reduced field size (see Fig. 2) and a target dose of 16 Gy.

As can be seen from Table 2 the effective dose at Leiden is 65 mGy and at Essen 34 mGy. The lower values at Essen have to be attributed to the higher photon energy, the reduced field size and smaller target dose (16 Gy versus 20 Gy).

The risk factor for fatal cases in the high dose region as derived from human epidemiology (1) is presently assumed to be 10 per cent per Sv. Therefore, an effective dose of 64.6 mSv could carry a risk of 0.0065 (or 7 per 1000 persons) for fatal radiogenic cancers in patients treated for Graves' ophthalmopathy (GO). The incidence value for radiation induced cancers could be twice as high. Trott and Kamprad (5) state that our study deserves thorough critical consideration due to its uniqueness and careful conduct, although they come to a somewhat different conclusion. They mention a risk of 0.2 per cent for induction of meningiomas, 0.2 per cent for leukaemia and a life time risk for basalioma of up to 2 per cent. Since the latter type of malignancy will not necessarily be fatal, the estimates of Trott and Kamprad would lead to a mortality risk value of 0.4 per cent.

The implementation of Monte Carlo algorithms and the use of mathematically defined phantoms allow the calculation of effective doses in radiology. The risk factor for induction of fatal malignancies after retrobulbar irradiation can vary between 0.1 and 0.7 per cent and the risk for tumour induction between 0.2 and 1.4 per cent. Since radiation induced malignancies have latency periods of decades the risk for the elderly patient might be limited. At the LUMC, however, we are hesitant to irradiate patients at young age without serious clinical indications.

¹ Alfried Krupp Hospital, Essen, Germany

² Dept. Clinical Oncology, Leiden University Medical Center, Leiden, The Netherlands

1. ICRP Publication 60.

1990. Recommendations of the International Commission on Radiological Protection. Annals of the ICRP, vol. 21, 1-3, 1991.

2. JThM Jansen.

Monte Carlo calculations in diagnostic radiology: dose conversion factors and risk benefit analyses. Thesis, University Leiden, 1998.

3. A Snijders-Keilholz, RJW de Keizer, BM Goslings, EWCM van Dam, JThM Jansen and JJ Broerse.

Probable risk of tumour induction after retro-orbital irradiation for Graves' ophthalmopathy. *Radiother Oncol* 38, 69-71, 1996.

4. LECM Blank, GW Barendsen, MF Prummel, L Stalpers, W Wiersinga and L Koornneef.

Probable risk of tumour induction after retro-orbital irradiation for Graves' ophthalmopathy. *Radiother Oncol* 40, 187-188, 1996.

5. KR Trott and F Kamprad.

Side effects and long-term risks from radiotherapy of benign diseases. In press.

6. ICRP Publication 23.

Reference man: Anatomical, Physiological and Metabolic Characteristics, 1975.

7. A Alavi, S Heyman, T Ka Ming and D Munz.

Bone marrow imaging. In: *Diagnostic Nuclear Medicine*, 3rd edition, vol. 2, Williams and Wilkins, 1993.

Table 1. Nominal probability coefficients for stochastic effects in individual tissues and organs for the whole population and associated tissue weighting factors according to the ICRP (1).

Tissue or organ	Probability of fatal cancer (10^{-2}Sv^{-1})	Probability of severe hereditary disorders (10^{-2}Sv^{-1})	Tissue weighting factor wT	Normalised probability (10^{-2}Sv^{-1})
Gonads		1.00	0.20	
Red bone marrow	0.50		0.12	0.75
Colon	0.85		0.12	0.75
Lung	0.85		0.12	0.75
Stomach	1.10		0.12	0.75
Bladder	0.30		0.05	0.31
Breast	0.20		0.05	0.31
Liver	0.15		0.05	0.31
Oesophagus	0.30		0.05	0.31
Thyroid	0.08		0.05	0.31
Skin	0.02		0.01	0.07
Bone surface	0.05		0.01	0.07
Remainder	0.50		0.05	0.31
Sum	5.00	1.00	1.00	5.00

Table 2. Organ doses and effective doses for radiotherapy of Graves' disease at Leiden and Essen

Organ	Leiden: 5 MV, 20 Gy		Essen: 12 MV, 16 Gy	
	Average organ dose (mGy)	Contribution to effective dose (mSv)	Average organ dose (mGy)	Contribution to effective dose (mSv)
Red marrow	184	22.0	98	11.8
Lung	3	0.3	1	0.1
Oesophagus	8	0.4	2	0.1
Thyroid	45	2.3	9	0.5
Skin	72	0.7	38	0.4
Bone surface	291	2.9	162	1.6
Brain	1437	35.9	774	19.3
Rest of remainder	3	0.1	1	0.0
Effective dose		64.6		33.8

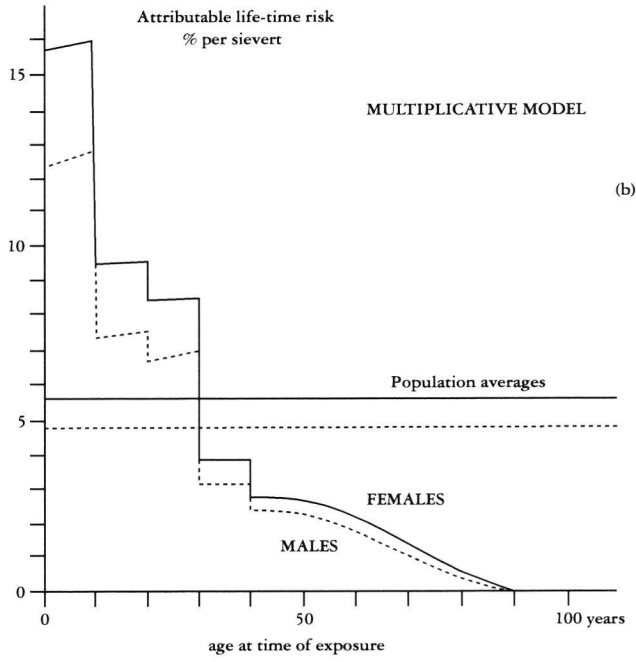


Figure 1. Attributable life time risk from a single small dose at various ages at time of exposure assuming a dose, dose rate effectiveness factor (DDREF) of two (1).

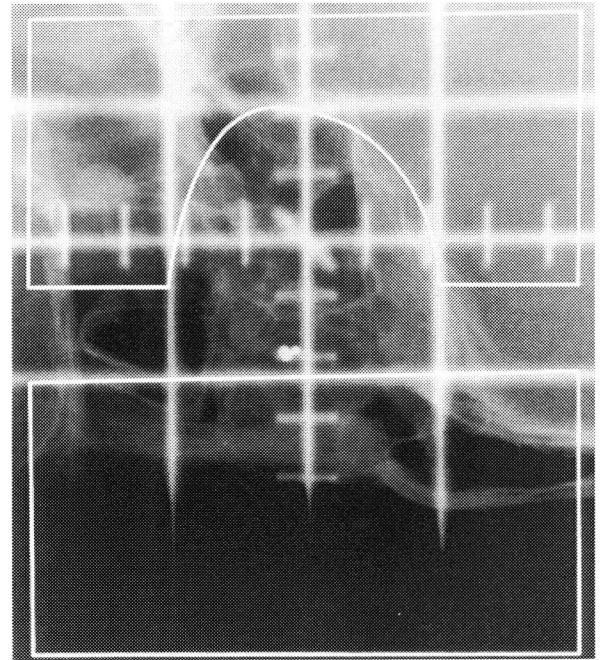


Figure 2. Treatment plan for irradiation of Graves' ophthalmopathy with a field according to the conical outline of the orbit.



3. Environmental protection

Radon is a chemically inert, naturally occurring radioactive gas. The radon concentration in Dutch dwellings ranges from 10 to 140 Bq·cm⁻³ with a mean value of about 30 Bq·cm⁻³. The main risk to humans is the induction of lung cancer. TNO has reliable measurement techniques for measuring radon concentrations in air as well as in other matrices such as building materials, soil and drinking water. Also computer models have been developed for estimating radon concentrations inside houses and for determining the effect of counter measures. A laboratory test dwelling for testing counter measures is available. In the following contributions radon counter measures are evaluated in the laboratory radon test dwelling (3.1.). The influence of building parameters on radon exhalation is described (3.2) and the magnitude of the effective dose of radon in The Netherlands (3.3) and results of epidemiological studies (3.4) are discussed. Preliminary results on health effects of rats exposed in utero to radon in the radon inhalation facility (3.5) will be discussed in the last contribution.

3.1. Efficacy of air treatment devices in controlling indoor radon decay products

P. de Jong and W. van Dijk

Reduction of the dose to the respiratory tract of inhabitants due to radon progeny, can be achieved by several methods.

Roughly, these methods can be subdivided into four classes:

- Methods that affects the radon source in the dwelling itself, for example the use of building materials which have a low exhalation rate;
- Methods aiming at the reduction of the infiltration rate of radon into houses such as application of paints (building material) or tightening of the ground floor;
- Increase in the ventilation rate of the living rooms;
- Application of air cleaning devices, such as mixing fans and filtration units.

In this study, the efficacy of a number of air treatment devices is investigated. The mechanism of these systems is based on either the reduction of the airborne short-lived radon daughters or the enhancement of the air motion in a room, resulting in higher deposition rates. The aim is to lower the concentrations of the radon progeny and thus decrease the bronchial dose.

The experiments are performed in a conditioned 25 m³-test facility, provided with an aerosol generator and equipment to record continuously the temperature, relative humidity, ventilation rate, number of particles per m³ and radon-222 concentration. Air samples were collected in batches from the interior and analysed for the radon daughter concentrations of

both the attached and free fraction by alpha spectrometry.

From these results the equilibrium factor and the free fraction are calculated.

Much effort is made to simulate a reproducible 'standard' living room atmosphere. The average results, as determined over nine different days, were found to be 0.45 ± 0.02 for the equilibrium factor and 0.031 ± 0.007 for the free fraction. The free fraction is much more sensitive to small variations in the aerosol concentration, and therefore shows a larger uncertainty.

In a number of experiments, it has been investigated whether the installation of a small mixing fan or a ceiling fan affects the radon-daughter concentrations and the distribution over the different air fractions. As an additional parameter, the number of revolutions of the fans per unit of time has been noted. Table 1 contains a comprehensive summary of the results.

From the table, it can be concluded that the use of a mixing fan can reduce the equilibrium factor by 20 per cent at maximum. In general, the effect on the free fraction is not significantly different from the starting-point, without air treatment device. Model calculations show a maximum dose reduction of about 15 per cent. Studies on other treatment devices, such as filter units and ion generators, are in progress.

Table 1. Effect on equilibrium factor and free fraction

Description	Equilibrium factor	Free fraction
Starting point	0.45 ± 0.02 (n=9)	0.031 ± 0.007 (n=9)
Small mixing fan (slow)	0.38 ± 0.01 (n=4)	0.038 ± 0.006 (n=4)
Small mixing fan (fast)	0.37 ± 0.05 (n=2)	0.035 ± 0.009 (n=2)
Ceiling fan (slow)	0.44 (n=2)	0.032 ± 0.007 (n=2)
Ceiling fan (fast)	0.35 ± 0.02 (n=4)	0.054 ± 0.015 (n=4)

3.2. The efficacy of the composition and production process of concrete on the ²²²Rn exhalation rate

P. de Jong and W. van Dijk

Radon in houses is the main source of exposure of man to ionising radiation. Radon concentrations vary considerably and depend mainly on the influx from soil and building materials. Among the building materials, concrete generally

accounts for the highest contribution. The large number of variables of this material can be altered over fairly wide ranges. Some of these variables are related to the manner of production, others to the composition of the concrete products.

Both classes of variables are known to affect the capillary pores, the residue of the water-filled spaces in the fresh paste. These capillary pores form an extensive, interconnected network of voids, responsible for the permeability of the concrete and the exchange of water and gases. In this study, the radon emanating power was determined as a function of the amount and type of cement, the water-cement ratio, curing time, type of aggregates and compressive strength. Since earlier studies showed that the moisture content of the concrete samples strongly influences the exhalation rate, the evaporation rate during conditioning was determined as an additional parameter. Some of the results are presented below.

Figure 1 shows the results of the emanating power as a function of the loss of water after six months of conditioned curing. For the concrete slabs prepared with blast furnace cement, a clear relation is shown between both parameters.

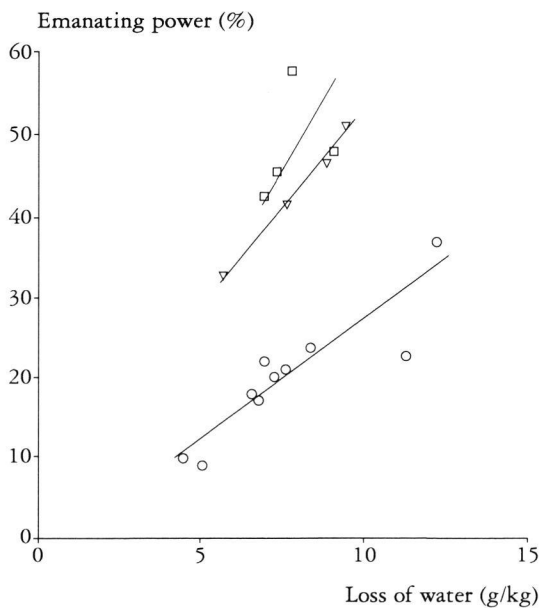


Figure 1: Emanating power as a function of the loss of water after six months of conditioning at 20°C, 50 per cent RH. Samples concreted with Portland cement (□), Portland fly-ash cement (▽), and blast furnace cement (O). Line for blast furnace cement fitted using method of least squares ($r=0.89$). Other lines drawn by eye.

Although there were only four test samples for Portland and Portland fly-ash cement, the same conclusion holds true for these types of cement. The coherence between the two parameters indicates that, with an increase of the evaporation rate, more internal emanating pore surface will be available,

allowing more radon to escape from the interior of the walls. The effect of the cement type is clearly demonstrated. Given a certain loss of water, concretes fabricated with blast furnace cement show the lowest emanating power. Since this type of cement has smaller capillary pores in comparison with concretes based on Portland cement, it is assumed that this related to the lower probability of an emanated radon atom to be stopped within the pore volume. The intermediate position of the concretes prepared using Portland fly-ash can be explained by the condensing, choking effect of fly-ash, which results in reduced pore sizes.

The water-cement ratio was varied from 0.40 – 0.65 in three slabs, using a fixed amount of blast furnace cement of 315 kg/m³. Raising the water-cement ratio also provides an increase of the capillary pore volume and consequently of the liberated amount of radon. A linear relation is obtained when the emanating power is plotted against the water-cement

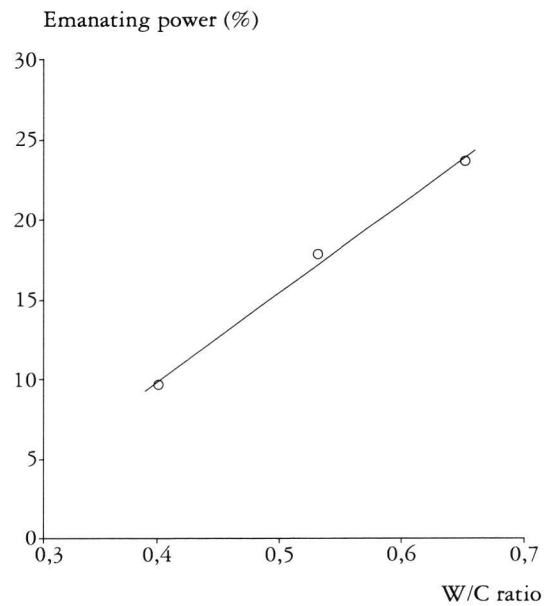


Figure 2: Emanating power as a function of water-cement ratio (blast furnace cement). Line fitted using method of least squares ($r=1.00$).

ratio (Fig. 2), which is in agreement with earlier studies.

Another indicator of the capillary pore volume of concrete samples is the compressive strength. The results showed that the emanating power decreases linearly with the compressive strength, confirming that the coherence within the cement paste decreases in favour of the emanating internal surfaces. A last series of observations concerns the type of aggregates in the concrete samples. Some alternatives for river-gravel were incorporated into this study, to find out whether

comparable exhalation rates could be obtained. The results showed that replacement of river-gravel by limestone or sea gravel actually results in the same exhalation rates.

However, the sample concreted with recycled masonry and concrete granulates shows an increased rate, probably due to its high porosity. Although this material is an attractive alternative from an environmental point of view, more research into its applicability in residential concrete is necessary.

Table 1. Results of measurements

Sample code and short description	Compressive strength (MPa)	Loss of water* (g/kg)	Exhalation rate (Bq.m ²)	Emanating power (%)	²²⁶ Ra content (Bq/kg)
Amount of cement					
1 280 Blast furnace	39.3 ± 1.3	6.9	3.9 ± 0.4	22 ± 3	20 ± 2
2 315 Blast furnace	44.6 ± 0.8	7.2	3.7 ± 0.2	20 ± 2	21 ± 2
3 350 Blast furnace	25.1 ± 0.8	12.2	6.3 ± 0.4	37 ± 4	20 ± 2
4 280 Portland	49.4 ± 1.1	7.3	3.9 ± 0.3	45 ± 7	10 ± 2
5 315 Portland	49.3 ± 1.0	7.8	4.5 ± 0.3	58 ± 9	9 ± 2
6 350 Portland	44.7 ± 0.2	9.0	4.6 ± 0.2	48 ± 6	11 ± 2
7 280 Portland fly-ash	41.2 ± 2.0	7.6	4.2 ± 0.3	41 ± 6	12 ± 2
8 315 Portland fly-ash	43.6 ± 1.5	8.8	4.7 ± 0.2	46 ± 6	11 ± 2
9 350 Portland fly-ash	41.0 ± 1.0	9.4	5.4 ± 0.4	51 ± 7	12 ± 2
Pre-fab concretes					
10 0.40 Portland	56.3 ± 2.7	6.9	3.5 ± 0.3	42 ± 7	9 ± 2
11 0.40 Portland fly ash	52.1 ± 2.0	5.7	3.9 ± 0.4	33 ± 5	13 ± 3
Water-cement ratio					
12 0.40 Blast furnace	46.4 ± 4.4	4.5	2.3 ± 0.1	10 ± 1	26 ± 2
13 0.53 Blast furnace	41.2 ± 1.3	6.6	3.3 ± 0.2	18 ± 1	21 ± 1
14 0.65 Blast furnace	25.7 ± 2.6	8.3	5.5 ± 0.3	24 ± 3	26 ± 2
Time in plastic					
12 0 days	44.6 ± 0.8	7.2	3.7 ± 0.2	20 ± 2	21 ± 2
13 3 days	41.2 ± 1.3	6.6	3.3 ± 0.2	18 ± 1	21 ± 2
15 28 days	42.8 ± 1.4	6.8	3.2 ± 0.2	17 ± 2	21 ± 2
Aggregates					
13 Meuse gravel	41.2 ± 1.3	6.6	3.3 ± 0.2	18 ± 1	21 ± 2
16 Limestone	49.7 ± 0.3	5.0	3.1 ± 0.2	9 ± 1	39 ± 2
17 Granulates	39.4 ± 3.1	11.2	4.8 ± 0.2	22 ± 2	26 ± 2
18 Sea gravel	45.8 ± 2.4	7.6	3.2 ± 0.3	21 ± 3	17 ± 2

* Loss of water after six months curing.

3.3. The effective dose of radon in The Netherlands

H.B. Kal

In publication no. 65 of the International Commission on Radiological Protection (1) risk factors for workers and members of the public are provided for exposure to radon. These factors were derived from risk factors for radon-exposed miners. The effective dose in The Netherlands due to radon exposure with a mean concentration of 29 Bq.m^{-3} on the base of the ICRP 65 publication is estimated to be 0.5 mSv per year. This value, first mentioned in a publication of the Netherlands Society for Radiological Protection (2), is lower than the value of 1.0 mSv per year mentioned in the final report on radiation exposures in The Netherlands (3). An explanation will be provided for the factor 2 difference in effective dose and a conclusion will be made which effective dose will be useful for the situation in The Netherlands.

The excess relative risk on mortality due to lung cancer in 6 cohorts uranium miners and 1 cohort iron miners according to ICRP 65 is 3.79 per J.h.m^{-3} , and the absolute risk 0.08 per J.h.m^{-3} . This latter value is also applicable to members of the general public (1). For radiation protection purposes this value can also be applied for the detriment (this factor includes mortality risk, non-fatal cancer and hereditary risks) as defined by the ICRP in publication 60 (4). The detriment per unit effective dose as defined by the ICRP (4) is 5.6×10^{-5} per mSv for workers and 7.3×10^{-5} per mSv for the general public.

The detriment per unit exposure to radon progeny is, as said, 0.08 per J.h.m^{-3} , that is 8.0×10^{-5} per mJ.h.m^{-3} for workers, and the same figure for members of the public (1). In terms of detriment, an exposure to radon progeny of 1 mJ.h.m^{-3} is equivalent to an effective dose of 1.43 mSv for workers or 1.10 mSv for members of the public.

The effective dose, due to radon, is mainly determined by the short-lived daughters emitting alpha particles. At equilibrium of radon and its progeny 1 Bq Rn-222 deposits in lung tissue energy of $55.4 \times 10^{-10} \text{ J}$. In Dutch dwellings the mean equilibrium factor is about 0.4. Hence 1 Bq Rn-222 deposits energy of $22.16 \times 10^{-10} \text{ J}$.

In Dutch dwellings the mean radon concentration is 29 Bq.m^{-3} and outdoors 3 Bq.m^{-3} . A member of the population spends on average 7000 h per year indoor and 1760 h per year outdoors. Thus, the energy deposited due to exposure to radon is $[29 \times 7000 + 3 \times 1760] \times 22.16 \times 10^{-10} = 0.46 \text{ mJ.h.m}^{-3}$. Using the value of 1 mJ.h.m^{-3} equivalent to an effective dose of 1.10 mSv for members of the public, the effective dose will then be 0.5 mSv per year. This is the value said in the first paragraph.

The value obtained is a logical consequence of a consistent ICRP policy to include not only mortality but also non-fatal cancer and hereditary effects into the risk factor. The Dutch

authorities however use mortality as endpoint with a risk factor of 5×10^{-5} per mSv. The effective dose due to radon exposure will then be 0.7 mSv.

The excess relative risk of 3.79 per J.h.m^{-3} was converted by the ICRP (1) to a life time risk using a value of 4.2 per cent for all causes of death due to lung cancer. However, in The Netherlands the mortality rate due to lung cancer is 6.4 per cent. The resulting effective dose will then be 1.1 mSv and this value is close to the 1.0 mSv reported by Blaauboer et al. (3).

In conclusion: using the detriment concept and the mortality rate for lung cancer the calculated effective dose is 0.5 mSv (1,2). Using the mortality risk factor and the mortality rate for lung cancer in The Netherlands the calculated effective dose due to radon exposure is 1.1 mSv (5), a value close to the 1.0 mSv reported earlier (3).

With respect to the uncertainties in the risk factors for protection purposes, it is questionable whether it is worthwhile to change a risk factor when the change is equal to or less than a factor of 2. Furthermore, in The Netherlands the effective doses are used for comparison of the mortality risks (not detriment) due to exposure to ionising radiations. We feel that the figure of 1 mSv per year as the effective dose due to radon exposure -as mentioned in the final report on radiation exposures in The Netherlands (3)- can be maintained.

1. Protection against radon-222 at home and at work.

ICRP publication 65. Annals of the ICRP 1993; 23 (2).

2. S van Dulleman, AS Keverling Buisman and CZuur.

Veel gestelde vragen over ioniserende straling. NVS publicatie 25, 1995.

3. RO Blaauboer, LH Vaas and HP Leenhouts.

Stralingsbelasting in Nederland in 1988. Bilthoven: RIVM, 1991. Rapport nr. 249103001.

4. Recommendations of the International Commission on Radiological Protection.

ICRP publication 60. Annals of the ICRP 1991, 21 (13).

5. HB Kal.

De effectieve dosis van radon in Nederland. NVS-Nieuws 22, 1, 4-7, 1997.

3.4 The epidemiology of the association between domestic radon concentrations and lung cancer mortality: an ever ending story?

P.A.J. Bentvelzen, A. van Rotterdam and R.W. Bartstra

The carcinogenicity of radon daughter products has been convincingly demonstrated by the dose-dependent elevation of lung cancer risk of underground miners (1). The risk of fatal lung cancer due to exposure to radon in homes is calculated by linear extrapolation of the estimated risk of highly exposed miners. It was concluded that approximately one tenth of the lung cancer deaths in the United States would be due to exposure to indoor radon (1). Epidemiological studies on the relationship between radon concentrations in homes and lung cancer mortality yielded inconclusive results, however (2).

The combined analysis of eleven cohorts of underground miners resulted in a statistically significantly elevated risk for exposures higher than 50 Working Level Months (WLM). The dose-effect relationship was not statistically deviant from linearity (1). A recent update of the same miner cohorts and a new analysis showed at lesser exposures in mines to radon (30-50 WLM) a significantly elevated lung cancer risk. The data in this low-exposure category are compatible with a linear dose-effect relationship as obtained for considerably higher rates of exposure (3). If exposure to radon in homes would be completely comparable to that in mines continuous residence in a dwelling with an average radon concentration of 150 Bq.m^{-3} would give a relative risk of 1.13. It must be mentioned here that in view of the inverse dose-rate effect found only at high cumulative doses, such an extrapolation may result in an overestimation of the domestic radon risks (4).

A meta-analysis of eight published case-control studies on residential radon concentrations and lung cancer mortality has been performed by Lubin and Boice (5). This study does not contain a new analysis of all the pooled detailed data in the separate investigations but a statistical analysis of the combined gross results in the eight publications. This meta-analysis comprises six studies discussed in our former report (2): women in New Jersey (USA), women in Shenyang (China), women in the county of Stockholm (Sweden); men and women all over Sweden; non-smoking white women in Missouri (USA); men and women in Winnipeg (Canada). It also includes a study on men in rural Southern Finland (6) as well as a nested case-control study on men and women in Finland, who have lived at least eighteen years in their last homes (7). Both studies did not yield a statistically significant excess relative risk of lung cancer in relation to elevated indoor radon concentrations. The meta-analysis, however, showed a significant upward trend between lung cancer risk and radon concentrations. At 150 Bq.m^{-3} the relative risk of 1.14 (95% confidence interval 1.0 - 1.3), was found, which would be compatible with the linear extrapolation of the miner data.

The eight separate studies differed considerably in various aspects, like gender and smoking habits, the period in which the radon concentration is determined, the sites at which the measuring devices are located, the technique of determining the radon concentration, the number of years of patients or controls have lived in their last homes. Imprecision in retrospective radon exposure assessment may have significant consequences for the lung cancer risk estimates, as was concluded in a Monte Carlo technique modelling study of the large Swedish epidemiological investigation (8). The great variation in set-up of the eight studies raises the question whether a meta-analysis would be warranted. However, the omission of a single study did not affect much the overall estimates of relative risk (5). It seems that at radon concentrations higher than 150 Bq.m^{-3} , there is a significantly elevated relative risk of lung cancer (5). The results of the meta-analysis with regard to lower radon concentrations neither contradict nor support the linear extrapolation no-threshold hypothesis. They strongly contradict, however, the negative linear exposure-response relationship over a range of 0-300 Bq.m^{-3} , as found by Cohen (9) in a large ecological study on average radon concentrations and lung cancer mortality in 1601 US countries.

Re-analysis of the data of this ecological study (without input of new data) led Cohen to the conclusion that they would be best fitted by a linear-quadratic model (10). This implies a sharp decline in lung cancer mortality with increasing radon concentrations in the range of 4-75 Bq.m^{-3} , a levelling off of this decline in the range 75-150 Bq.m^{-3} , and an upward curve at concentrations higher than 150 Bq.m^{-3} . Cohen furthermore tried to prove that the correction for smoking habits in his 1995 paper has been done in an adequate way. He obtained roughly the same relationships between radon concentrations and lung cancer mortality for countries with the fewest smokers as for countries with average number of smokers or with the highest numbers of smokers.

Neither the eight separate case-control studies, nor the meta-analysis of these studies provide an indication of a sharp decline in lung cancer mortality in the range of 4-75 Bq.m^{-3} , but the numbers of individuals in the low-concentration range are quite small. A very large case-control study is needed particularly in areas with low average radon concentrations to answer the question whether there is a concentration-dependent elevation or a decline of lung cancer risk in the range of 4-75 Bq.m^{-3} . The picture emerges that at concentrations higher than 150 Bq.m^{-3} , there is a small but significant elevation of the relative risk of lung cancer. *U*

1. JH Lubin, JD Boice Jr, E Edling, et al.

Lung cancer in radon-exposed miners and estimation of risk from indoor exposure. *J Nat Cancer Inst.* 87, 817-827, 1995.

2. PAJ Bentvelzen, A van Rotterdam and RW Bartstra.

Survey of epidemiological literature since 1990 on the association between radon and lung cancer. TNO-CSD Progress Report 1995, 27.

3. JH Lubin, I Tomásek, E Edling, et al.

Estimating lung cancer mortality from residential radon using data for low exposures of miners. *Radiat Res* 147, 126-134, 1997.

4. DJ Brenner.

The significance of dose rate in assessing the hazards of domestic radon exposure. *Health Physics* 67, 76-79, 1994.

5. JH Lubin and JD Boice Jr.

Lung cancer risk from residential radon: meta-analysis of eight epidemiological studies. *J Nat Cancer Inst.* 89, 49-57, 1997.

6. E Rusteenoja, I Mäkeläinen, T Rytömaa, et al.

Radon and lung cancer in Finland. *Health Physics* 71, 185-189, 1996.

7. A Auvinen, I Mäkeläinen, M Hakama, et al.

Indoor radon exposure and risk of lung cancer: a nested case-control study in Finland. *J Nat Cancer Inst.* 88, 966-972, 1996.

8. F Lagarde, G Pershagen, G Åkerblom, et al.

Residential radon and lung cancer in Sweden: risk analysis accounting for random error in the exposure assessment. *Health Physics* 72, 269-276, 1997.

9. BL Cohen.

Test of the linear no-threshold theory of radiation carcinogenesis for inhaled radon decay products. *Health Physics* 68, 157-175, 1995.

10. BL Cohen.

Lung cancer rate versus mean radon level in US countries of various characteristics. *Health Physics* 72, 114-119, 1997.

3.5. Health effects on rats exposed to radon *in utero*

H.B. Kal, H.H. Goedoen, J.W. Noomen and R.W. Bartstra

The present risk factors for exposure to radon are derived from epidemiological studies concerning mineworkers exposed to high radon concentrations as compared to indoor concentrations (1). No data are available for exposure of young people to high radon concentrations. In general, for children and foetuses the risk factor for tumour induction is considered to be twice that in adults (2).

Preliminary experiments were performed to answer the question whether high radon concentrations to unborn animals may result in malignancies at young age and whether the frequency of malignancies at older age is increased as compared to control animals.

Three pregnant Wag/Rij rats were exposed to high radon concentrations in the Rijswijk radon inhalation facility.

Two foetuses of rat 1 were surgically removed after the second exposure and activity measurements were performed. The exposure conditions and estimated doses to the foetus are listed in Table 1.

One new-born animal (#3-1) was sacrificed at the age of one month to examine its haematological status. No abnormalities were observed.

The remaining 18 animals were allowed to live their life span. Causes of death and life span are shown in Table 2.

The mean survival time and 95 per cent confidence interval of the 18 rats exposed *in utero* to radon is 113 ± 14 weeks. The mean survival time of rats exposed to 0.6 Sv is 114 ± 13 weeks, that of rats exposed to 0.1 and 0.3 Sv taken together is 113 ± 23 weeks. There is no significant difference in mean

Table 1. Exposure of pregnant rats to radon

rat#	exposure time (h)	radon concentration (MBq/m ³)	time after mating (d)	number of litter mates	foetal dose (Sv)
rat 1	6	900	13		
	5	1000	19	7	0.6
rat 2	6	900	13	8	0.3
rat 3	6	300	14	4	0.1

survival time between the animals exposed to 0.6 Sv and the group exposed to 0.3 and 0.1 Sv as determined with the logrank test. The mean survival time for control WAG/Rij rats is about 130 weeks (3). The mean survival time of the exposed group of 18 rats is significant different from that of controls ($p = 0.03$).

Two out of 7 animals in the 0.6 Sv group developed malignancies about two years after exposure. In the 0.1 and 0.3 Sv group three out of 11 animals developed malignancies at ages of 138 week or older. The frequencies are not significant different, however, there may be a trend for development of tumours earlier in the highest exposed group.

From this experiment it can be concluded that exposure of rats in utero results in a shorter life span. No malignancies at young age were observed, an increased risk of malignancies in the highest dose group may be present.

1. International Commission on Radiological Protection.

Protection against radon-222 at home and at work. ICRP publication 65. Annals of the ICRP 1993; 23 (2).

2. International Commission on Radiological Protection.

1990 Recommendations of the ICRP, publication 60, Pergamon Press, Oxford, 1991.

3. MJ van Zwieten.

The rat as animal model in breast cancer research. Thesis, Univ. Utrecht, 1984.

Table 2. Life span and causes of death of rats exposed in utero to radon

rat#	life span (week)	causes of death
foetal dose is 0.6 Sv		
1-1	114	spontaneous, liver and lung tumour
1-2	108	spontaneous
1-3	103	killed, otitis
1-4	103	killed, moribund, mammary tumour
1-5	128	killed, moribund
1-6	144	spontaneous
1-7	96	spontaneous
foetal dose is 0.3 Sv		
2-1	96	spontaneous
2-2	82	spontaneous, blood in brain
2-3	103	spontaneous
2-4	20	spontaneous
2-5	138	spontaneous, lung tumour
2-6	139	spontaneous
2-7	140	killed, moribund, liver tumour
2-8	150	spontaneous, brain tumour
foetal dose is 0.1 Sv		
3-1	5	killed for haematology
3-2	138	spontaneous
3-3	126	spontaneous
3-4	112	spontaneous



4. Radiation dosimetry research

The development and improvement of dosimetric methods is a general task of TNO-CSD. Adequate dosimetry is required for studies in all fields of radiological protection, i.e., protection of workers, patients, the general public and the environment.

The first contribution (4.1) refers to calculated energy-response correction factors for TLD dosimeters. In (4.2) recent EULEP dosimetry intercomparisons for whole body irradiation of mice are discussed. In the third contribution the relative neutron sensitivity of ionisation chambers for boron-neutron capture therapy is presented and in the last contribution compartmental models for internal dosimetry are described.



4.1 Calculated energy response correction factors for Thermo-Luminescent Dosimeters (TLD) employed in the seventh EULEP dosimetry intercomparison

J. Zoetelief and J.Th.M. Jansen

To derive absorbed dose to muscle tissue from the readout of a thermoluminescent dosimeter (TLD) it is necessary to know its response per unit of absorbed dose. Free-in-air, this information can be obtained by exposing TLDs at different radiation qualities (characterised by HVL) and comparing the TLD readings with muscle tissue doses measured with a calibrated ionisation chamber. Inside the mouse phantom, however, a deviation from the incident spectrum can occur due to two opposing phenomena, i.e., a contribution from scattered radiation produced inside the phantom and, if applicable, back and side scatter material will cause a decrease in effective energy; filtration of the incident radiation with depth in-phantom will result in an increase in effective energy.

The aim of the present study was to calculate energy response correction factors for LiF TLDs exposed in various irradiation geometries to X rays with reference to the calibration situation, i.e., ^{60}Co gamma irradiation of TLDs in the centre of a single mouse phantom. To verify the radiation transport calculations, measurements were made with an ionisation chamber and LiF TLDs for various exposure geometries at two radiation qualities.

The EULEP mouse phantom (1) is a polymethylmethacrylate (PMMA) block with a length of 65 mm, a height (beam direction) of 25 mm and a width of 20 mm. The reference positions at depths in-phantom of 4, 12.5 and 21 mm are referred to as positions, 1, 2 and 3, respectively. For the measurements, the phantoms were machined to fit either 4 TLDs per measurement position or the ionisation chamber used. The top and bottom positions of the TLDs in-phantom are shifted by approximately 1.9 cm out of the central beam axis in the longitudinal phantom directions. This was done to avoid shielding by TLD material for central and bottom positions.

Four exposure geometries were studied, i.e., the mouse phantom flanked on either side by two additional mouse phantoms and employing a PMMA back scatter plate (thickness 8 cm, other dimensions 30 cm) referred to as 5+ geometry; the same situation without back-scatter plate referred to as 5- geometry, a single mouse phantom referred to as 1- and free-in-air referred to as 0-.

For the calculations, various X-ray spectra were selected from the catalogue published by Seelentag et al. (2). In addition, calculations were made for ^{137}Cs and ^{60}Co gamma rays. For the experiments, two X-ray spectra were selected, i.e., first, tube voltage: 180 kV and filter: 0.59 mm Cu and 1 mm Al and second, tube voltage: 250 kV and filter: 2.80 mm Cu and 1 mm Al.

These radiation qualities were produced by a Philips Müller model 320 X-ray generator (Philips, Hamburg, Germany). The corresponding spectra used for the calculations are C102 and C122 and are characterised by HVLs of 1.06 and 2.90 mm Cu, respectively. Ionisation chamber measurements were made with a Farmer type chamber (Nuclear Enterprises Technology, Reading, UK, model NE 2571) connected to a Keithley (Keithley, Cleveland Ohio, USA, model 617) electrometer and a high voltage supply operated at 250 V employing mass energy absorption coefficients and overall chamber correction factors published elsewhere (3). Calibration of the ionisation chamber system in terms of air kerma free-in-air was performed at the Dutch Standards Laboratory at X rays with HVLs of 0.60, 1.55 and 2.94 mm Cu as well as at ^{60}Co gamma rays.

Experiments with TLDs were made with LiF chips (Harshaw-Bicron, Solon Ohio, USA, type TLD-100) having dimensions of 3.2 mm x 3.2 mm x 0.9 mm. TLDs were pre-selected from a batch of 200 after exposure to 10 mGy ^{60}Co gamma rays.

Cameron annealing was used, and the readout of the TLDs was made at a home-made hot nitrogen gas reader (4). The radiation transport calculations were performed with the Monte Carlo N-particle code (MCNP) version 4.2 (5). For the calculations, 107 photon histories were simulated and the energy cut-off for the photon transport was 1 keV. The resulting statistical uncertainty at one standard deviation confidence level was typically 0.7 per cent and 2.3 per cent at maximum.

The first HVLs measured for the experimental conditions were 1.05 mm Cu and 3.01 mm Cu for the X rays generated at tube voltages of 180 and 250 kV employing the filtrations mentioned before. These findings are in good agreement with the values of 1.06 mm Cu and 2.94 mm Cu, respectively, quoted by Seelentag et al. (1979) and calculated values of 1.03 mm Cu and 2.88 mm Cu, respectively. The calculated HVLs of the incident X-ray beams are used for further presentation of results.

The homogeneity of the radiation fields across the area relevant for the exposure of the mouse phantom measured with the ionisation chamber showed a maximum deviation of 2.3 per cent. This implies that measurements at the top and bottom positions, i.e., positions 1 and 3 can yield somewhat lower (1 to 2 per cent) values as these are somewhat (1.9 cm) outside of the central beams axis. A comparison of the results of ionisation chamber measurements with those from the calculations for the three irradiation geometries 5+, 5- and 1- relative to the situation free-in-air, 0-, is shown in Figure 1.

The maximum difference obtained between measurements and calculations amount to 4.4 per cent (250 kV, 5+ geometry, position 2). Also for the other in-phantom positions irradiated in the 5+ geometry relatively large (about 3 to 4 per cent) deviations are found. During the measurements in the 5+ geometry, the backscatter plate was placed on the floor of the irradiation room, which caused an additional backscatter of about 1.4 to 2.4 per cent. Application of this scatter correction reduced the maximum difference to less than 2.5 per cent, except for 180 kV X rays in the 1- geometry, position 3 which is somewhat larger (3.5 per cent).

The results of the measurements with LiF TLDs compared to those obtained from the calculations for various measurement positions and exposure geometries at 180 kV and 250 kV X rays are shown in Figure 2. The calculated values include the correction for additional backscatter from the floor in the 5+ geometry, and scatter from the use of four chips simultaneously free-in-air. The largest difference between the doses calculated in LiF in-phantom normalised to LiF kerma free-in-air compared to the readings from the LiF chips in-phantom relative to free-in-air amounts to about 6.5 per cent (180 kV, 5+, position 3). This difference is reduced by about 2 per cent due to the inhomogeneity of the irradiation field to approximately 4.5 per cent. Based upon the expected uncertainties for TLD measurements (3 per cent at a confidence level of 1 SD resulting in an uncertainty for the ratio in-phantom to free-in-air of 4 per cent) and those in the calculations (less than 1 per cent at a confidence level of 1 SD) the observed differences are not significant except for 180 kV, 5+, position 3). The largest difference remains well within 2 standard deviations, which is not unacceptable in view of the number of measurement conditions (n=24).

The results of the comparisons of the dose calculations with the ionisation chamber as well as the TLD dose measurements confirmed the validity of the calculational procedures. Therefore, it seems appropriate to determine the energy response correction factors to be applied to the TLD readout for the various photon spectra, irradiation geometries and measurement positions on the basis of the Monte Carlo calculations.

In Figure 3, the energy response correction factors for position 2 to be applied to the TLD readout when the calibration is made in terms of muscle tissue dose at ^{60}Co gamma rays, $C_{x,g,2}$, are shown as a function of the irradiation geometry and the HVL of the incident photon beam. For incident X rays ranging from 1 to 2.9 mm Cu, the ratio of the energy response correction factor free-in-air to the energy response correction factor for the 5+ geometry, $C_{x,0-2}/C_{x,5+,2}$, varies by about 3 to 4 per cent.

The results of the energy response correction factors for the full scatter conditions (5+) are significantly smaller than

those for exposure geometries with less scatter (5- and 1-) by up to about 3 per cent at maximum. The uncertainties in the energy response correction factors are estimated to be about 1 per cent at maximum. The present results reduce the uncertainties in the TLD measurements significantly as different correction factors can be applied for different exposure geometries. In previous dosimetry intercomparisons a distinction between full scatter conditions and geometries in which full scatter conditions are not met, was not possible. The differences found in the present study of 3 per cent at maximum are considerable in view of the requirement of 5 per cent accuracy in dosimetry for radiobiology.

Conclusions

- Validation of the calculation procedures has been shown by experiments with an ionisation chamber and TLDs.
- Energy response correction factors to be applied to LiF TLD measurements when TLDs calibrated in terms of muscle tissue dose at ^{60}Co gamma rays, $C_{x,g,i}$, are presented on the basis of Monte Carlo radiation transport calculations.
- The variation in the energy response correction factor $C_{x,g,i}$, with irradiation geometry is about 4 per cent at maximum.
- The variation in $C_{x,g,i}$, among the 5+, 5- and 1- geometries is about 3 per cent at maximum.

1. J Zoetelief, JJ Broerse and RW Davies.

EULEP protocol for X-ray dosimetry, EUR 9507 (Luxembourg: Commission of the European Communities), 1985.

2. WW Seelentag, W Panzer, G Drexler, L Platz and S Santner.

A catalogue of spectra for the calibration of dosimeters. GSF Bericht 560 (München; GSF), 1979.

3. J Zoetelief and JThM Jansen.

Calculated energy response correction factors for LiF thermoluminescent dosimeters employed in the seventh EULEP dosimetry intercomparison. Phys Med Biol 42, 1491-1504, 1997.

4. HW Julius, CW Verhoef and FAI Busscher.

A universal automatic TLD-reader for large-scale radiation dosimetry. In: Proc Third Int Cong IRPA (Washington DC, USA: IRPA) 563-567, 1973.

5. J Briesmeister.

MCNP - A general Monte Carlo Code for Neutron and Photon Transport, version 3A, LA-7396-M Rev2 (Los Alamos NM, USA: Los Alamos National Laboratory), 1986.

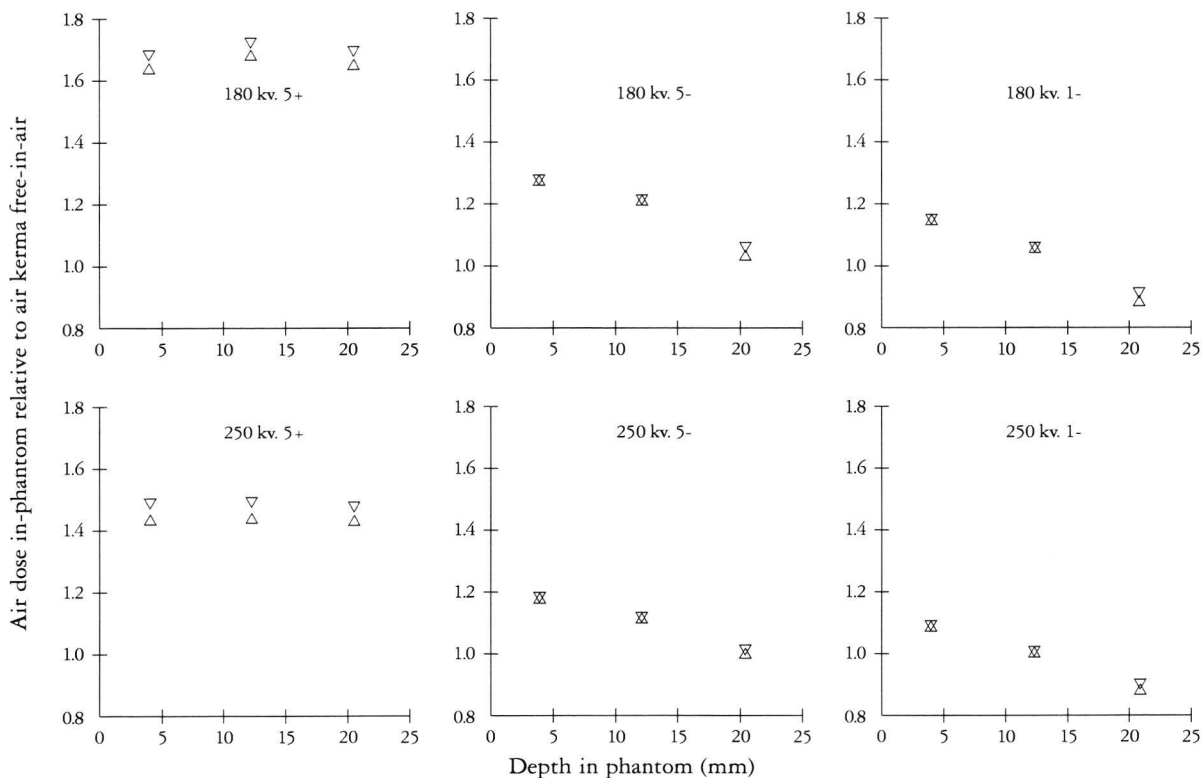


Figure 1: Comparison of results from Monte Carlo radiation transport calculations with those from ionisation chamber measurements for three depths (4, 12.5 and 21 mm referred to as positions 1, 2 and 3, respectively) inside a mouse phantom at various irradiation geometries, i.e., the mouse phantom flanked by two mouse phantoms on each side employing an 8 cm-thick back-scatter plate (5+), the same situation without back-scatter plate (5-) and a single mouse phantom (1-). Given are the calculated (Δ) and measured (∇) values for the air kerma at the in-phantom positions relative to air kerma free-in-air for the radiation qualities generated at tube voltages of 180 kV (measured HVL: Cu 1.05 mm) and 250 kV (measured HVL: Cu 3.01 mm).

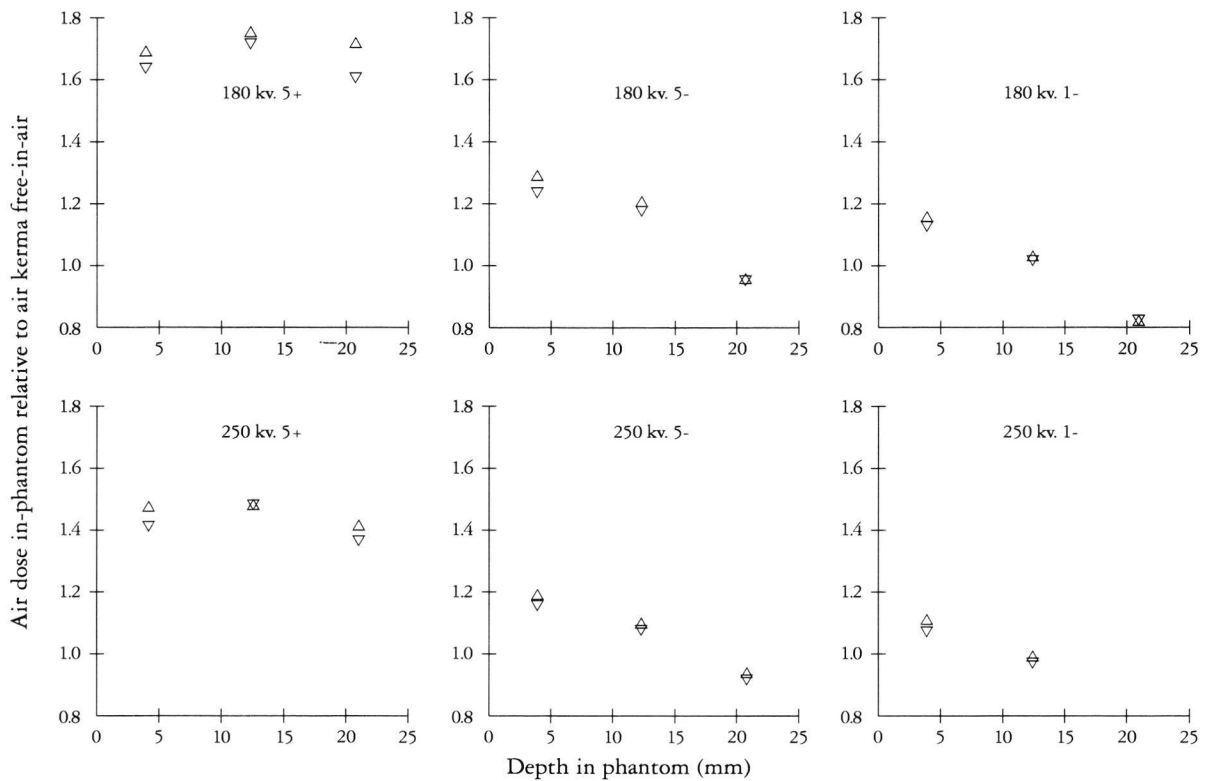


Figure 2: Comparison of results from Monte Carlo calculations with those from LiF TLD measurements. The reference positions in-phantom and irradiation geometries are the same as in Figure 1. Shown are, for various in-phantom positions and irradiation geometries the dose in LiF calculated (Δ) in-phantom relative to free-in-air and the LiF TLD readout (∇) in-phantom relative to free-in-air.

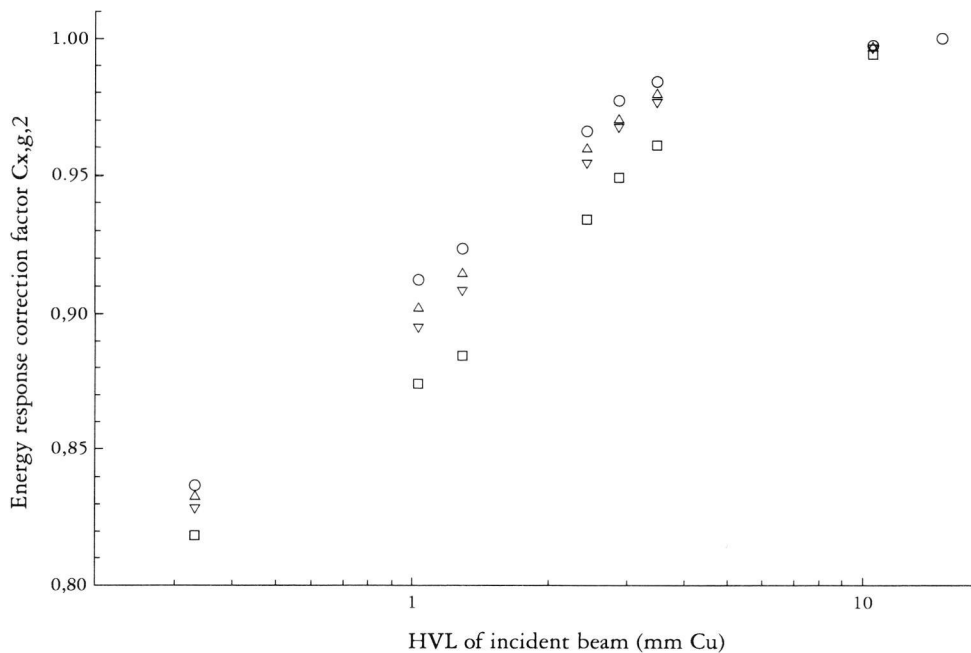


Figure 3: Energy response correction factors for position 2, $C_{x,g,2}$, calculated as a function of HVL of the incident beam for LiF TLDs exposed in various irradiation geometries, i.e., 5+ (\square), 5- (∇) and 0- (\circ).

4.2. Recent EULEP dosimetry intercomparisons for whole body irradiation of mice

J. Zoetelief, J.J. Broerse, F.A.I. Busscher, W.P. Hiestand, H.W. Julius and J.Th.M. Jansen

Incentives for dosimetry intercomparisons are the following:

- Providing the possibility to participants of checking the accuracy and precision of their irradiations and the homogeneity of their dose distributions.
- Repeated intercomparisons provide information on the long-term stability of irradiation procedures and stimulate the participants to improve dosimetry.
- Special assistance to institutes showing discrepancies in their dose assessment.
- Intercomparisons are certainly valuable for new participants, co-operating within the European Late Effects Project Group (EULEP).

The present contribution summarises both the procedures and the results obtained during EULEP dosimetry intercomparison for whole body irradiation of mice.

All participants in the seventh intercomparison (Table 1) received for each irradiation facility two polymethylmethacrylate (PMMA) mouse test phantoms (20 mm x 25 mm (radiation direction) x 65 mm) loaded with LiF thermoluminescent dosimeters (TLD). The measurement positions at depths of 4, 12.5 and 21 mm are referred to as top, central and bottom, respectively. A control badge filled with both irradiated and unirradiated TLD was provided to each participant. The participants were requested to irradiate the test phantoms in their actual arrangements used for whole body irradiation of mice, such that the absorbed dose in muscle tissue in the centre of the test phantom was 2 Gy and the dose distribution was uniform, i.e., a ratio of less than 1.10 between maximum and minimum doses in the phantom (1). The control badges, which were to be kept in a radiation free area, served to investigate the influence of transport. Detailed instructions were given in a procedure form. For background information reference was made to the code of practice given in the EULEP dosimetry protocol (2). Detailed information on the exposure conditions was collected through a questionnaire. In some of the earlier intercomparisons the participants received a single mouse phantom and the procedure was repeated once or twice.

In the seventh intercomparison, calibration of the TLD was obtained by exposing a single mouse phantom to a muscle tissue dose of 2 Gy of ^{60}Co gamma rays. The responses of the LiF TLD are dependent on the radiation quality. The determination of the correction factors for the energy response of LiF TLD in various irradiation geometries as a function of the HVL of the incident photon beam has been presented elsewhere (3). The accuracy (overall uncertainty) in the dose determination from the TLD is estimated to be 3.3 per cent

at a 66 per cent confidence level.

In the earlier intercomparisons, calibration of TLD was obtained for exposure to X rays free-in-air at the Dutch Standards Laboratory. Experimentally determined energy correction factors (4) were employed to derive the absorbed dose in-phantom under full scatter conditions.

In all intercomparisons, the readout of the TLD from the control badges showed no unexpected fading or irradiation. The information obtained through the questionnaires was checked for all participants. In some cases where inconsistencies were found, the responsible scientists were consulted to resolve these.

In Figure 1, the results for the 1996 EULEP dosimetry intercomparison concerning absorbed dose in the central position of the mouse phantom are shown. Eleven facilities yielded satisfactory results. For one facility a deviation between 5 and 10 per cent was found, whereas for two facilities the discrepancy was in excess of 10 per cent. The scientists responsible for the facilities, at which dose discrepancies were observed, were approached to obtain additional information. After consultation two out of the three discrepancies were resolved, and the 19 per cent discrepancy was reduced to 9 per cent.

In Figure 2, the results for the dose distribution in the mouse phantom in the 1996 intercomparison are shown. It can be seen that for six out of the 13 facilities the conditions for a uniform irradiation were not fulfilled. One institute explicitly stated that uniformity of the dose distribution was not important in view of their studies and thus not aimed for. The causes for non-uniform dose distributions were mainly related to unilateral irradiation.

A comparison of the results of all intercomparisons concerning the dose in the centre of the mouse phantom can be made from the data in Figure 1. The lowest number (none) of discrepancies in dose in excess of 10 per cent was observed during the third (1976) intercomparison and the largest number (four) in the first (1971) intercomparison. The most considerable improvement was obtained between the first and second intercomparison. This was due, in part, to site visits made by members of the EULEP dosimetry committee to help improve the dosimetry. The large dose discrepancies in the second, fourth and fifth intercomparisons were also resolved through site visits. The two institutes where dose discrepancies in excess of 10 per cent were found in the sixth intercomparison did not respond to an offer by the EULEP dosimetry Committee to resolve the dosimetric problems.

Concerning the uniformity of the dose distributions (Fig. 2)

a gradual improvement is observed during the consecutive intercomparisons. However, the results for the seventh intercomparison are still not satisfactory for a considerable number of irradiation facilities.

Conclusions

- The results of the seventh EULEP dosimetry intercomparison for whole body irradiation of mice are satisfying with regard to the assessment of the absorbed dose for 11 out of the 14 irradiation facilities. For two facilities showing a dose discrepancy the causes were identified, for one facility the dose discrepancy was considerably reduced.
- Almost all intercomparisons revealed discrepancies in X-ray dosimetry beyond 10 per cent. This indicates the need for repeated intercomparisons.
- With regard to the dose distribution in a mouse phantom, a gradual improvement is observed since the first intercomparison. However, in the seventh intercomparison still 6 out of the 13 facilities deliver non-uniform dose distributions.

1. ICRU (International Commission on Radiation Units and Measurements).

Quantitative Concepts and Dosimetry in Radiobiology, ICRU report 30 (Bethesda, MD, USA: ICRU), 1979.

2. J Zoetelief, JJ Broerse and RW Davies.

EULEP Protocol for X-ray Dosimetry, EUR 9507 (Luxembourg: Commission of the European Communities), 1985.

3. J Zoetelief and JThM Jansen.

Calculated correction factors for energy dependence of LiF thermoluminescent dosimeters employed for the seventh EULEP dosimetry intercomparison. Phys Med Biol 42, 1491-1504, 1997.

4. KJ Puite and DLJM Crebolder.

Energy dependence of thermoluminescent dosimeters for X-ray dose and dose distribution measurements in a mouse phantom. Phys Med Biol 19, 341-347, 1974.

5. J Zoetelief, JJ Broerse, FAI Busscher, WP Hiestand, HW Julius and JThM Jansen.

Recent EULEP dosimetry intercomparisons for whole body irradiation of mice. Int J Radiat Biol 72, 627-632, 1997.

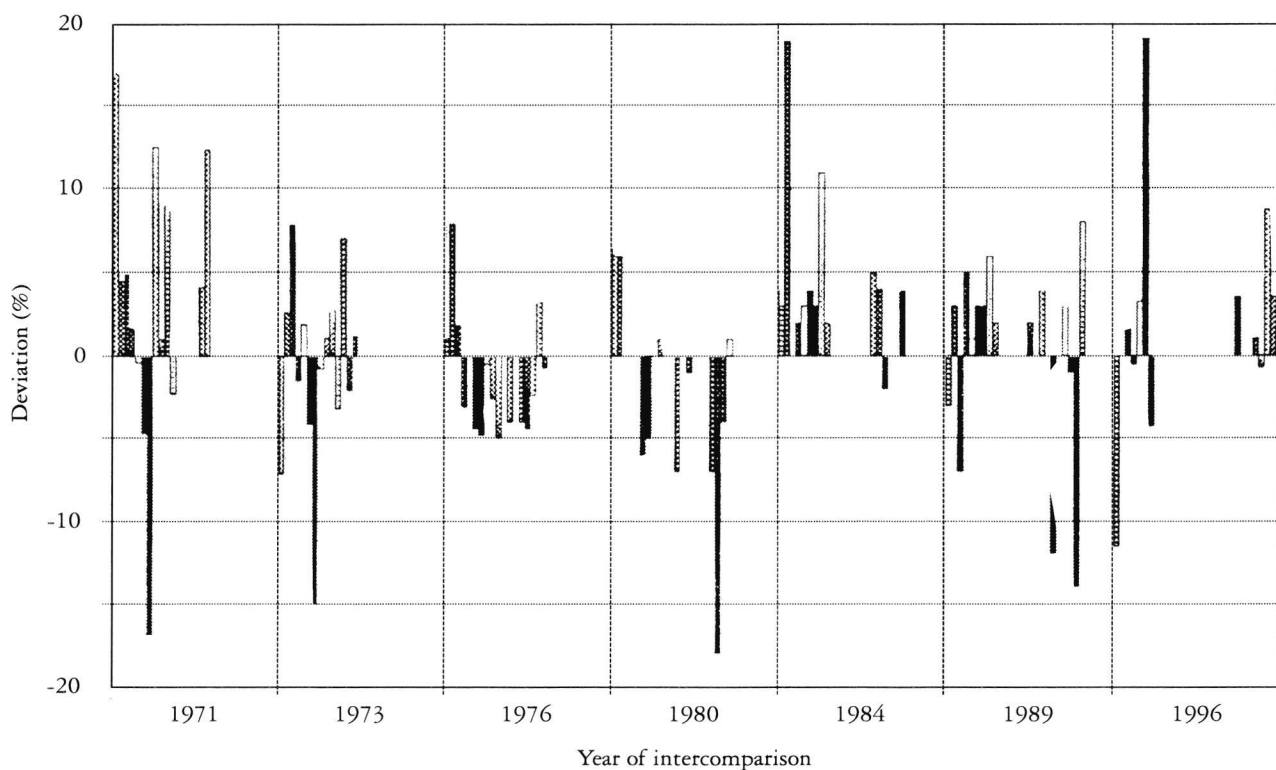


Figure 1: Results for absorbed dose in muscle tissue in the centre of the mouse phantom for seven EULEP dosimetry intercomparisons (1971-1996). The deviation of the measured dose from the dose quoted by each participant is shown by the individual columns (5).

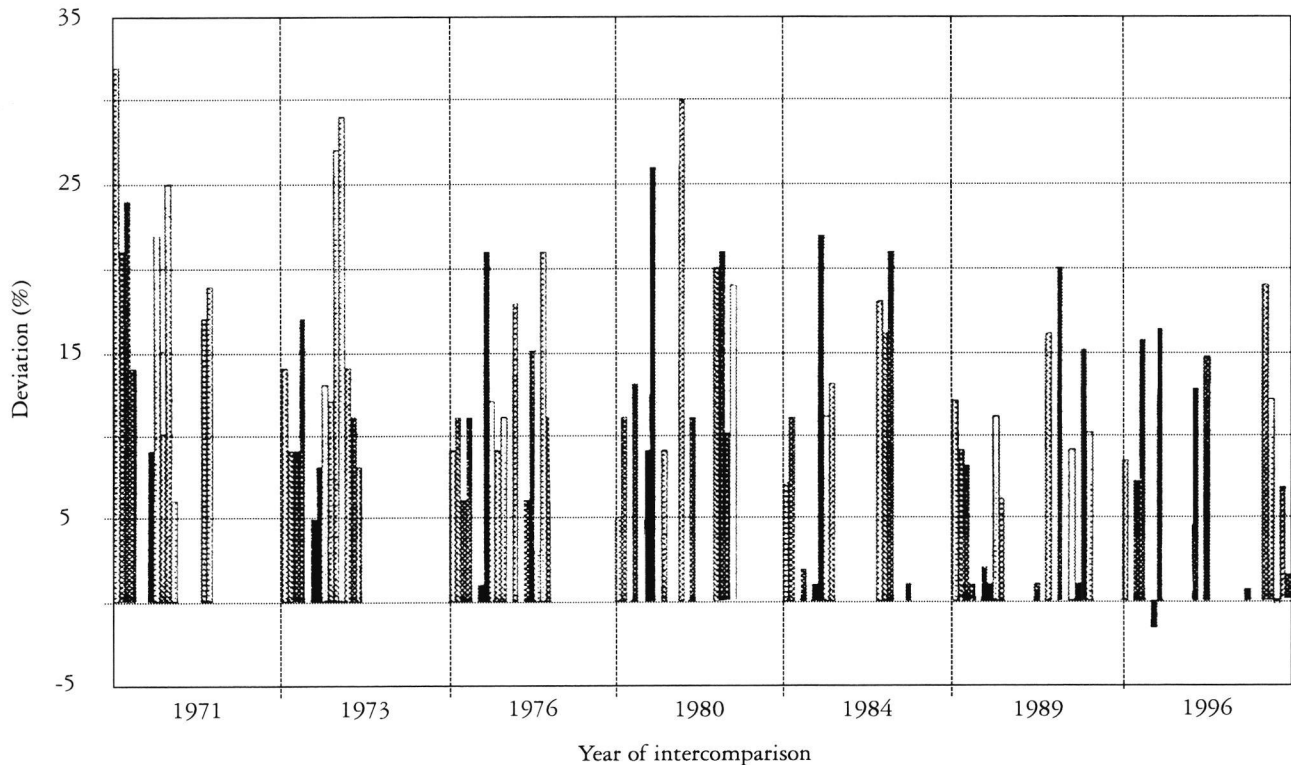


Figure 2: Results for dose distribution in the mouse phantom for seven EULEP dosimetry intercomparisons. The dose distribution is presented as the difference in dose between top and bottom positions relative to the dose in the central position $(D_{\text{top}} - D_{\text{bottom}}) / D_{\text{centre}}$ (5).

4.3 Relative neutron sensitivity of tissue-equivalent ionisation chambers in an epithermal neutron beam for boron neutron capture therapy

J.Th.M. Jansen, C.P.J. Raaijmakers¹, B.J. Mijnheer¹ and J. Zoetelief

During recent years, boron neutron capture therapy received renewed interest as new promising boron compounds and epithermal neutron beams have become available. For establishment of the different dose components in epithermal neutron beams, various techniques are applied, including the use of tissue-equivalent (TE) ionisation chambers for the determination of the intermediate and fast neutron dose. This paper is directed towards the calculation of the relative neutron sensitivity of TE ionisation chambers, k_T , for the free-in-air spectrum at the HB11 epithermal beam facility of the High Flux Reactor in Petten.

According to ICRU Report 45 (1), the relative neutron

sensitivity, k_T , of a TE ionisation chamber can be expressed by:

$$k_T = \frac{W_c}{W_n} \left[\frac{((\bar{L}/\rho)_m / (\bar{L}/\rho)_g)_c}{(I_{m,g})_n} \right] \left[\frac{((\mu_{en}/\rho)_t / (\mu_{en}/\rho)_m)_c}{(K_t K_m)_n} \right]$$

where the subscripts c and n refer to the calibration and mixed field situation, respectively; the subscripts m, g and t indicate the chamber wall material, chamber gas and ICRU muscle tissue, respectively; W represents the average energy required to form an ion pair in the chamber gas; $(L/\rho)_c$ is the mean restricted collision mass stopping power for the

slowing down electrons produced by the photons used for calibration; $(r_{m,g})_n$ is the gas-to-wall absorbed dose conversion factor for an ionisation chamber in a mixed field; (μ_{en}/r) is the mass energy absorption coefficient; and K is the kerma.

The following simplifications and assumptions are made for the present calculation of K_T . The ratio of the gas-to-wall absorbed dose conversion factor and the ratio of mean restricted collision mass stopping powers, $(r_{m,g})_n / \{(\mu_{en}/\rho)_m / (\mu_{en}/\rho)_g\}_c$ is 1.00 ± 0.02 for neutron energies employed for fast neutron therapy (T). This might not be directly applicable to the present situation. The calculations of Burger and Makarewicz (2) suggest that cavity size effects are not maximal for infinite size. At energies below the values for which they performed calculations, the cavity size will approach more and more infinite size. Therefore, it is assumed that the ICRU recommendation for fast neutrons also holds true for the wide range of neutrons considered in the present study. The ratio $\{(\mu_{en}/\rho)_t / (\mu_{en}/\rho)_m\}_c$ can be calculated using data from ICRU Report 44 (3) and equals 1.000 for ^{60}Co γ rays and 1.003 for ^{137}Cs γ rays. For the present calculations, this ratio is taken to be equal to unity. A value of 29.2 eV has been taken for W_c for the methane-based TE gas which is based on the value for W_{air} of 33.97 eV from Boutillon and Perroche-Roux (4) and the estimate for W_{air}/W_g of 1.166 derived from measurements with ionisation chambers filled with TE gas and air (5). Data on kerma factors are obtained from ICRU Report 44 (3). To arrive at values of W_n for various neutron energy bins, the Caswell-Coyne code for calculation of energy deposition and ion yield (6) is used after replacing the functions and numerical values for W of charged particles by those presented by Taylor et al. (7). The neutron spectrum was calculated using Monte Carlo simulations for the free-in-air condition at the HB11 epithermal neutron beam facility of the High Flux Reactor in Petten (8).

W_n values calculated for neutrons in the energy range 2.6–10–8 to 20 MeV are shown in Figure 1. Also shown in this figure are data published previously by Makarewicz and Burger (9). The W_n values show a distinct peak around about 0.3 keV for both sets of calculations. The largest difference in W_n value between the present calculations and those of Makarewicz and Burger amounts to about 40 per cent and occurs in the energy bin 0.14 to 0.26 keV. This difference is most likely due to the different mathematical expressions used for W values of charged particles as a function of energy. It is expected that the largest differences between different calculations will occur at the largest W_n values, since at these neutron energies the charged particles with the lowest energies are produced. Both sets of W_n values indicate that the linear extrapolation of W_n values below 0.1 MeV made by Rogus et al. (10) is not justified.

Relative neutron sensitivities of TE ionisation chambers

calculated as a function of neutron energy are shown in Figure 2. The present calculations show that the highest k_T value is 1.04 (at about 18.5 MeV) and the lowest k_T is 0.19 (at about $3.6 \cdot 10^{-4}$ MeV). For thermal neutrons k_T is approximately 0.94. These results are quite different from the values published by Rogus et al. (10) as shown in Figure 2. The differences are mainly due to the approximations used for W_n values below 0.1 MeV by Rogus et al. They either extrapolated W_n values of Goodman and Coyne (11) linearly to neutron energies below 0.1 MeV or applied for this neutron energy region W_p data of Leonard and Bohring (12) that result in infinite W values below about 10^{-3} MeV. More recent information of Huber et al. (13) showed that W_p does not increase as rapidly as found by Leonard and Bohring.

Spectral data of the HB11 beam at the HFR in Petten have been used in combination with W_n and kerma factors for the neutron energy bins to calculate average W and k_T values with the code developed in-house. Since the thermal neutron response of the chamber is treated separately, the thermal part of the spectrum has not been included in the calculations. The k_T value calculated using the W_n values of Makarewicz and Burger (9) for the total spectrum resulted in a value of 0.87 which is in good agreement with the k_T values calculated using the W_n values from the present study. The present k_T value is about 10 per cent smaller than the value of 0.95 proposed by Rogus et al. (10) and Raaijmakers et al. (14) which is important in view of the required accuracy for dosimetry in radiotherapy.

¹ The Netherlands Cancer Institute, Antoni van Leeuwenhoek Huis, Amsterdam.

1. ICRU.

Clinical Neutron Dosimetry. Part 1: Determination of absorbed dose in a patient treated by external beams of fast neutrons. Report 45 (ICRU Publications, Bethesda, MD, USA), 1989.

2. G Burger and M Makarewicz.

Average energy to produce an ion pair in gases (W -values) and related quantities of relevance in neutron dosimetry. In: Nuclear and Atomic Data for Radiotherapy and Related Radiobiology, (IAEA, Vienna), pp. 225-238, 1987.

3. ICRU.

Tissue substitutes in radiation dosimetry and measurement. Report 44 (ICRU Publications, Bethesda, MD, USA), 1989.

4. M Boutillon and AM Perroche-Roux.

Re-evaluation of the W value for electrons in dry air. Phys Med Biol 32, 213-219, 1987.

5. J Zoetelief and H Schraube.

Experimental procedures for the on-site neutron dosimetry intercomparison ENDIP-2. In: Proc. Fifth Symposium on Neutron Dosimetry. Eds. H Schraube, G Burger and J Booz. EUR 9762 (Brussels and Luxembourg: Commission of the European Communities) pp. 1179-1190, 1985.

6. RS Caswell and JJ Coyne.

Energy deposition spectra for neutrons based on recent cross section evaluations. In: Proc. Sixth Symp. on Microdosimetry. Eds. J Booz and HG Ebert (Commission of the European Communities, Brussels) EUR-6064, Vol. II, pp. 1159-1171, 1978.

7. GC Taylor, JTM Jansen, J Zoetelief and H Schuhmacher.

Neutron W -values in methane-based tissue equivalent gas up to 60 MeV. Radiat Prot Dosim 61, 285-290, 1995.

8. P Watkins, MW Konijnenberg, G Constantine, H Reif, R Ricchena, JBM de Haas and W Freudenreich.

Review of the physics calculations performed for the BNCT facility at the HFR Petten. In: Boron Neutron Capture Therapy: Toward Clinical Trials of Glioma Treatment. Ed. D Gabel and R Moss (New York: Plenum Press) pp 47-58, 1992.

9. M Makarewicz and GW Burger.

W_n for methane-based TE gas and carbon dioxide and W_n and gas-to-wall dose conversion factors for TE/TE cavities. In: Proc. Fifth Symp. on Neutron Dosimetry, Eds. H Schraube, G Burger and J Booz (Commission of the European Communities, Luxembourg) EUR 9762, pp. 275-286, 1985.

10. RD Rogus, OK Harling and JC Yanch.

Mixed field dosimetry of epithermal neutron beams for boron neutron capture therapy at the MITR-II research reactor. Med Phys 21, 1611-1625, 1994.

11. LJ Goodman and JJ Coyne.

W_n and neutron kerma for methane-based tissue-equivalent gas. Radiat Res 82, 13-26, 1980.

12. BE Leonard and JW Bohring.

The average energy per ion pair, W , for hydrogen and oxygen ions in a tissue equivalent gas. Radiat Res 55, 1-9, 1973.

13. R Huber, D Combecher and G Burger.

Measurements of average energy required to produce an ion pair (W value) for low-energy ions in several gases. Radiat Res 101, 237-251, 1985.

14. CPJ Raaijmakers, MW Konijnenberg, HW Verhagen and BJ Mijnheer.

Determination of dose components in phantoms irradiated with an epithermal neutron beam for boron neutron capture therapy. Med Phys 22, 321-329, 1995.

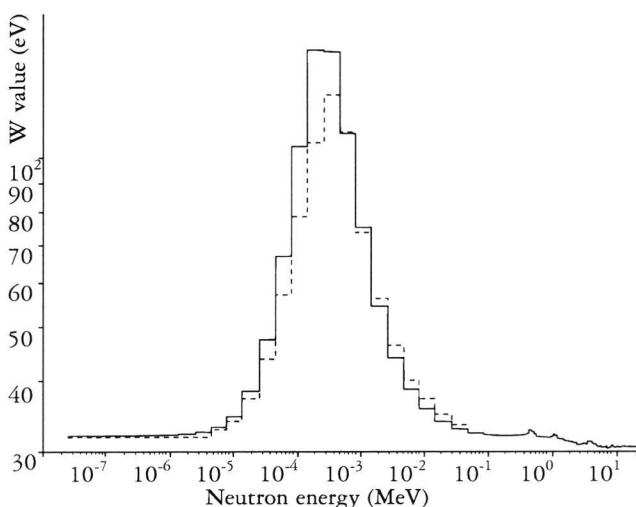


Figure 1: Average energy required per ion pair formed, W_n , in methane-based TE gas as a function of neutron energy. Shown are the results from the present calculations (solid line) and data from Makarewicz and Burger (9) (broken line).

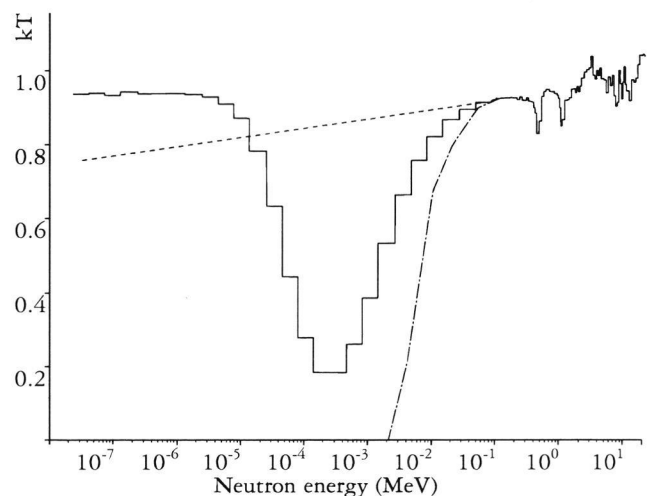


Figure 2: Relative neutron sensitivity of a tissue-equivalent ionisation chamber filled with methane-based TE gas as a function of neutron energy. Shown are results from the present calculations (solid line) and extrapolations made by Rogus et al. (10) based on data on W_n of Goodman and Coyne (11) (broken line) and on data on W_p of Leonard and Bohring (12) (dot, line, dot representation).

4.4 Compartmental models for internal dosimetry

F.W. Schultz and A. van Rotterdam

Metabolic models for the deposition, retention, transport and clearance of activity in the body are necessary to evaluate effective dose after injection, ingestion or inhalation of radionuclides. Usually, linear multicompartiment models are used, in which activity in each compartment as a function of time is described by a set of linear first order differential equations. Given the input of activity, the behaviour of the model (model response) is determined by the values of its parameters, i.e., the transfer rate constants (amount of activity transported per unit of time from one compartment to another). For larger models analytical evaluation of the response becomes unpractical. In principle, it can be calculated numerically. To do this a number of standard numerical methods exists. However, new methods are still being developed to improve performance and solve convergence problems. Especially when parameter values differ by large orders of magnitude the standard methods have difficulties in approximating the true model response satisfactorily (1). A second problem is in model development, i.e., in the determination of the correct values of the parameters. In the past the International Commission on Radiological Protection (ICRP) has established transfer rate constants for various radioactive compounds, based on experimental data from literature (2). Because of new data being gathered continuously, updates of models and parameters are required from time to time, e.g., the new respiratory tract model (3). Even then, in view of the variability in experimental data and, for instance, inevitable extrapolations from laboratory animal to man, uncertainties in the transfer rate constants remain large. Therefore, sensitivity analysis is proposed, to identify critical areas in biokinetic model development and to investigate effects of variability and uncertainty in the parameters. Within the framework of a larger EC research project on internal dosimetry (contract FI4P-CT95-0011) computer code is being developed at TNO-CSD that can serve as a generally applicable tool for such sensitivity analyses.

Two approaches are being followed. In the first one the maximum likelihood (ML) optimisation technique is employed to estimate parameter values and their variances. Results of ML estimation are asymptotically unbiased and efficient, i.e., for large numbers of observations, respectively, the estimated parameter values tend to the true values and their variances tend to a lower limit (the so-called Cramer-Rao lower limit of the variance-covariance matrix of the parameters). So, this method requires the availability of sufficient measured activity values in several, but not necessarily all, compartments. As a model for measurement noise, i.e., deviations between model response and the

measured activities in the compartments, a normal distribution is assumed, with zero mean and some, time-invariant, variance. A Gaussian probability density function (likelihood function) can then be drafted, which should be maximised with respect to the parameters to yield the optimum match of the model response to the observations. Starting with an arbitrary set of parameter values, the computer code maximises the likelihood function by iteratively computing steps in parameter space according to the Gauss-Newton method, modified to improve convergence (4). In the process the Cramer-Rao lower boundary of the parameter variances is also estimated. From the uncertainties in the final (optimal) parameter values, best estimates of uncertainties in the (cumulated) activities in the compartments, and hence in the absorbed doses, can be derived.

The computer code (Fortran 77) was tested, first on simple three and four compartment models and later on the more complex old and new ICRP biokinetic models for ^{59}Fe ingestion. The latter are, respectively, a chain model of ten compartments with nine parameters (2) and a recycling model of eighteen compartments with twenty-seven parameters (5). Table I may serve as a preliminary illustration of how the computer code meets its design purposes. The likelihood function is maximised by starting from a parameter set that deviates ± 10 per cent from the true set and by using simulated observations (taken from model response for true parameter set, to which ± 10 per cent deviation is added). Not all parameters can be estimated well, even if observations are present in all compartments. However, in general better estimates are produced when all compartments have observations rather than observations being present in only a few compartments. In the latter case, confidence intervals, or uncertainties in parameter values, are much larger. On a Hewlett Packard HP9000/777C110 workstation a typical execution run requires less than 10 iteration steps, lasting about 7 min for the old ^{59}Fe model and about 2 h for the new one.

In many cases no, or insufficient, observations will be available for a meaningful application of the ML method. Therefore, in a second approach to sensitivity analysis, the variability of the model response is evaluated through direct variation of the parameter values. The code for this method is also written in Fortran 77. First, the model response is calculated for a nominal set of parameter values, e.g., the values recommended by the ICRP. Then, sequentially a minimum and a maximum value is assigned to each parameter, whereas the other parameters keep their nominal value. Such minimum and maximum values may follow from literature review or may be based on expert judgement. After

every change the model response is recalculated, using the same (one-time) input of activity. For a model with L parameters this requires 2L recalculations. This will yield an estimate of the maximum influence of every single parameter on the model response.

Alternatively, the 2L combinations of extreme parameter values may be used to recalculate the model response. That will yield an estimate of the maximum variability that the model response can exhibit. For larger models this alternative is not practical. With L=9 (old ⁵⁹Fe model) 512 recalculations at 0.09 s on the HP9000 require 45 s cpu time to cover all extreme combinations. However, with L=27 (new ⁵⁹Fe model) more than 134 million recalculations are necessary, which at 0.42 s each would consume over a year and a half of cpu time.

To illustrate sensitivity analysis by the method of direct variation Figure 1 shows activities in the ten compartments of the old ⁵⁹Fe model (Figure 2), cumulated over 360 d after ingestion of 1 Bq, for nominal (ICRP) values of the transfer rate constants. Bars reflect the result of direct variation of the parameters by a factor of 25, from 0.2 to 5.0 times the nominal

value (except parameter 1: maximum 1.2 times nominal value) and using all extreme combinations. In most compartments the cumulated activity may change by a few orders of magnitude. Intake compartment 1 (stomach) is least affected and, by comparison, the influence on excretion compartment 5 (faeces) is not large either. Varying only parameter seven has relatively little effect on the cumulated activity in all compartments, except for the excretion in compartment 10 (Fig.1, bottom panel). The single action of parameter 3 is larger (Fig. 1, top panel). Increase in parameter 3 causes more activity in compartments 6 through 10 and less activity in compartments 2 through 5. Influence on compartments 3 through 5 is relatively small. Compartment 1 is hardly affected at all.

At present both methods, ML estimation and direct variation of parameters, developed to serve as a tool for the sensitivity analysis of biokinetic multicompartment models, are available in an elementary form. More testing and refinements are necessary before the computer codes can be released for general, user-friendly, application.

Figure 1.

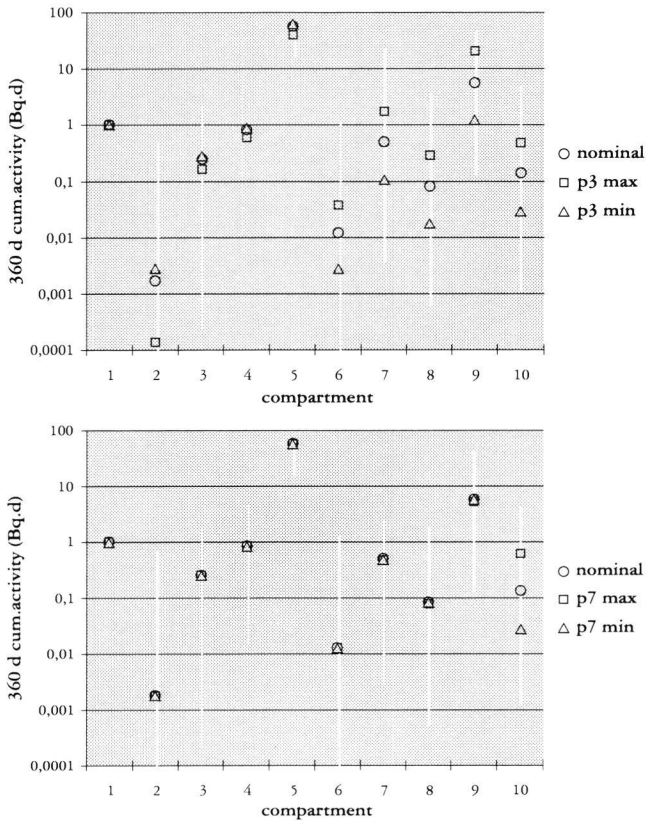
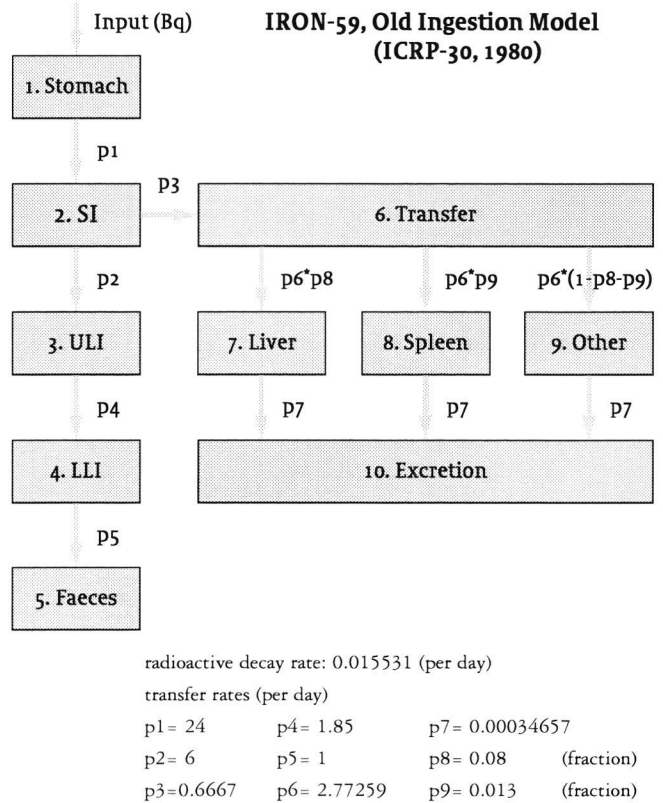


Figure 2.



1. A van Rotterdam.

An algorithm for solving compartmental models describing the stochastic behaviour of radioactive compounds in the body. TNO-CSD Progress Report 1995, pp 18-21, 1996.

2. ICRP (1979-1988).

Limits for intakes of radionuclides by workers. ICRP publication 30. Pergamon Press.

3. Human respiratory tract model for radiological protection.

ICRP publication 66. Pergamon Press, 1994.

4. FW Schultz.

Mathematical modeling in support of optimization of treatment of leukemia. Thesis, Erasmus University Rotterdam, pp 123-161, 1994.

5. Age-dependent doses to members of the public from intake of radionuclides: Part 3

Ingestion dose coefficients. ICRP publication 69. Pergamon Press, 1995.

Table 1. ML parameter estimation using the new iron-59 model

Case A	All compartments observed
Case B	Observations only for plasma, red blood cells, red marrow, urine, faeces
Input	1 Bq in stomach at time 0
Observations	True model response (ICRP parameter values) with assumed ± 10 per cent uncertainty added at ten time points between 0 and 360 d

A Parameter	Transfer		true	Value (1/day)		95% confidence		EC
	from	to		initial	final			
1	Plasma synthesis	red marrow	6	5.4	5.98	5.34	6.63	1.0028
3	Plasma	liver transfer	1.5	1.65	1.49	1.27	1.72	1.0037
5	Plasma	urinary bladder	0.02	0.022	0.02	0.018	0.022	1.0029
15	Liver transfer	small intestine	0.00045	0.00041	0.00058	-0.025	0.026	1.2954
23	Small intestine	plasma	0.6667	0.6	0.6632	0.64	0.69	1.0052
B Parameter	Transfer		true	Value (1/day)		95% confidence		EC
	from	to		initial	final			
1	Plasma	red marrow	6	5.4	5.99	3.75	8.23	1.0021
3	Plasma	liver synthesis transfer	1.5	1.65	1.47	-13.92	16.86	1.0200
5	Plasma	urinary bladder	0.02	0.022	0.02	0.01	0.03	1.0200
15	Liver transfer	small intestine	0.00045	0.00041	-0.0012	-1.22	1.21	—
23	Small intestine	plasma	0.6667	0.6	0.6592	-0.24	1.56	1.0114

EC = $\exp(x)$ where $x = |\ln(p \text{ true}/p \text{ estimated})|$

EC the closer to one, the better the estimated parameter value approximates the true value



5. Biological consequences of exposure to radiation

Exposure to ionising radiations with relatively high doses results in deterministic effects. Acute deterministic effects are for instance reddening of skin and skin burns, late deterministic effects are for instance cataract, loss of organ function such as in kidney and lung, and myelopathy. All these effects will occur when a threshold dose is exceeded. After low as well as high doses stochastic effects may occur for which no threshold doses are assumed. Tumour induction is the most studied stochastic effect. In radiation protection the aim is to prevent deterministic effects and to limit the frequency of stochastic effects to a reasonable extent.

In the following contributions the induction of mammary tumours in rats and the effect of the age at irradiation is described (5.1). In a rat lung tumour model the introduction of a molecular tumour marker for detection of minimal tumour load and the sensitivity of low tumour load for high-dose chemotherapy with bone marrow rescue (5.2 and 5.3) are presented. In contribution 5.4 the chemosensitivity of rat lung tumours and in 5.5 the long-term effects of total body irradiation on the heart of rhesus monkeys are investigated.

5.1. Induction of mammary tumours in rats by single dose gamma irradiation at different ages

R.W. Bartstra, P.A.J. Bentvelzen, J. Zoetelief, A.H. Mulder¹,
J.J. Broerse and D.W. van Bekkum².

Breast cancer is the most frequent malignancy among women in Western countries. Approximately 40 per cent of women with breast cancer will die from the disease, but early detection of mammary tumours reduces mortality considerably. At present, mammography is the most effective method for the early detection of malignant mammary lesions. Therefore, nation-wide breast cancer screening programs have been started in many Western countries. Consequently, the mammary glands of many women (usually in the age range of 50-70 years) will be regularly exposed to low doses of radiation, typical average glandular doses being 1-4 mGy per mammogram. Human epidemiological studies have clearly demonstrated a carcinogenic risk for doses higher than approximately 0.1 Gy. It remains to be established whether irradiation of the mammary gland due to mammographic screening carries a risk of breast cancer induction. To estimate this risk, animal studies in which experimental conditions can be controlled, may provide valuable information. Previous studies at TNO with rats suggested that age at exposure could play an important role (1). Rats irradiated with a dose of 1.2 Gy at 8 weeks of age had an approximate twofold higher risk of mammary carcinoma than rats irradiated at 17 weeks of age. At these ages, rats can be considered as relatively young, both with respect to life-span (100-150 weeks) and to the end of the fertile period (40-60 weeks). Since women participating in breast cancer screening programs are usually beyond the menopause, the sensitivity of the rat mammary gland to irradiation at middle age (>60 weeks) may be more relevant to mammography than at a relatively young age. Therefore, a new study has been performed on the induction of mammary carcinoma by gamma irradiation, using ages at exposure from 8 to 64 weeks. Radiation doses of 1 and 2 Gy have been used to obtain statistically significant results with a limited number of animals per group.

Specific-pathogen-free inbred female WAG/Rij rats were irradiated with ¹³⁷Cs gamma rays, at a dose rate of 0.75 Gy/min. Single total body doses of 1 or 2 Gy were administered at ages 8, 12, 16, 22, 36 or 64 weeks. Each irradiated group comprised 40 rats, the control group of unirradiated animals included 120 rats. The mammary gland regions of the rats were palpated weekly for the presence of nodules or other abnormalities, the date of detection of which was recorded. Mammary lesions persisting for 6 weeks were removed by surgery, and the rats remained under observation. Animals were sacrificed only when moribund. At necropsy all palpable mammary nodules were excised. Tissues taken at surgery or at necropsy were histologically examined.

Only the first detected carcinoma of each rat was taken into account in the data analysis. For each experimental group, a Weibull function was fitted to the tumour data, which was used to derive the value of excess normalised risk (ENR) with reference to the control group (2).

Figure 1 shows the ENR as a function of age at exposure for single doses of 1 and 2 Gy. In either case, there is no statistically significant difference between the groups exposed at ages 8, 12, 16, 22 or 36 weeks (one-sided χ^2 -test of 1 Gy results: $p \geq 0.09$; 2 Gy results: $p \geq 0.16$), neither do these groups suggest any age-specific trend when the two curves of Figure 1 are compared. It seems, therefore, justified to pool the age groups 8 to 36 weeks for both dose levels separately. In the pooled analysis, the ENR at a dose of 2 Gy is approximately twice the risk at 1 Gy. For exposures at 64 weeks of age, not only is the ENR significantly reduced as compared to the risk in the younger age groups, but it is negative, i.e., these animals have a risk of developing mammary cancer that is smaller than that in unirradiated control rats. This effect is observed for both 1 and 2 Gy, but it is statistically significant only for a dose of 1 Gy ($p=0.016$). As we have observed similar effects in a study in which the rats were treated with oestrogens (3), it seems highly unlikely that the phenomenon is due to chance. This oestrogen study also rejects explanations, that are based on changes in the plasma oestrogen level in rats as a result of the total body dose, such as radiation induced anovulation. The negative ENR may neither be adequately explained by a reduction with age of the number of clonogenic mammary cells, or of their susceptibility with respect to malignant transformation, since even a reduction down to zero would not yield a cancer risk below the control level. A possible explanation may be that initiated and premalignant mammary cells, that have occurred spontaneously up to the moment of irradiation, may be sterilised by the radiation, therefore no longer being capable of developing into a tumour. The present results on the influence of age at exposure on the risk of mammary cancer in rats show a similar trend as the available epidemiological data in women (4, 5).

Dose-response curves, i.e., excess normalised risk as a function of dose, are presented in Figure 2 for the combined age groups (exposed at 8-36 weeks) and for the groups exposed at 64 weeks of age. Also included are the results obtained previously by Broerse et al. (1) for ages at exposure 8-17 weeks, after a reanalysis of their data (2). A linear dose-response model was fitted to the data obtained in age groups 8-36 weeks of the present study, and in age groups 8-17 weeks of the previous one, yielding a value of 1.1 Gy⁻¹ for the

ENR per unit of dose (95%-CI: 0.8, 1.4). The dose-response curve for irradiation at 64 weeks of age has a negative initial slope, and cannot be described by a straight line (Fig. 2).

In rats, an age of 64 weeks may correspond to an age of approximately 45 years in women (2). Therefore, our results suggest that irradiation of the mammary gland with doses below 1 Gy at ages currently adopted for regular mammographic screening, does not carry a risk of breast cancer induction.

Conclusions:

Irradiation of WAG/Rij rats with a total body dose up to 2 Gy at younger ages will result in an induced excess risk of mammary cancer that is approximately linear with dose, but the excess risk vanishes for exposures at middle age. The latter exposures may even yield a negative excess relative risk, i.e., a reduction of the risk of mammary cancer below the control level. Although these results have been obtained with single, relatively high total body doses, they suggest that dose reduction in mammography is important for young women, but probably not crucial for elderly women.

¹ Pathological Anatomical Laboratory, Dordrecht;

² Intogene B.V., Leiden.

1. JJ Broerse, DW van Bekkum and C Zurcher.

Radiation carcinogenesis in experimental animals. *Experientia* 45, 60-69, 1989.

2. RW Bartstra, PAJ Bentvelzen, J Zoetelief, AH Mulder, JJ Broerse and DW van Bekkum.

Induction of mammary tumors in rats by single dose gamma irradiation at different ages. *Radiat Res* 150, 442-450, 1998.

3. RW Bartstra, PAJ Bentvelzen, J Zoetelief, AH Mulder, JJ Broerse and DW van Bekkum.

The influence of estrogen treatment on induction of mammary carcinoma in rats by single dose gamma irradiation at different ages. *Radiat Res* 150, 451-458, 1998.

4. A Mattsson, BI Rudén, P Hall, N Wilking and LE Rutqvist.

Radiation-induced breast cancer: long-term follow-up of radiation therapy for benign breast disease. *J Natl Cancer Inst* 85, 1679-1685, 1993.

5. GR Howe and J McLaughlin.

Breast cancer mortality between 1950 and 1987 after exposure to fractionated moderate-dose-rate ionizing radiation in the Canadian fluoroscopy cohort study and a comparison with breast cancer mortality in the atomic bomb survivors study. *Radiat Res* 145, 694-707, 1996.

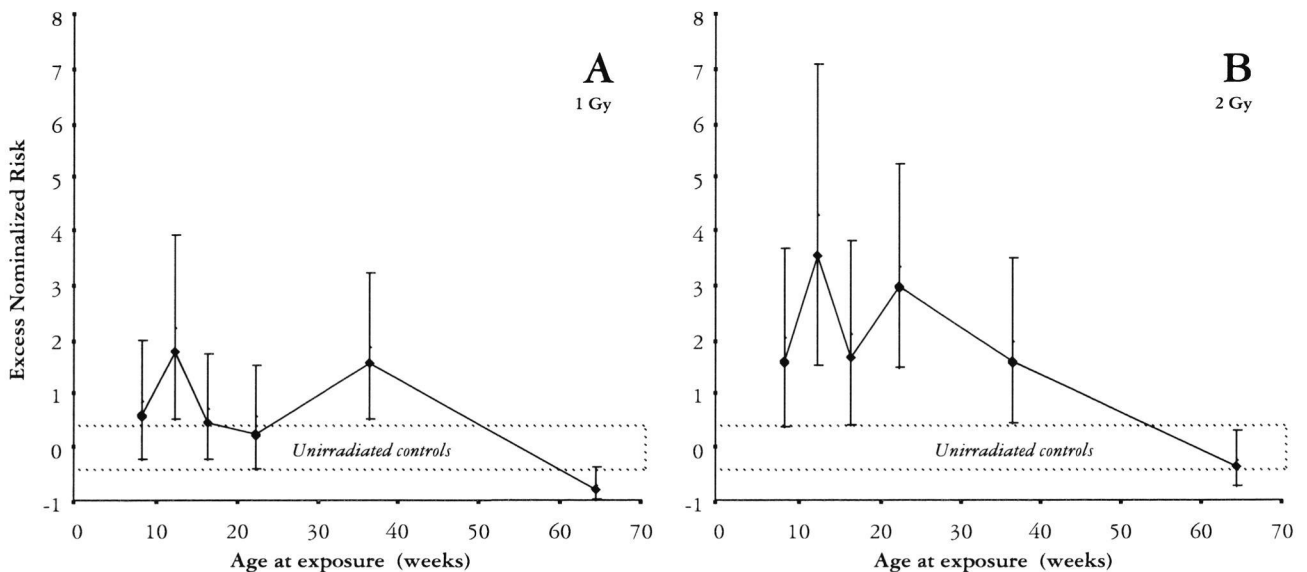


Figure 1. Excess normalised risk of mammary carcinoma in WAG/Rij rats, after single dose gamma irradiation with 1 Gy (panel A) or 2 Gy (panel B) at different ages. Error bars represent the 95 per cent confidence intervals.

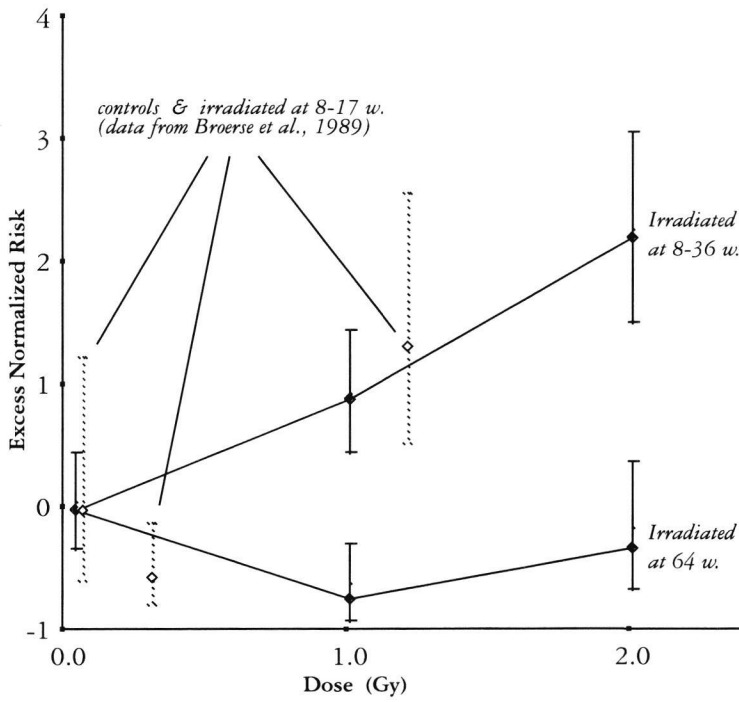


Figure 2. Dose-response curves for induction of mammary carcinoma in WAG/Rij rats, after single dose gamma irradiation at ages 8-36 or 64 weeks. Also shown is the result of a reanalysis of the data obtained previously for ages at exposure 8-17 weeks (1). Error bars represent the 95 per cent confidence intervals.

5.2. Introduction of a molecular tumour marker in rat lung tumour cells for detection of minimal tumour load

P.J.N. Meijnders¹ and H.B. Kal

An important parameter for the efficacy of an experimental cancer therapy is the maximum tumour load reduction that can be achieved. For solid tumours, a sensitive and reliable measurement of tumour load in case of minimal residual disease or metastases is currently not available.

For detection of low tumour load the lacZ gene was introduced in rat lung tumour cells as a marker gene. Its product, β -galactosidase, can be detected histochemically by staining tissues or cultured cells with X-Gal (5-chloro-4-bromo-3-indolyl- β -D-galactosidase). A technique was developed to determine the tumour load quantitatively (1).

L37 and L44 rat lung tumour cells were infected in vitro with the retroviral shuttle vector BAG, containing the lacZ gene. After subcutaneous inoculation of the transduced cells, tumours developed with preservation of their characteristics compared to the parental line.

The β -galactosidase activity in cell lysates could be measured spectrophotometrically using ONPG (o-nitrophenyl- β -D-galactosidase) as a substrate, or fluorometrically using MUG (4-methylumbelliferyl β -D-galactopyranoside) as a substrate. Spectrophotometrical as well as fluorometrical measurements of cell suspensions revealed a linear increase of β -galactosidase activity with increasing cell numbers. Mixing cell lysates of cultured cells with homogenated total lung lysates demonstrated the possibility of detecting β -galactosidase activity in lung lysates.

After iv injection of transduced L44 tumour cells lung nodules developed. Measuring β -galactosidase activity in

lysates of lungs with tumour deposits revealed a linear increase of enzyme activity with increasing tumour weight. Expressed in enzyme activity per gram tumour, 0.5 gram tumour cells could be detected in lung lysates, that is about $5 \cdot 10^8$ cells. The in vitro experiments demonstrated that the lower detection limits are about $2 \cdot 10^4$ cells for the spectrophotometrical assay (ONPG) and about 200 cells for the fluorometrical assay (MUG). Thus, less tumour cells were detected in the in vivo experiments than expected from the in vitro data.

The discrepancy between the in vitro and in vivo - experiments is probably related to down-regulation of the lacZ gene in the absence of the drug G418 or loss of enzyme activity in the lysates. It might also be a phenomenon of dying cells that down-regulate all non-vital genes. Suggestions for improvement are made varying from better designed gene constructs to a better selection for high-titre producing cell lines and the use of mutant green fluorescent protein (GFP) genes for transfection experiments in tumour models (1).

¹ Algemeen Ziekenhuis Middelheim, B-2020 Antwerp.

1. P.J.N. Meijnders.

The application of rat lung tumour models in experimental therapy of bronchial cancer. Thesis, University of Leiden, 1998.

5.3. Sensitivity of low tumour load in rats for high dose chemotherapy with bone marrow rescue

P.J.N. Meijnders¹ and H.B. Kal

If loco-regional control can be achieved in lung cancer patients, at least half of them will die eventually due to distant metastasis. It seems therefore sensible to treat them with adjuvant chemotherapy. Unfortunately, effective chemotherapeutic regimens for non-small cell lung cancer do not yet exist. In most cases haematological toxicity is dose limiting. The limits posed by haematological toxicity can be increased by bone marrow transplantation. The effectivity of supralethal chemotherapy and bone marrow support for the treatment of non-small cell lung cancer is explored in the rat lung tumour model (1-3).

The LD50 values for WAG/Rij rats could be increased

with bone marrow support for ifosfamide in combination with mesna, TCNU, etoposide and vinblastine but not for carboplatin (Table 1).

Dose-response relationships as well tumour volume dependency were established for single drugs with and without bone marrow rescue, an example is shown for L37 tumours treated with ifosfamide at a tumour volume of 200 mm³ (Table 2).

In order to evaluate the effects of treatment on minimal residual disease 6 to 8 tumour fragments were implanted subcutaneously in the flanks and treated early on day 7 after implantation. These tumours served as model for small

metastases. In this way the sensitivity was established for small L37 rat lung tumours. The implant of 6 to 8 tumours per animal was feasible, and tumour growth delay data could be obtained per individual tumour. Treatment of small (<10 mm³) L37 tumours resulted in a higher tumour growth delay (TGD) for TCNU than for larger tumours (500 mm³) (Table 3). Dose-response relationships were also shown for etoposide and ifosfamide/ mesna, but not for vinblastine. In case of ifosfamide, the number of cures increased with augmented dose.

In this rat lung tumour model ifosfamide, etoposide, vinblastine and TCNU were appropriate for high-dose chemotherapy with bone marrow support. A dose-response relationship was demonstrated for ifosfamide, TCNU and etoposide.

¹ Algemeen Ziekenhuis Middelheim, B-2020 Antwerp.

1. PJN Meijnders.

The application of rat lung tumour models in experimental therapy of bronchial cancer. Thesis, University of Leiden, 1998.

2. HB Kal, AH van Berkel, C Zurcher, T Smink and DW van Bekkum.

A rat lung cancer model based on intrapulmonary implantation of tumour material. Radiotherapy & Oncology 6, 231-238, 1988.

3. HB Kal.

In vivo models for testing of cytostatic agents in non-small cell lung cancer. Chapter 8 in: Lung Cancer, HH Hansen (ed.), 1994.

Table 1. LD50 values for WAG/Rij rats with or without bone marrow transplantation (BMT)

Drug	LD50 without BMT (mg/kg)	LD50 with BMT (mg/kg)	DMF*
IFO/mesna	628	1000	1.6
TCNU	64	>75	>1.2
Etoposide	42	60	1.4
Vinblastine	4.3	6.0	1.4
Carboplatin	99	99	1.0

* DMF: dose-modifying factor = LD50 with BMT/LD50 without BMT

Table 2. Dose-response relationship of L37 tumours for ifosfamide and mesna determined at a tumour volume of 200 mm³

Dose (mg/kg)	survival ¹	TGD (d)	SGD	cure	SGD*
300	2/2	26.5	7.0		
400	2/2	31.7	8.3		
500	2/2	26.9	7.1		
600	4/4	33.0	8.7	1	13.1
with BMT					
400	4/4	30.8	8.1		
600	4/4	37.6	8.8	2	18.1
800	4/4	40.3	10.6	1	14.5
1000	2/4			2	26.3

* SGD assuming a TGD of 100 d for 1 cure

¹ Number of surviving animals/total number of animals per group

Table 3. Dose-response relationship of the L37 tumour for TCNU treatment: tumour growth delay (TGD) and specific growth delay (SGD)

n1	n2	treatment at day	Td(d)	TGD (d) and (SGD)		
				20 mg/kg	25 mg/kg	30 mg/kg
1	5	39.5**	8.2	10.4 (1.3)	21.2 (2.6)	22.0 (2.7)
1	5	7***	8.2	16.3 (2.0)	20.2 (2.5)	54.1 (6.6)*
8	5	7***	6.3	20.4 (3.2)	24.9 (4.0)	45.1 (7.2)*

* 1 cure

** tumour volume is 500 mm³*** tumour volume is < 10 mm³

n1: number of tumours per animal

n2: number of animals per group.

5.4. Thermosensitivity of experimental rat lung tumours

P.J.N. Meijnders¹ and H.B. Kal

Local control is an important requirement for improvement of the survival of lung cancer patients. Hyperthermia is a well-established treatment modality in tumour therapy. A cytotoxic effect at temperatures above 42°C has been established. Hyperthermia has shown to enhance local control probability in locally advanced mammary carcinomas and cervical carcinomas. The rat lung tumour model was used to explore the responsiveness of lung tumours to hyperthermia in an experimental set-up (1-3).

A capacitive RF external heating system was used working at 27 MHz, delivering energy deposition with an applicator consisting of 2 condensator plates surrounded by a temperature regulated 1 % saline bolus (Fig. 1). Subcutaneously implanted L33, L41 and L44 rat lung tumours were carefully positioned between the applicator plates. Temperatures were measured with an optic ASEA fiber thermometer inserted in a set of catheters placed inside the tumour (Fig. 1). The temperatures in the central catheter were kept constant using a feedback-regulatory unit. Temperatures achieved were between 43 and 50°C. At the higher temperatures the skin was temporarily removed during treatment to prevent excessive skin damage. Treatment endpoint was tumour growth delay or cure. In some experiments the effects of hyperthermia combined with chemotherapy (melphalan and ifosfamide) was studied.

Tumour growth delay with hyperthermia alone was seen when a high tumour temperature was obtained. Even tumour cures were seen in the highest dose groups (Table 1). Skin damage in these groups was however considerable. Removing the skin during treatment was sometimes successful.

Pulsed-dose hyperthermia (or cyclic heating, e.g. 10 s

power on, 5 s power off) did not decrease the amount of skin damage, but appeared to be a valuable tool to deliver heat to a tumour in a very homogeneous way. Ifosfamide and melphalan enhanced the effects of hyperthermia by at least a factor of 2 (Table 2).

The results demonstrate that high heat doses applied for a short treatment time can be curative in vivo and can be administered with acceptable toxicity to normal tissues. With the capacitive 27 MHz system, tumour temperatures of 50°C were achieved in a controlled way.

¹ Algemeen Ziekenhuis Middelheim, B-2020 Antwerp.

1. PJN Meijnders.

The application of rat lung tumour models in experimental therapy of bronchial cancer. Thesis, University of Leiden, 1998.

2. HB Kal, AH van Berkel, C Zurcher, T Smink and DW van Bekkum.

A rat lung cancer model based on intrapulmonary implantation of tumour material. Radiotherapy and Oncology 6, 231-238, 1988.

3. HB Kal.

In vivo models for testing of cytostatic agents in non-small cell lung cancer. Chapter 8 in: Lung Cancer, HH Hansen (ed.), 1994

Table 1. Thermosensitivity of L44 tumours growing subcutaneously: tumour growth delay and specific growth delay as a function of treatment time and temperature, saline bolus temperature is 39°C.

treatment temp. (°C)	time (min)	EHD	TGD (d)	SGD
43	60	1	1.3	0.4
45	30	2	3.0	1.0
48	5	3	3.0	1.0
50	5	11	2.8	0.6
50	9*	19	15.9	5.5**
50	20*	42	26	9

* saline bolus temperature is 49°C.

** 2 cures are not included in this figure

*** cyclic hyperthermia, bolus temperature 47°C

EHD: equivalent heat dose= equivalent to hyperthermic treatment of 43°C for 60 min

TGD: tumour growth delay

SGD: specific growth delay= tumour growth delay/tumour doubling time

Table 2. Combined effects of chemotherapy and hyperthermia on rat lung tumours growing subcutaneously

tumour	drug	dose (mg/kg)	temp (°C)	time (min)	TGD (d)	SGD
L44	ifosfamide	250			19	4.8
			45	5	2	0.6
	ifosfamide	250	45	5	34	8.5
L33	melphalan	5			0	0
			45	15	1.5	0.2
	melphalan	5	45	15	15.6	2.2

TGD: tumour growth delay

SGD: specific growth delay= tumour growth delay/tumour doubling time

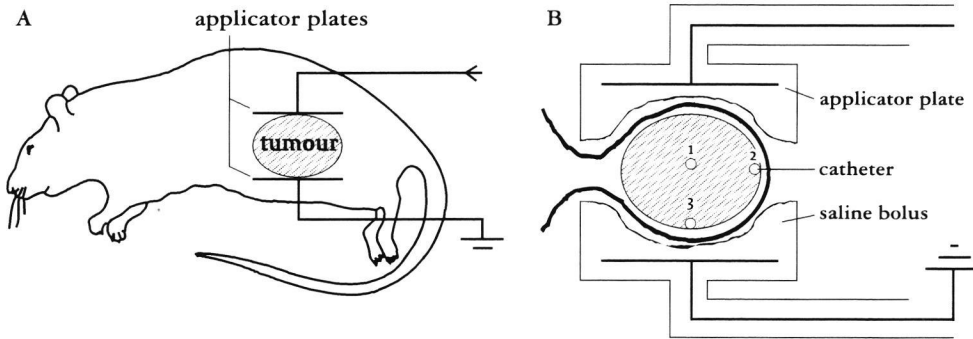


Figure 1. Hyperthermic treatment with the capacitive RF applicator. Application of the hyperthermic device around the flank tumour; (B) coronal view of the capacitive plates and the saline bolus around the tumour (1: core catheter, 2 and 3: peripheral catheters).

5.5. Long-term deterministic effects of high-dose total-body irradiation on the heart of rhesus monkeys; are changes in circulating atrial natriuretic peptide relevant?

J. Wondergem¹, C.C.M. Persons¹, M. Fröhlich², C. Zurcher¹ and J.J. Broerse

In this project, the relation between echocardiographic parameters and plasma-ANP (atrial natriuretic peptide) values was studied in rhesus monkeys previously treated with total body irradiation (TBI) without additional chemotherapy, at post irradiation intervals up to 30 years, at the former TNO Primate Centre at Rijswijk. The present data show that screening of ANP plasma concentrations is important since circulating levels of ANP correlate with the degree of cardiac damage, even when cardiac disease is still subclinical. Echocardiographic parameters also used in this study did not reveal differences in cardiac function between the experimental groups.

Bone marrow transplantation (BMT) has become the major salvage treatment approach for patients with relapsed haematological malignancies. Increasing numbers of patients have been successfully treated using high-dose therapy (high-dose chemotherapy combined with total body irradiation) and BMT. With the increasing number of surviving BMT recipients, more emphasis is being placed on the long term adverse effects of the "conditioning" treatment. At present, several long-term sequelae have been reported after high-dose therapy including intensive chemotherapy combined with TBI. Long-term effects (both stochastic and deterministic) of TBI of rhesus monkeys have been studied by Broerse and colleagues. Recent data on the effect of TBI on different organ systems of the rhesus monkey have been presented during the EULEP TBI symposium in Oxford in 1997. Radiation experiments with primates are of great importance since the radiation response of monkeys closely matches that of man. Cardiac toxicity is an important clinical complication of some chemotherapeutic drugs, such as anthracyclines and cyclophosphamide, and of mediastinal irradiation. Since both modalities are used as conditioning treatment for BMT, long-term survivors may have a potential risk for cardiac complications. To date only limited information on the effect of BMT on cardiac function is available yet. Moreover, no data are available on the presumed cardiotoxic effect of TBI as a single factor. Based on clinical and experimental data the use of plasma ANP as a marker for cardiac damage is suggested. Atrial natriuretic peptide (ANP) is a peptide hormone produced predominantly in the right atrium of the heart. The physiological role of ANP is to activate the homeostatic mechanism that restores normal blood volume (and pressure) and electrolyte levels. It has potent diuretic and vasorelaxant properties and an inhibitory effect on renin and aldosterone secretion. The biological half life of ANP in plasma is 30 - 90 s. Elevated plasma-ANP levels have been

found in heart failure both in patients and in animals.

In order to determine the presence of cardiac damage associated with TBI, both circulating levels of ANP and echocardiographic parameters (to determine cardiac function and cardiac dimensions) were studied. Cardiac function was studied in different cohort of monkeys, their age ranging from 6 to 24 years. A total of 45 (22 irradiated and 23 controls) animals were evaluated 5 - 20 years after treatment. Blood was collected in pre-chilled EDTA tubes from the femoral vein in order to screen the animals for changes in plasma-ANP levels. Plasma was prepared immediately by centrifugation for 10 min at 1800 g and 4°C, frozen under liquid nitrogen and stored at -70°C until analysis. The ANP was extracted from plasma samples using Sep-Pak1B cartridges. ANP levels were measured by radioimmuno-assay (Peninsula Laboratories Inc., Belmont, Ca, USA). Blood pressure was measured by the cuff method. Echocardiograms were recorded by using standard echocardiographic techniques and positions (combined 2-dimensional and M-mode echocardiography, and doppler), with a Hewlett Packard Sonus 1000 ultrasound system.

Before cardiac evaluation all animals underwent a general physical examination. No clinical signs of cardiac disease were present upon cardiac examination. Irradiation and gender had a large influence on body weight of rhesus monkeys. Animals which received TBI had highly significantly lower bodyweights compared to that of non-treated animals. Males were heavier than females both in the irradiated and non-irradiated group. In contrast to body weight, final height (size) of the animals was hardly influenced by irradiation to a lesser extent. Males were significantly longer than females. Calculated Body Surface Area (BSA) was strongly dependent on treatment and gender. In spite of the fact that this monkey population was very heterogeneous, plasma-ANP levels of animals which received TBI were significantly ($p=0.015$) elevated when compared to age-matched controls (64.2 ± 9.4 pg/ml vs. 39.9 ± 5.7 pg/ml). When plasma-ANP values were plotted as function of time post treatment a positive relationship became evident (Fig. 1); ANP-values increased with increasing time interval between irradiation and evaluation. Autopsy reports demonstrate light but consistent cardiovascular damage in several animals treated with TBI (increased incidence of mild epicardial and perivascular fibrosis). No clear differences in "classical" cardiac parameters such as blood pressure and heart rate were observed between the different groups. Table 1 shows echocardiographic measurement of cardiac dimensions of animals, which

received TBI and age-matched controls. Since cardiac dimensions measured by echocardiography are strongly influenced by BSA, all data were corrected for differences in BSA. After TBI, L. ventricular dimensions (both diastolic and systolic dimensions) were significantly smaller when compared with untreated controls. No effect of irradiation on L. atrial dimensions, aortic dimensions, posterior wall thickness and interventricular septum thickness was observed. As parameters of L. ventricular systolic function both Fractional Shortening (FS) of the left ventricle was measured. FS was calculated as the difference between end-diastolic and end-systolic LV dimensions expressed as a percentage of the end-diastolic dimension. No change in FS as a result of TBI could be observed.

Conclusions:

The concentration of plasma-ANP proved to be important since the present data show that circulating levels of ANP correlate with the degree of cardiac dysfunction, even when cardiac diseases is still subclinical. In the clinic, serial determinations of plasma ANP in individual patients might provide important information about the cardiac status after TBI.

¹ Department of Clinical Oncology and
² Department of Clinical Chemistry, Leiden University Medical Center, Leiden, The Netherlands.

Table 1. Effect of total body irradiation on cardiac dimensions* (cm) using echocardiography (M mode; long axis)

	Age-matched controls (n=23)	irradiated animals (n=22)	
Intercentricular septum	0.56 ± 0.03	0.55 ± 0.03	(NS)
Posterior wall	0.56 ± 0.02	0.58 ± 0.02	(NS)
Left ventricle (d)	3.21 ± 0.08	2.86 ± 0.06	(p=0.002)
Left ventricle (s)	1.90 ± 0.07	1.75 ± 0.03	(p=0.069)
Left atrium	2.08 ± 0.07	2.06 ± 0.09	(NS)
Aorta	1.75 ± 0.05	1.68 ± 0.05	(NS)

* cardiac dimensions (CD) are corrected for differences in body surface area (BSA) according to: $CD(\text{corr}) = CD \times (BSA)^{-1/3}$.

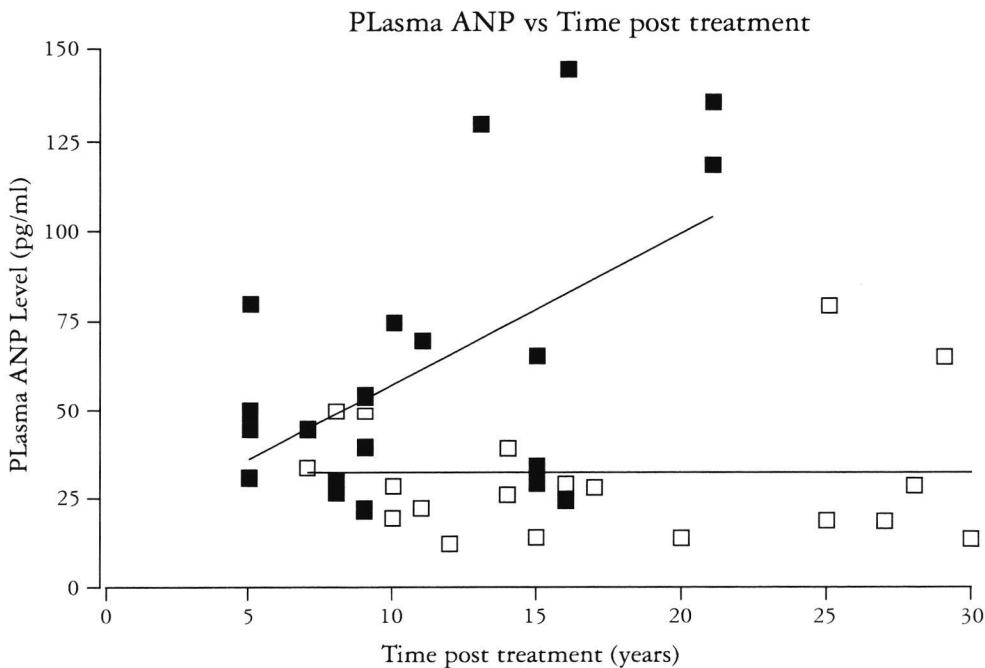


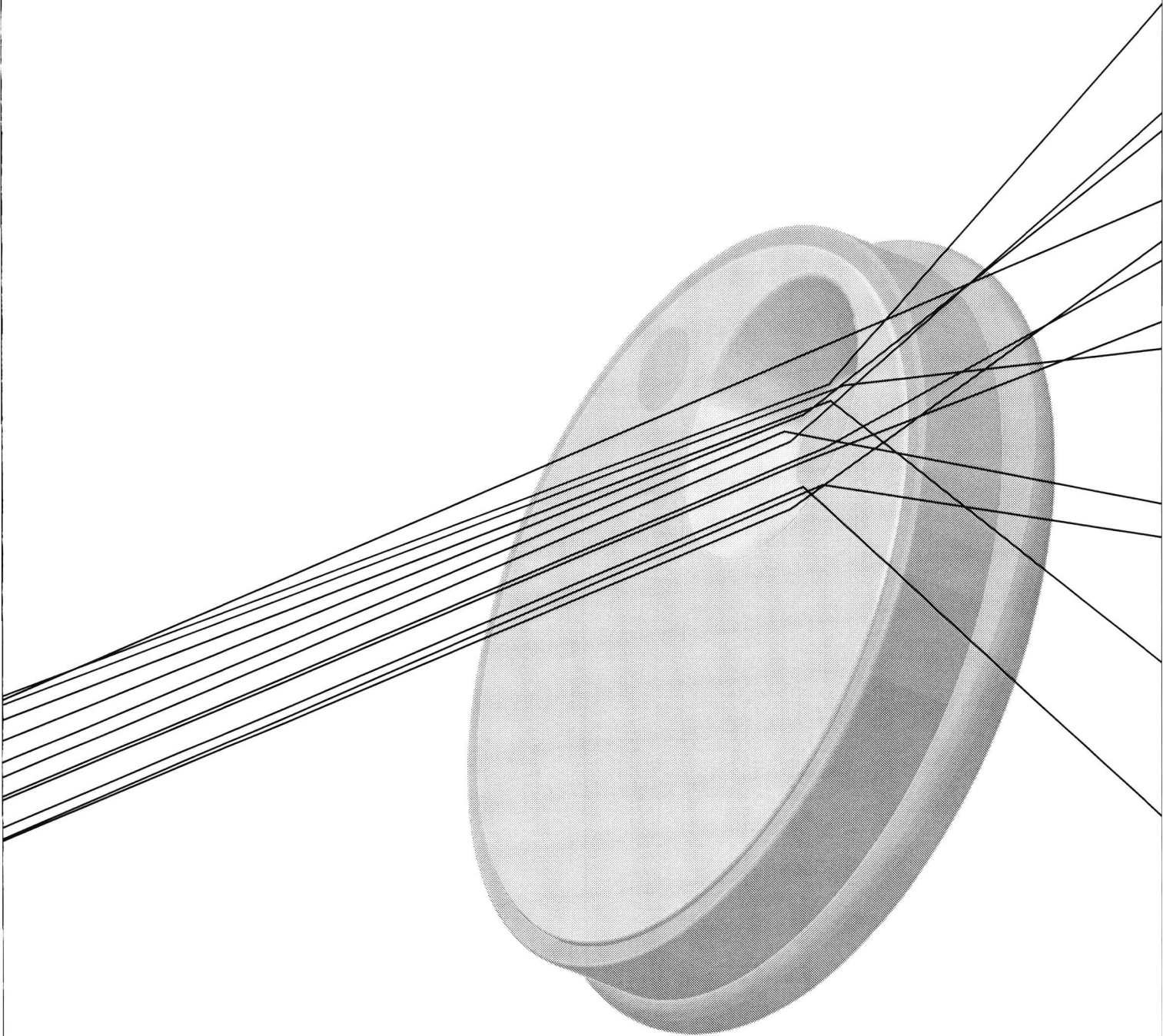
Figure 1. Relation between plasma ANP concentration and the time post treatment (years). Irradiated hearts: closed squares; age-matched control hearts: open squares. N=45 animals (22 irradiated and 23 controls).



I. Research and Development

II. Services

III. Publications and Reports





Services

TNO-CSD offers a variety of services among which:

- Thermoluminescence dosimetry for individual monitoring and other dosimetry services of special applications.
- A number of analytical services for both environmental and worker conditions. Standard protocols are available for a number of radioactivity analyses. Most of these protocols are tested in international comparisons.
- Quality Assurance (QA) developed for equipment in diagnostic radiology departments. These QA services are intended for those hospitals that do not have the necessary expertise and technical facilities available.
- Assistance to investigate the working environment in order to verify that exposure of the radiation worker is kept as low as reasonably achievable.
- A wide range of radiation sources and measuring equipment for calibration and type testing of instruments.
- Computer (Monte Carlo) simulations of radiodiagnostic procedures that can be performed to obtain quantitative information on dosimetric quantities in case making measurements is impossible or impractical, i.e., calculation of effective doses, depth-dose curves, influence of filters applied.
- Measurements of various patient-related dosimetric quantities, as well as for the assessment of image quality by performing measurements on images of contrast-detail phantoms. This is to ascertain that the radiation exposure to the patient should be kept as low as possible, but still compatible with the image quality required for an adequate diagnosis.

More information about these services are provided in the following contributions.

1. Thermoluminescence dosimetry

J.W.E. van Dijk

Individual monitoring

The individual Monitoring Service of TNO-CSD is an Approved Dosimetry Service, licensed by the Ministry of Social Affairs and Employment. The thermoluminescence dosimeters (TLDs) are issued on a bi-weekly and four-weekly basis. Two types of dosimeters are used, one type is designed to measure both photons (X and gamma rays) and beta's, the other to detect photons only. The quantities measured are body dose, $H_p(10)$, and skin dose, $H_p(0.07)$. The dosimetry system complies with the 'Technical Recommendations for Monitoring Individuals Occupationally Exposed to External Radiation' (EURATOM document EUR 14852) with respect to energy and angular response and with respect to precision and accuracy (detection limit 0.01 mSv). The dosimetry, the dose record keeping system and the administrative procedures are all included in an extensive Quality Assurance program. TNO monitors approximately 27,000 radiation workers,

which is 85 per cent of the national need. The service offered includes return mail, periodical dose reports (English optional), an annual dose report and same day reports for doses higher than 1 mSv.

Special TLDosimetry

The TNO thermoluminescence dosimetry system is a flexible system that allows to offer various TLD based services. Single detectors can be encapsulated in plastic after which they can be swallowed by patients to be treated with ionising radiation. On the other end, detectors with a more robust casing are used in oil production platforms for cost effective measurements of radioactive scaling in the piping. The high reproducibility and low detection limits allow the TNO-TLDs to be used for environmental dosimetry and experimental studies.

2. Radioactivity analyses

P. de Jong and W. van Dijk

TNO Centre for Radiological Protection and Dosimetry provides a number of analytical services, for both environmental and worker oriented research. The many years of experience, together with an adequate quality control system, guarantees highly accurate results that meet international standards. Standard protocols are available for the following services:

- Determination of the natural radioactivity of industrial by-products (inhomogeneous) waste, building materials, gravel, soils, etc.
- Determination of internal contamination by whole-body counting.
- Analysis of excreta to estimate the degree of uptake of radionuclides and to determine the effective dose in individuals.
- Wipe and leak tests of encapsulated sources.
- Determination of artificial radionuclides in food stuff and environmental samples.
- Air monitoring in working environments.
- Determination of radon in air, both long-term (integrated) and instantaneous.
- Environmental monitoring of radiation fields by thermoluminescence dosimetry or ionisation chambers.

A method was developed for the determination of radium

(Ra-226) and radon (Rn-222) concentrations in water. In this method the sample of interest is purged by nitrogen gas and the outflowing radon trapped on silica gel at -190°C .

Approximately 16 h after sampling, the silica gel is analysed by liquid scintillation counting to determine the radon level. The reliability of the method was verified by means of an international intercomparison, organised by the World Health Organisation (WHO), the results of which are shown in Table 1. The same method is applied for the determination of the radon exhalation rate of building materials, amongst others employed in studies after the retarding effect of paint systems and the effects of the production process and composition of concrete slabs. During all investigations, the results of the sampling and the counting facility were verified using a laboratory standard phosphogypsum block. Its repeatability was found to be 5 per cent (relative standard

Table 1. Results of an international intercomparison on the determination of Ra-226 concentrations in water

	Ra-226 concentration (Bq/l)	
	Mean	95% confidence interval
All participants	2.07	1.71 - 2.43
WHO results	2.33	2.26 - 2.40
TNO-CSD results	2.26	2.14 - 2.38

deviation) overall period of 8 years.

A method was developed to assess radon progeny concentrations in air, taking into account both the attached and the unattached fractions. In the radon inhalation facility

a detection limit was obtained of approximately 1 Bq.m^{-3} Rn-EEC for PAEC-values, based on a single measurement. Research is in progress to verify the method under more realistic conditions in a physical model of a dwelling.

3. Quality assurance in diagnostic radiology

L. van den Berg and J. Moor

Since the publication of the EU Directive Euratom 1984/466 (often referred to as "Radiation Protection of the Patient") and its implementation in the Dutch legislation, attention has increasingly been focused on Quality Assurance (QA) in medical diagnostic radiology. The main aim of QA is to provide good quality diagnostic images, while keeping the dose to the patient as low as reasonably achievable.

Achieving and demonstrating good quality requires implementation of a QA programme. A QA programme includes systematic testing of diagnostic X-ray equipment and related tools (e.g. viewing boxes and film processors) and an organisational structure describing the responsibilities of the staff of the radiology department.

Ideally the performance of a diagnostic X-ray unit would be characterised by two key parameters: the effective dose to the patient and the quality of the image produced. However, methods to quantify the image quality are still subject of

scientific research, while determination of the dose to the patient is far from straight forward. In practice, QA in hospitals can best be assured by testing a set of physical (technical) parameters of the equipment, such as kVp, tube load, beam limitation, filtration, focal spot size and several others.

TNO-CSD, participating in the Working Group "Quality Criteria for diagnostic X-ray Equipment" developed measuring protocols for evaluating the performance characteristics ("status") of X-ray equipment in co-operation with medical professionals and hospital physicists. So far, eleven protocols have been prepared (see 2.5). These protocols have been tested in medical practice.

TNO-CSD provides QA services for diagnostic radiology departments in those hospitals that do not have the necessary expertise and technical facilities available.

4. Radiation safety at the workplace

L. van den Berg and J. Moor

The working conditions of persons working in the vicinity of sources or using sources of ionising radiation should comply with radiation protection criteria. Individual monitoring, necessary to verify that no worker receives a dose in excess of the specified dose limits, may provide useful information on the radiation safety of the work place. It is, however, often desirable to investigate the working environment to verify that exposure of the worker is kept as low as reasonably achievable (ALARA). In cases where local expertise and/or measuring facilities are not available, TNO-CSD provides assistance. Investigations are made using calibrated instruments and following working procedures approved by the government.

When existing facilities need remodelling or when new constructions meant to accommodate radiation sources are being designed (e.g. X-ray rooms in hospitals), radiation

protection aspects, i.e. shielding, require careful consideration. This is another area where TNO-CSD can give advice, having the facilities to assist in making calculations for optimal shielding.

5. Calibration of instruments

L. van den Berg and J. Moor

A wide range of radiation sources and measuring equipment is of paramount importance for scientific research in radiation dosimetry. These facilities are available at TNO-CSD and are also used to evaluate, type test or calibrate radiation protection instruments for suppliers, hospitals and (nuclear) industry. To report the results certificates are issued. The sources and ionisation chambers/electrometers used by CSD are traceable to primary standards, calibration procedures are based on standard protocols. The following radiation sources are available:

Radiation source	(max) energy (keV)	remarks
Co-60	1250	4 sources
Cs-137	662	4 sources
X rays	10-320	filtered beams
Beta rays	225-2300	¹⁴⁷ Pm, ²⁰⁴ Tl, ⁹⁰ Sr/ ⁹⁰ Y

If the customer so desires reference radiations as specified by ISO (International Standards Organisation) are used (Narrow as well as Wide Spectrum Series).

6. Monte Carlo computer codes

F.W. Schultz

When measuring is impractical or impossible computer simulation employing Monte Carlo (MC) techniques may offer an alternative way of evaluating dosimetric quantities. During the past few decades sophisticated computer codes have been developed, tested and benchmarked, against each other and against physical experiments, with satisfactory results. Such computer codes are based on mathematical models of radiation physics and use compiled numerical data on interactions of radiation and matter. In essence, MC techniques determine the fate of radiation particles, transported along simulated paths through matter in a region of interest, by random selection from probability density distributions that describe the likelihood of the direction of the path and the events encountered (e.g., scatter, energy deposition, creation of secondary particles). The probability density distributions depend on the nature of the simulated particle (type, energy) and on the nature of the material it crosses (density, composition). The contribution of each particle to a sought dosimetric quantity is recorded. By simulating a great many random particle histories statistically reliable average values and uncertainty estimates are calculated. Users must supply details about the radiation source, shape and quality of the beam, the irradiated object and any other parts of the exposure geometry.

At TNO-CSD the MC code "MCNP" (Monte Carlo Simulation of N Particles) version 4A (released in 1993) is being used. This is a general-purpose code for simulation of neutrons, photons and electrons. The software package was developed at Los Alamos National Laboratory.

The well-known code "EGS4" (Electron Gamma Shower 4) originating from Stanford Linear Accelerator Center is also available. Both codes run on a Hewlett-Packard HP9000

model 777/C110 workstation.

A number of mathematical anthropomorphic phantoms are available for application in combination with MCNP. They can be used, for instance, to calculate organ dose distributions. All organs that are of importance to radiological protection are modelled. The phantoms represent the reference adult male and female, and a seven years old girl. Another phantom family consists of male and female children of ages 15, 10, 5 and 1 year, and new-born babies.

At TNO-CSD the majority of problems being solved by means of MCNP concerns calculation of dose distributions and (effective) dose conversion factors for medical applications in diagnostic radiology, radiotherapy and nuclear medicine. It is also used to support experimental dosimetry and radiobiology, and for personal dosimetry, in conjunction with radiation protection of patients, radiation workers and general public.

7. Patient dosimetry and assessment of image quality in medical diagnostic radiology

J. Zoetelief, J.Th.M. Jansen and F.W. Schultz

Application of the general principles of radiation protection to medical radiology implies that clinical procedures involving X rays or radionuclides are to be justified and optimised. For diagnostic radiology, optimisation means that the radiation dose to the patient should be kept as low as possible, but still compatible with the image quality necessary for an adequate diagnosis. Optimisation concerns the balance between patient dose and image quality, i.e., radiation risk versus adequate medical diagnosis. Assessment of image quality is of great importance in this respect. The most appropriate dosimetric quantity for risk assessment is the effective dose (1). Presently, a key question in diagnostic radiology is to what extent digital techniques should replace conventional methods, e.g. film/screen radiography.

In practice, the assessment of organ effective doses in diagnostic radiology is based upon measurement of relatively simple dosimetric quantities, e.g., entrance surface dose (ESD), X-ray tube output (i.e., air-kerma free-in-air per unit of tube-current exposure-time product, mAs), computed tomography dose index (CTDI) and dose-area-product (DAP). Conversion factors, which depend on additional information including radiation quality specified by for instance half value layer and exposure geometry, provide a relation between the basic dosimetric quantities and effective dose.

Practical dose measurements

For the measurement of various dosimetric quantities TNO-CSD can provide adequate means. These include thermoluminescent dosimeters (TLD) in various arrangements for ESD measurement on patients as well as various types of ionisation chambers which in combination with appropriate electrometers, can be used for measurement of tube output, CTDI and DAP. The use of TLD has as advantages that these can easily be applied by the local staff of a diagnostic radiology department and can be evaluated at TNO-CSD. Ionisation chamber measurements, however, require a TNO employee visiting the department.

Assessment of organ and effective doses for patients

The same value of a basic dosimetric quantity for different exposure conditions may result in considerable differences in organ and effective doses. It is, therefore, important to apply appropriate factors to convert dosimetric quantities into organ and effective doses. TNO-CSD has available or access to almost all world-wide available data bases of conversion factors. In addition, TNO-CSD has the facilities to calculate conversion factors if adequate information is lacking.

Image quality assessment

Dosimetric information without knowledge of the related image quality provides only a basis for risk assessment, i.e., only half the information necessary to demonstrate compliance with good medical practice. Therefore, demonstration of adequate image quality is vital. TNO-CSD can provide means for the assessment of image quality by performing measurements on images of contrast-detail phantoms. Although this method provides only semi-quantitative information it still allows clear demonstration of differences in image quality for different situations. The development of techniques for quantifying image quality is an important research area of TNO-CSD.

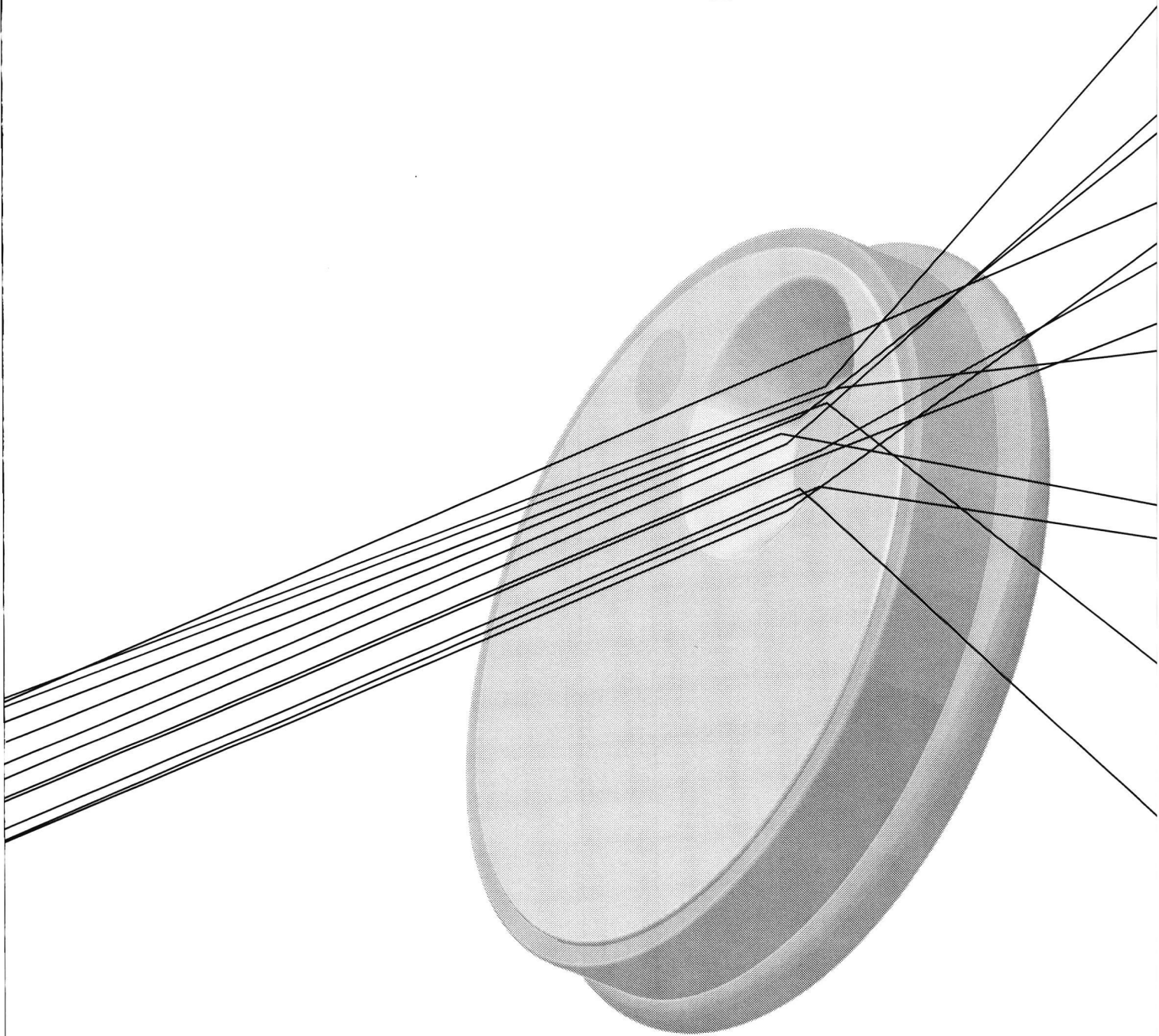
1. International Commission on Radiological Protection (ICRP).

1990 Recommendations of the International Commission on Radiological Protection. ICRP publication 60 (Oxford: Pergamon Press, ICRP), 1991.

I. Research and Development

II. Services

III. Publications and Reports





List of publications

1996

- **L.B. Beentjes and J.J. Broerse.**
Biologische effecten en stralingsbescherming. In: Fundamente van de radiologie. Edited by J.H.J. Ruijs and J.A.M. Lemens. Utrecht: Wetenschappelijke Uitgeverij Bunge, p. 55-74, 1996.
- **P. Bentvelzen.**
Het belang van het CDKN2A-gen voor de oncologie. IKR Bulletin 20(1) 38, 1996.
- **P. Bentvelzen.**
Humane kankervirussen. IKR Bulletin 20(1) 66-78, 1996.
- **P. Bentvelzen.**
Bijdrage van het moderne experimentele kankeronderzoek aan de kankertherapie. IKR-Bulletin 20(3), 42-45, 1996.
- **P. Bentvelzen.**
Human herpes-virus 8 geassocieerd met Kaposi sarcoom. Tijdschrift Kanker 20(4), 19, 1996.
- **P. Bentvelzen.**
Roken, p53 en longkanker. Tijdschrift Kanker 20(6), 31, 1996.
- **L. van den Berg, J. Zoetelief, H.W. Julius and H.B. Kal.**
Kwaliteitsborging in de medische radiodiagnostiek. Klinische Fysica, 3, 11-17, 1996.
- **J.J. Broerse and F.W. Schultz.**
Dose assessment-possibilities and limitations. In: Proc. ERPET Course of Radiation Accident Management. Institute of Occupational and Social Medicine. IOSM, pp. 102-112, 1996.
- **J.J. Broerse.**
Book review: Basic Clinical Radiobiology. Eur. J. Nucl. Med. 22, 1459-1460, 1996.
- **J.J. Broerse, B. Bakker, J. Davelaar, J.W.H. Leer, M.M.B. Niemer-Tucker and E.M. Noordijk.**
The effects of single dose TBI on hepatic and renal function in non-human primates and patients. In: The radiological consequences of the Chernobyl accident. ISBN no. 92-827-5248-8. Proc. First Int. Conf. Minsk, Belarus (18-22 March 1996) (EUR 16544 EN), ed.: A. Karaoglou, G. Desmet, G.N. Kelly and H.G. Menzel. Brussels: European Commission on the Belarus, Russian and Ukrainian Ministries on Chernobyl Affairs Emergency Situations and Health 1996, pp. 611-617, 1996.
- **J.J. Broerse.**
Zijn magnetische velden bij hoogspanningskabels nadelig voor de gezondheid? Vademecum 14, no. 22, 1-3, 1996.
- **J.J. Broerse and L.B. Beentjes.**
Dosimetrie van ioniserende straling. In: Fundamente van de radiologie. Ed.: J.H.J. Ruijs and J.A.M. Lemmens. Utrecht: Wetenschappelijke Uitgeverij Bunge, pp. 35-54, 1996.
- **J.J. Broerse.**
De potentiële gevaren van straling en radioactiviteit in onze leefomgeving. In: Vragen over kanker, het antwoord van de huisarts. Ed.: M.E.T.C. Muijsenbergh. Leiden: Boerhaave Commissie, pp. 71-83, 1996.
- **J.J. Broerse and M. Coppola.**
Differences in wT for radiation carcinogenesis in various organs. In: Radiation Research 1895-1995. Ed.: U. Hagen, D. Harder, H. Jung and C. Streffer. Würzburg: The International Association for Radiation Research, pp. 177-180, 1996.
- **J.W.E. van Dijk and H.W. Julius.**
Dose thresholds and quality assessment by statistical analysis of routine individual monitoring TLD data. Radiat. Prot. Dosim. 66, 17-22, 1996.
- **J.Th.M. Jansen, J. Geleijns, D. Zweers, F.W. Schultz and J. Zoetelief.**
Calculation of computed tomography dose index to effective dose conversion factors based on measurement of the dose profile along the fan shaped beam. Brit. J. Radiol 69, 33-41, 1996.
- **J.Th.M. Jansen and J. Zoetelief.**
Model for optimising mammography screening protocols. In: Proc. Tenth Int. Congr. Radiation Research. Eds: U. Hagen, D. Harder, H. Jung, C. Streffer. Würzburg: ICRR, pp. 1175-1178, 1996.
- **H.W. Julius.**
Some remaining problems in the practical application of the ICRU concepts of operational quantities in individual monitoring (11 SSDS, Boedapest, 1995). Radiat. Prot. Dosim. 66, nos. 1-4, pp.1-8, 1996.
- **H.B. Kal.**
Tumorbiologie. In: Radiobiologie en Stralenbescherming. Edited by V. de Ru and H. Welleweerd, 1996.

- **C.P.J. Raaijmakers, P.R.D. Watkins, E.L. Nottelman, H.W. Verhagen, J.Th.M. Jansen, J. Zoetelief and B.J. Mijnheer.**
The neutron sensitivity of dosimeter applied to boron neutron capture therapy. *Med. Phys.* 23, 1581-1589, 1996.
 - **F.W. Schultz and J. Zoetelief.**
Organ and effective doses in the male phantom Adam exposed in AP direction to broad unidirectional beams of monoenergetic electrons. *Health Phys.* 70, 498-504, 1996.
 - **A. Snijders-Keilholz, R.J.W. de Keizer, B.M. Goslings, E.W.C.M. van Dam, J.Th.M. Jansen and J.J. Broerse.**
Probable risk of tumour induction after retro-orbital irradiation for Graves' ophthalmopathy. *Radiother. Oncol.* 38, 69-71, 1996.
 - **A. Snijders-Keilholz, R.J.W. de Keizer, B.M. Goslings, E.W.C.M. van Dam, J.Th.M. Jansen and J.J. Broerse.**
To the editor: Response to Blank et al. The probable risk of tumour induction after retro-orbital irradiation for Graves' ophthalmopathy. *Radiother. Oncol.* 40, 188-189, 1996.
 - **J.C. Strong, J.P. Morlier, G. Monchaux, R.W. Bartstra, J.S. Groen and S.T. Bakker.**
Intercomparison of measurement techniques used in radon exposure facilities for animals in Europe. *Applied Radiation and Isotopes* 47, 355-359, 1996.
 - **J. Zoetelief, M. Fitzgerald, W. Leitz and M. Säbel.**
European Protocol on Dosimetry in Mammography. European Commission Report EUR 16263EN. Luxembourg: EC, 1996.
- 1997**
- **R.W. Bartstra.**
Prediction of hormesis in radon carcinogenesis. Proc. 27th Annual Meeting ESRB, Montpellier, September 1-4, 1996. *Radioprotection* 32(CI), 419, 1997.
 - **P. Bentvelzen, A. van Rotterdam and R.W. Bartstra.**
Radon in woningen en kans op longkanker. *NVS-Nieuws* 21(5), 8-11, 1997.
 - **P. Bentvelzen.**
Genetische instabiliteit. Chromosoomafwijkingen dragen bij aan het ontstaan van darmkanker. *Tijdschrift Kanker* 21(3), 36, 1997.
 - **P. Bentvelzen.**
ATM-mutaties en de kans op borstkanker. *Tijdschrift Kanker* 21(4), 26, 1997.
 - **J.J. Broerse, J. Geleijns and J. Zoetelief.**
Doses en risico's in de radiodiagnostiek - een stralende toekomst? *Gamma* 47, 78-81, 1997.
 - **J. Geleijns, J.J. Broerse, M.P. Chandie Shaw, F.W. Schultz, W. Teeuwisse, J.G. van Unnik and J. Zoetelief.**
Patient dose due to colon examination: dose assessment and results form a survey in The Netherlands. *Radiology* 204, 553-559, 1997.
 - **J. Geleijns, W. Teeuwisse and J.J. Broerse.**
Radiodiagnostisch onderzoek met betrekkelijk hoge doses. *Klinische Fysica* 2, 15-17, 1997.
 - **J.Th.M. Jansen and J. Zoetelief.**
Optimisation of breast cancer screening using a computer simulation model. *Eur. J. Radiol.* 24, 137-144, 1997.
 - **J.Th.M. Jansen and J. Zoetelief.**
Assessment of lifetime gained due to mammographic breast cancer screening using a computer model. *Brit. J. Radiol.* 70, 619-628, 1997.
 - **J.Th.M. Jansen, C.P.J. Raaijmakers, B.J. Mijnheer and J. Zoetelief.**
Relative neutron sensitivity of tissue equivalent ionisation chambers in an epithermal neutron beam for boron capture therapy. *Radiat. Prot. Dosim.* 70, 27-32, 1997.
 - **H.B. Kal.**
De effectieve dosis van radon in Nederland. *NVS-Nieuws* 22, nr. 1, 4-7, 1997.
 - **R. Klein, H. Aichinger, J. Dierker, J.T.M. Jansen, S. Joite-Barfuss, N. Säbel and J. Zoetelief.**
Determination of average glandular dose with modern mammography units for two large groups of patients. *Phys. Med. Biol.* 42, 561-572, 1997.
 - **J.L. Noteboom, W.A. Hummel, J.Th.M. Jansen, D.W. van Bekkum and J.J. Broerse.**
Simulation of measurements of uptake of ¹²³Iodide in the thyroid of foetal chimpanzees. *Radiat. Res.* 147, 686-690, 1997.
 - **J.L. Noteboom, W.A. Hummel, J.J. Broerse, J.J.M. de Vijlder, T. Vulsma, J.Th.M. Jansen and D.W. van Bekkum.**
Protection of the maternal and foetal thyroid from radioactive contamination by the administration of stable iodide during pregnancy. An experimental evaluation in chimpanzees. *Radiat. Res.* 147, 691-697, 1997.

- **J.L. Noteboom, W.A. Hummel, J.J. Broerse, J.J.M. de Vijlder, T. Vulsma and D.W. van Bekkum.**
Protection of the infant thyroid from radioactive contamination by the administration of stable iodide. An experimental evaluation in chimpanzees. *Radiat. Res.* 147, 698-706, 1997.
 - **F.W. Schultz and J. Zoetelief.**
Effective dose per unit fluence calculated for adults and a 7-year old girl in broad antero-posterior beams of monoenergetic electrons of 0.1 to 10 MeV. *Radiat. Prot. Dosim.* 69, 179-186, 1997.
 - **J.G. van Unnik, J.J. Broerse, J. Geleijns, J.Th.M. Jansen, J. Zoetelief and D. Zweers.**
Survey of CT techniques and absorbed dose in various Dutch hospitals. *Brit. J. Radiol.* 70, 367-371, 1997.
 - **J. Zoetelief, J.Th.M. Jansen and J.J. Broerse.**
Dosimetrie in de radiobiologie: internationale activiteiten. *Klinische Fysica* 2, 13-14, 1997.
 - **J. Zoetelief and J.Th.M. Jansen.**
Calculated energy response correction factors for LiF thermoluminescent dosimeters employed in the Seventh EULEP dosimetry intercomparison. *Phys. Med. Biol.* 42, 1491-1504, 1997.
 - **J. Zoetelief, J.J. Broerse, F.A.I. Busscher, W.P. Hiestand, H.W. Julius and J.Th.M. Jansen.**
Recent EULEP dosimetry intercomparisons for whole body irradiation of mice. *Int. J. Radiat. Biol.* 72, 627-632, 1997.
 - **J. Zoetelief.**
Stralingsbescherming van de patiënt en kwaliteitscontrole in de radiodiagnostiek. NVS-publicatie 29, 37-53, 1997.
 - **R.W. Bartstra.**
Prediction of hormesis in radon carcinogenesis. In: Proc 27th Annual Meeting of the European Society for Radiation Biology (F Daburon and M Martin, eds), Special Issue of *Radioprot* 32, 418, 1997.
 - **R.W. Bartstra.**
Theoretical plausibility of a non-linear dose-response relationship in low-dose radon carcinogenesis. In: Abstracts of International Workshop on Indoor Radon Exposure and its Health Consequences. Nat Inst of Radiological Sciences, Chiba, Japan, 1997.
 - **J. Zoetelief, J.J. Broerse, F.A.J. Busscher, W.P. Hiestand, H.W. Julius and J.T.M. Jansen.**
Recent EULEP dosimetry intercomparisons for whole body irradiation of mice. *Int J Radiat Biol* 72, 627-632, 1997.
 - **J. Zoetelief.**
Stralingsbescherming van de patiënt en kwaliteitscontrole in de radiodiagnostiek. NVS publicatie 29, 37-53, 1997.
 - **J. Zoetelief, J.T.M. Jansen and J.J. Broerse.**
Dosimetrie in de radiobiologie: internationale activiteiten. *Klinische Fysica* 2, 13-14, 1997.
- 1998**
- **R.W. Bartstra, P.A.J. Bentvelzen, J. Zoetelief A.H. Mulder J.J. Broerse and D.W. van Bekkum.**
Induction of mammary tumors in rats by single-dose gamma irradiation at different ages. *Radiat Res* 150, 442-450, 1998.
 - **R.W. Bartstra, P.A.J. Bentvelzen, J. Zoetelief A.H. Mulder J.J. Broerse and D.W. van Bekkum.**
The influence of estrogen treatment on induction of mammary carcinoma in rats by single-dose gamma irradiation at different ages. *Radiat Res* 150, 451-458, 1998.
 - **P.A.J. Bentvelzen.**
Oorzaken van kanker anno 1998. *Tijdschrift kanker* 22(1), 10-11, 1998.
 - **P.A.J. Bentvelzen.**
Röntgenfoto is niet zó gevaarlijk. *Tijdschrift Kanker* 22(4), 19, 1998.
 - **L. van den Berg.**
Loodschort en handschoen verplicht. Stralingsveiligheid en kwaliteit van röntgentoestellen. In *Praktijk, vaktijdschrift voor Dierenarts en Dierenassistenten*, nr 2, 23-26, 1998.
 - **L. van den Berg, J.C.N.M. Aarts, L.B. Beentjes, A. van Dalen, P. Elsackers, H.W. Julius, P.J.H. Kicken, F. van der Meer, W. Teeuwisse, M.A.O. Thijssen and J. Zoetelief.**
Guidelines for quality control of equipment used in diagnostic radiology in The Netherlands. *Rad Prot Dosim.* 80, 95-97, 1998.

- **J.J. Broerse and J. Geleijns.**
The relevance of different quantities for risk estimation in diagnostic radiology. *Rad Prot Dosim* 80, 33-37, 1998
- **F. Darroudi, A.T. Natarajan, P.A.J. Bentvelzen, P.J. Heidt, A. van Rotterdam, J. Zoetelief and J.J. Broerse.**
Detection of total-and partial-body irradiation in a monkey model: a comparative study of chromosomal, micronucleus and premature chromosome condensation assays. *Int J Radiat Biol* 74, 207-215, 1998
- **J.W.E. van Dijk.**
Quality assurance in individual monitoring: 10 years of performance monitoring of the TLD based TNO individual monitoring service. *Rad Prot Dosim* 77, 235-240, 1998
- **J. Geleijns, J.J. Broerse, M.P. Chandie Shaw, F.W. Schultz, W. Teeuwisse, J.G. van Unnik and J. Zoetelief.**
A comparison of patient dose for examinations of the upper gastrointestinal tract at 11 conventional and digital X-ray units in The Netherlands. *Brit J Radiol* 71, 745-753, 1998
- **J. Geleijns and J.J. Broerse.**
Dosimetrie bij inhomogene blootstelling. *EDURAD* 33, 11-16, 1998
- **J. Geleijns, J.J. Broerse, W.A. Hummel, M.J. Schlij, L.J. Schultze-Kool, W. Teeuwisse and J. Zoetelief.**
Preference dose rates for fluoroscopy guided interventions. *Radiat Prot Dosim*, 135-138, 1998
- **J.T.M. Jansen.**
Monte Carlo calculations in diagnostic radiology: dose conversion factors and risk benefit analyses. Thesis, Leiden, 1998
- **P. de Jong, W. van Dijk and H.P. Burger.**
²²⁶Ra and ²²⁸Ra concentrations in gypsum plasters and mortars used in The Netherlands. Proceedings Second International Symposium on Naturally Occurring Radioactive Materials (NORM II), November 10-13, 1998, Krefeld, Germany
- **H.W. Julius.**
Quo vadis in radiological protection? *Rad Prot Dosim* 77, 231-234, 1998
- **H.B. Kal.**
Gezondheidsraad-rapport 'Radiofrequente elektromagnetische velden (330 Hz-300 GHz)'. *Ned. Tijdschr. Geneesk.* 142, 1546-1550, 1998
- **H.B. Kal, SY El Sharouni and H. Struikmans.**
Postoperative radiotherapy in non-small-cell lung cancer. Correspondence. *The Lancet* 352, 1385, 1998
- **W. Teeuwisse, M.P. Chandie Shaw, J. Geleijns and F.W. Schultz.**
Stralenbelasting van patiënten tijdens colon-onderzoek. *Gamma* 48 (1), 3-12, 1998
- **J. Zoetelief.**
Quality control in diagnostic radiology in The Netherlands. *Radiat Prot Dosim* 77, 257-265, 1998
- **J. Zoetelief.**
Kwaliteitscontrole van radiodiagnostiekapparatuur. *EDURAD* 33, 22-27, 1998
- **J. Zoetelief, M. Fitzgerald, W. Leitz and M. Säbel.**
Dosimetric methods for and influence of exposure parameters on the establishment of reference doses in mammography. *Radiat Prot Dosim*, 175-180, 1998
- **J. Zoetelief and J. Geleijns.**
Patient doses in spiral CT. *Brit J Radiol* 71, 584-586, 1998
- **J. Zoetelief, J. Geleijns, P.H.J. Kicken, M.A.O. Thijssen and J.G. van Unnik.**
Diagnostic reference levels derived from recent surveys on patient dose for various types of radiological examination in The Netherlands. *Radiat Prot Dosim*, 109-114, 1998
- **J. Zoetelief, G. Wagemaker and J.J. Broerse.**
Dosimetry for total body irradiation of rhesus monkeys with 300 kV X-rays. *Int J Radiat Biol* 74, 265-272, 1998
- **D. Zweers, J. Geleijns, N.J.M. Aarts, L.J. Hardam, J.S. Laméris, F.W. Schultz and L.J. Schultze-Kool.**
Patient and staff radiation dose in fluoroscopy-guided TIPS procedures and dose reduction, using dedicated fluoroscopy exposure settings. *Brit J Radiol* 71, 672-676, 1998

List of reports

- **R.W. Bartstra, P. de Jong and H.B. Kal.**
Ontwikkeling van een meetmethode voor de bepaling van de activiteitsconcentraties van radonochters in lucht. Rapport RD-I9601-364, 1996.
- **J.Th.M. Jansen, H.B. Kal, J. Zoetelief and J.J. Broerse.**
Stralingsbelasting en stralingsrisico's als gevolg van langdurige doorlichting bij hartkatheterablatie. Rapport RD-I9608-371, 1996.
- **H.B. Kal and J. Zoetelief.**
Proposed criteria for acceptability of radiological and nuclear medicine installations. Rapport RD-I9602-367, 1996.
- **J.G. van Unnik, J.J. Broerse, J. Geleijns, F.W. Schultz, W. Teeuwisse and J. Zoetelief.**
Stralingsbelasting bij radiologisch colon- en maagonderzoek. Eindverslag VWS 148458.94, 1996.
- **J. Geleijns, F.W. Schultz and W. Teeuwisse.**
Stralingsbelasting van patiënten tijdens een colon-onderzoek; verslag van een vergelijkend onderzoek in negen Nederlandse ziekenhuizen. IRS Rapport 97-01, 1997.
- **H.B. Kal and J. Zoetelief.**
European Commission. Criteria for acceptability of radiological (including radiotherapy) and nuclear medicine installations. Radiation Protection 91. Directorate-General Environment, Nuclear Safety and Civil Protection, Luxembourg. ISBN 92-828-1140-9, 1997.
- **P. de Jong and J.T.M. Jansen.**
Berekening van de nucleaire afschermingsfactoren voor een luchtverdedigings- en commandofregat. Fase I: Beoordeling van de rekenmethode 'Van Grol'. TNO rapport nr. 98 CSD 275 PJ/VL, 1-18, 1998
- **F.W. Schultz, J.J. Broerse, J. Geleijns, H. Holscher, M. van Vliet, J. Weststrate, H.M. Zonderland and J. Zoetelief.**
Ontwikkeling van methoden voor de bepaling van stralingsbelasting en beeldkwaliteit bij kinderradiologie: bekkenopnamen en mictie-cysto-urethrografie. Eindverslag van een project uitgevoerd in opdracht van het Ministerie van VWS, DGV 1995-1997. Rapport RD-I/9806-392, 1998



